ALMA MATER STUDIORUM
UNIVERSITÀ DI BOLOGNA

DEPARTMENT OF PHYSICS AND ASTRONOMY "A. RIGHI"

SECOND CYCLE DEGREE

PHYSICS

Series expansions for scattering amplitudes

Supervisor
Prof. Dr. Tiziano Peraro

Co-supervisor
Prof. Dr. Lorenzo Tancredi

Defended by
Giovanni Luca Ferro

Graduation Session / October/ 2025

Academic Year 2024/2025

Abstract

This thesis investigates series expansion techniques for Feynman integrals and scattering amplitudes in quantum field theory. These integrals are reduced to linear combinations of an independent set of master integrals, via Integration By Parts identities. The master integrals, in turn, obey systems of differential equations, whose solution provides an efficient method for their evaluation. We focus on solving the differential equations using an iterative approach in the dimensional regulator ϵ, combined with a series expansion in the relevant kinematic scales.

To improve convergence, we study and systematically develop Bernoulli-like variable changes, which map nearby singularities to infinity. Starting from one-scale problems, we analyze their effectiveness and limitations, identifying some of their key features.

We then propose an extension of the method to multi-scale problems by introducing multiple Bernoulli-like variables. Applied to two-loop amplitudes for Higgs and Z decays into three gluons, this approach significantly reduces the number of required terms for accurate results. We also test it on a two-scale elliptic Feynman integral (the sunrise with two equal masses and a different mass), finding moderate improvements despite the complicated singularity geometry.

Our results show that Bernoulli-like transformations provide a general and efficient tool for accelerating series solutions, with potential applications to high-loop, multi-scale calculations where analytic methods are intractable.

Contents

1 Introduction

Theoretical particle physics aims to understand the fundamental constituents of matter and the interactions that govern their behavior. Quantum Field Theory (QFT) provides the foundational framework for this pursuit, combining the principles of quantum mechanics and special relativity into a unified description where particles arise as excited states of underlying quantum fields. Within this framework, the Standard Model (SM) stands as the most successful and experimentally validated theory to date. It describes all known elementary particles and three of the four fundamental interactions (electromagnetic, weak, and strong) based on a gauge symmetry structure, described by the symmetry group $SU(3)_C \times SU(2)_L \times U(1)_Y$. This symmetry governs how particles interact and gives rise to the rich phenomenology observed in high-energy physics experiments.

Scattering processes are the primary tools for probing the nature of particles and their interactions. By studying how particles deflect, merge, or transform when they collide, we gain insight into the underlying forces that govern their behavior and try to answer some of the most profound questions in fundamental physics. As experimental measurements at colliders reach ever higher levels of accuracy, on the theoretical side, making precise predictions is of fundamental importance to enable meaningful comparisons. High-precision comparisons are essential for both investigating properties of the known particles, testing the internal consistency of the Standard Model and its predictive power, and looking for signals of new physics beyond it.

In this context, scattering amplitudes have a central role: they are the primary interface between theory and experiments, as they encapsulate the probabilities for various outcomes of a scattering event, providing predictions that can be tested with high precision. In quantum field theory, scattering amplitudes are typically computed using perturbation theory, an approximation method that becomes valid when the coupling constant of the interaction is small. This allows one to express the amplitude as a power series in the coupling, where each order is represented by a finite sum of Feynman diagrams constructed according to the Feynman rules of the theory.

To obtain high-precision theoretical predictions, it is often necessary to go beyond the lowest-order (tree-level) approximation and include higher-order corrections. These correspond to diagrams with loops, which account for virtual particles circulating in intermediate states: these particles are not observed, hence we need to integrate over their momenta. As a result, the evaluation of loop diagrams naturally gives rise to Feynman integrals (FIs), multidimensional integrals whose computation is a very challenging task due to their complicated functional dependence on external momenta and masses and the presence of divergences, requiring regularization and renormalization. In particular, Feynman integrals are typically computed in dimensional regularization [6, 24],

where the spacetime dimension is continued to $d = d_0 - 2\epsilon$ ($d_0 \in \mathbb{N}$), to regulate divergencies. In most applications, one is only interested in their Laurent expansion around $\epsilon = 0$, up to a certain order dictated by the required precision.

For a given process, achieving the desired level of precision often requires the evaluation of hundreds or even thousands of Feynman integrals, particularly at higher orders in perturbation theory. Over the past two decades, powerful techniques have been developed to handle this complexity. Feynman integrals can be grouped into families based on their underlying topology, with each family characterized by a common set of propagators. The integrals within a given family are not all independent; they satisfy linear relations known as integration-by-parts (IBP) identities [12, 46]. These relations make it possible to systematically reduce the (infinite) set of integrals in a family to a finite [44] of linearly independent integrals known as master integrals (MIs).

The master integrals obey systems of differential equations [25, 39, 26] with respect to the kinematic invariants of the process (external momenta and internal masses). As a result, the problem of computing all integrals in the family reduces to solving these differential equations and imposing the appropriate boundary conditions.
In particular, it is convenient to look for a canonical basis [23, 22], i.e. a basis of MIs for which the ϵ-dependence in the differential equations factorizes. In this basis, the differential equations can be solved order by order in ϵ, allowing one, at least in principle, to compute all the Laurent coefficients up to the desired order. This method has become a cornerstone of modern multi-loop calculations in quantum field theory.

However, the complexity of the analytical results for FIs rapidly grows with the number of loops and external legs, so that it is not always possible to find global analytic solutions. Even when such solutions exist, they are often expressed in terms of highly nontrivial special function [8, 34] that are difficult to evaluate in practice.

Series expansion techniques are a powerful and pragmatic alternative. It is well known (see e.g. [7]) that, around any point that is not an essential singularity of a differential equation, local solutions can be expressed as generalized series expansions, which are guaranteed to converge at least up to the nearest singularity in the complex plane. In the context of Feynman integrals, the associated differential equations are typically Fuchsian [33], meaning that they possess only regular singular points, around which series solutions can be constructed. However, these techniques have important practical limitations: series have a limited radius of convergence, and even within that radius, the rate of convergence significantly decreases as one approaches the boundary. These challenges become particularly severe for problems involving multiple scales and multiple singularities.

A common strategy to improve convergence and extend the region of validity of a series solution involves performing a logarithmic change of variables [1] — known as a Bernoulli-like transformation — which maps the nearest singularity to infinity. This

technique has been applied to various one-scale problems [18, 37, 10], often in the spirit of experimental mathematics, where its use has been justified primarily by empirical success. However, to date, no comprehensive study of this method has been conducted. Moreover, a systematic generalization of the technique to multi-scale Feynman integrals or full scattering amplitudes has not yet been developed.

In this thesis, we focus on series expansion techniques for both Feynman integrals and scattering amplitudes, with particular attention to the convergence issues discussed above. We revisit the Bernoulli-like acceleration method from a more systematic perspective, with the goal of developing a deeper theoretical understanding and gaining greater control over its application. Then, we propose a generalization of the method to multi-scale problems. In particular, we demonstrate that significant improvements in convergence for two-scale problems can be achieved by introducing two Bernoulli-like variables (one for each scale) effectively mapping two nearby singularities to infinity and extending the region of convergence in both directions. We also briefly explore the possibility of constructing a generalized Bernoulli-like transformation capable of simultaneously pushing away multiple singularities, even within one-scale problems. However, this preliminary investigation did not lead to substantial improvements.

The work is structured around a series of case studies, from which we aim to extract general insights. We begin with simple one-scale problems, then move to more complicated two-scale examples. For the cases involving Feynman integrals, we solve the associated systems of differential equations, by combining an iterative (order-by-order in ϵ) procedure, facilitated by working in a canonical basis, with a series expansion in the relevant kinematic variables. In the case of full amplitudes, we directly analyze the series expansions of known analytic expressions [20, 21]. In both contexts, we study the convergence properties of the resulting series and investigate the effect of applying Bernoulli-like transformations to improve convergence.

The thesis is structured as follows:

- **Chapter 2** introduces the fundamentals of Feynman integrals: their definitions, main properties, parametric representations, and linear relations, with a focus on integration-by-parts (IBP) identities and the concept of master integrals.
- **Chapter 3** reviews the method of differential equations, emphasizing the canonical form and a recently proposed algorithm for constructing it, which is used throughout the thesis.
- **Chapter 4** provides an overview of the mathematical structures appearing in Feynman integrals, such as periods and iterated integrals, with particular attention to multiple polylogarithms (MPLs) and integrals over elliptic curves.
- **Chapter 5** discusses series solutions of differential equations, especially via the

Frobenius method. We then revisit the Bernoulli-like change of variable from an original perspective, deriving a general expression for it, and analyzing its convergence-accelerating properties.

- **Chapter 6** applies these methods to the bubble integral — the simplest one-loop case — which, despite its simplicity, reveals interesting aspects related to its convergence behavior and the properties of Bernoulli-like variables.

- **Chapter 7** focuses on the equal-mass sunrise integral — a two-loop, one-scale problem that allows us to refine our techniques. We also explore possible generalizations of the Bernoulli-like transformation to handle *multiple singularities*, though without significant results.

- **Chapter 8** presents the main original contribution of the thesis: a convergence acceleration method for multi-scale problems using multiple Bernoulli-like variables. We test this approach on two polylogarithmic amplitudes describing Higgs and Z-boson decays into three gluons at two loops.

- **Chapter 9** applies the series expansion techniques to a two-scale elliptic Feynman integral — the sunrise with two equal masses and one distinct mass — and assesses the *performance and limitations* of the proposed acceleration method in this more complicated setting.

- **Chapter 10** summarizes the main results of this thesis and outlines possible directions for future research.

2 Feynman Integrals

In this chapter, we introduce the foundational concepts of Feynman integrals (FIs), following mainly [2] and [48]. We assume the reader to be already familiar with QFT topics, which can be found in many textbooks [42, 47, 36].

We begin by presenting the main definitions and general properties of FIs. We then derive their principal parametric representations. Finally, we explore the linear relations among Feynman integrals, focusing on the notions of integral families,integration-by-parts identities (IBPs), and master integrals (MIs). These concepts will play a central role throughout the rest of this work.

2.1 Basic definitions and properties

Let us start with the precise definition of a scalar Feynman integral.

Def. 1 A scalar Feynman integral, associated to a L-loops amplitude with E external legs and P propagators, is an integral of the following form:

$$I(p_1,...,p_E;m_1^2,...,m_P^2;\nu;D)=\int\left(\prod_{j=1}^{L}e^{\gamma_E\epsilon}\frac{d^Dk_j}{i\pi^{D/2}}\right)\frac{\mathcal{N}\big(\{k_i\cdot k_j,k_i\cdot p_j\};D\big)}{\prod_{j=1}^{P}\big(q_j^2-m_j^2+i\delta\big)^{\nu_j}},\quad (1)$$

where $\nu=(\nu_1,...,\nu_p)\in\mathbb{Z}^p$ is the vector of (integer) propagator exponents, γ_E is the Euler-Mascheroni constant, m_j ($1\leq j\leq P$) are the propagator masses (assumed to be positive), k_j ($1\leq j\leq L$) are the loop momenta, p_j ($1\leq j\leq E$) are the external momenta.

We assume w.l.o.g. all external momenta to be incoming; they are real Minkowski momenta, only constrained by momentum conservation, expressed by: $\sum_{j=1}^{E}p_j=0$. The momenta flowing through propagators can be expressed as linear combinations of loop and external momenta of the form:

$$q_j=\sum_{j=1}^{L}\alpha_{ij}k_j+\sum_{j=1}^{E}\beta_{ij}p_j\qquad\text{with}\quad\alpha_{ij},\beta_{ij}\in\{-1,0,1\}.\quad (2)$$

The numerator of (1) is assumed to be a polynomial in the scalar products between loop and/or external momenta; in the denominator we use the usual Feynman-Stückelberg prescription to deform the integration contour away from propagator poles. We are working in dimensional regularization with $D=D_0-2\epsilon$ dimensions, where D_0 is a positive integer (in most cases $D_0=4$).

A scalar Feynman integral, like (1), is by definition invariant under Lorentz transformations in D dimensions:

$$I(\Lambda p_1,...,\Lambda p_E;m_1^2,...,m_P^2;\nu;D)=I(p_1,...,p_E;m_1^2,...,m_P^2;\nu;D).\quad (3)$$

As a consequence, it can only depend on the external scales: propagator masses and scalar products among external momenta, collectively denoted as:

$$x = \Big(\{p_i \cdot p_j\}_{1 \leq i,j \leq E}, \{m_j^2\}_{1 \leq j \leq P} \Big). \tag{4}$$

To simplify the notation and make Lorentz invariance manifest, in the following we will denote integral (1) as $I(x; \nu; D)$.

Let us recap the main basic properties of Feynman integrals in dim. reg.:

Prop. 1 (Invariance under shifts and rescalings of loop momenta)
Feynman integrals in dimensional regularization are invariant[1] under general linear changes of variables: $k_i^\mu \to \lambda k_i^\mu + v^\mu$, with λ a nonzero real number and v^μ a D-dimensional vector independent of k^μ.

Prop. 2 (Dependence on ϵ)
Feynman integrals are meromorphic functions of the regulator ϵ, i.e. they can have at most poles in the complex ϵ-plane, but no branch-cuts. We are usually interested in the first coefficients of the Laurent expansion around $\epsilon = 0$, $I = \sum_{k \geq k_0} I_k \epsilon^k$. If $k_0 < 0$, then the integral is divergent in D_0 dimensions.

Prop. 3 (Homogeneity)
Feynman integrals are homogeneous functions in the external scales, i.e. under a rescaling of all of them: $x \to \lambda^2 x$ (coresponding to $(p_j, m_j) \to (\lambda p_j, \lambda m_j)$) with $\lambda \in \mathbb{R}^*$, we have:

$$I(\lambda^2 x; \nu; D) = \lambda^\alpha I(x; \nu; D), \tag{5}$$

with α mass dimension of the integral: $\alpha = [I(x; \nu; D)] = [\mathcal{N}] + LD - 2\sum_{j=1}^P \nu_j$.

Prop.4 (Scaleless integrals)
A Feynman integral is said to be scaleless if it does not depend on any external scale, i.e. $x = \vec{0}$. Scaless integrals vanish in dimensional regularization.

Proof
Prop. 3 for a scaleless integral reduces to:

$$I(\vec{0}; \nu; D) = \lambda^\alpha I(\vec{0}; \nu; D), \qquad \forall \lambda \in \mathbb{R}^*. \tag{6}$$

Since[2] $\alpha \neq 0$ in dim. reg., the previous equation can only hold if $I(\vec{0}; \nu; D) = 0$.

Corollary
If $\nu_j \leq 0$ for all $1 \leq j \leq P$, then $I(x; \nu; D) = 0$ in dimensional regularization, being a linear combination of scaleless integrals.

Some of these properties will be useful to derive the main result of Section 2.3: the IBP relations.

[1] This property may seem trivial, but it is not: indeed, this is not true in other regularization schemes (e.g. with a cutoff as regulator).

[2] In fact, one can easily convince himself that $\alpha = [I(x; \nu; D)] = m - 2L\epsilon$ with $m \in \mathbb{Z}$.

2.2 Parametric representations

The representation of Feynman integrals in eq. (1) is known as the momentum representation: it is naturally connected to Feynman diagrams, but it is not the most convenient to compute these integrals and put their properties in evidence. For these purposes, many parametric representations have been introduced. In this section, we review the most common ones.

2.2.1 Schwinger representation

Each denominator $D_j = q_j^2 - m_j^2$ appearing in (1) can be rewritten using Schwinger's trick:[3]

$$\frac{1}{A_j^{\nu_j}} = \frac{1}{\Gamma(\nu_j)} \int_0^\infty d\alpha_j \, \alpha_j^{\nu_j - 1} e^{-\alpha_j A_j}, \qquad \text{for} \quad A_j > 0, \quad Re(\nu_j) > 0, \tag{7}$$

where in our case A_j is defined by:

$$A_j = Q_j^2 + m_j^2 = -q_j^2 + m_j^2 = -D_j, \tag{8}$$

with Q_j being the Euclidean version of momentum q_j. Thus, our Feynman integral (1), whose numerator has been set to one for simplicity, becomes:

$$I = \frac{e^{L\gamma_E \epsilon}}{\prod_{j=1}^{P} (-1)^{\nu_j} \Gamma(\nu_j)} \int_{\alpha_j \geq 0} d^P\alpha \left(\prod_{j=1}^{P} \alpha_j^{\nu_j - 1} \right) \int \left(\prod_{r=1}^{L} \frac{d^D k_r}{i\pi^{D/2}} \right) \exp\left[-\sum_{j=1}^{P} \alpha_j (-q_j^2 + m_j^2) \right], \tag{9}$$

where $\alpha = (\alpha_1, ..., \alpha_P)$ is the vector of the so-called Schwinger parameters.

Because of (2), the argument of the exponential will have a quadratic dependence on loop momenta of the form:

$$\sum_{j=1}^{P} \alpha_j (m_j^2 - q_j^2) = -k^T M k + 2k \cdot r + J, \tag{10}$$

where $k = (k_1, ...k_L)$ is as usual the vector of loop momenta, M is a $L \times L$ matrix whose entries are combinations of the Schwinger parameters, r is a L-dimensional vector whose components also involve the external momenta, J is a scalar.

We can perform the integration over loop momenta by Wick rotating and using the formula for an L-dimensional gaussian integral, which also extends to dimensional

[3] This follows directly from de definition of Euler's gamma function.

regularization. We get:

$$I = \frac{e^{L\gamma_E \epsilon}}{\prod_{j=1}^{P}(-1)^{\nu_j}\Gamma(\nu_j)} \int_{\alpha_j \geq 0} d^P\alpha \Big(\prod_{j=1}^{P} \alpha_j^{\nu_j - 1} \Big) [\mathcal{U}(\alpha)]^{-D/2} e^{-\frac{\mathcal{F}(\alpha;x)}{\mathcal{U}(\alpha)}}, \tag{11}$$

where we defined the graph polynomials (or Symanzik polynomials) $\mathcal{U}$ and $\mathcal{F}$ by:

$$\mathcal{U} = detM, \qquad \mathcal{F} = J + r^T M^{-1} r. \tag{12}$$

The integral representation (11) is known as the Schwinger parameter representation.

Note that $\mathcal{U}(\alpha)$ only depends on the Schwinger parameters, as it was for the matrix entries of M, while $\mathcal{F}(\alpha; x)$ also has a dependence on the external scales, coming from r and J. One can show [48] that they are homogeneous polynomials in the Schwinger parameters: $\mathcal{U}$ is of degree L, $\mathcal{F}$ is of degree $L + 1$. These properties are useful for deriving the Feynman representation.

2.2.2 Feynman representation

The Feynman representation is the one that is most well known, due to its usefulness in the computation of Feynman integrals by direct integration. It can be derived from the Schwinger representation or directly from the momentum representation; here, we choose the first option. We can write the following resolution of the unity in terms of Schwinger parameters:

$$1 = \int_{-\infty}^{\infty} dt\, \delta\Big(t - \sum_{j=1}^{p} \alpha_j\Big) = \int_{0}^{\infty} dt\, \delta\Big(t - \sum_{j=1}^{p} \alpha_j\Big), \tag{13}$$

where in the last step we used the fact that the sum is non-negative. For a generic integral over Schwinger parameters α_j, changing variables to $a_j = \alpha_j / t$ and inserting (13), we get the identity:

$$\int_{\alpha_j \geq 0} d^P\alpha\, f(\alpha_1, ...\alpha_p) = \int_{a_j \geq 0} d^P a\, \delta\Big(1 - \sum_{j=1}^{P} a_j\Big) \int_{0}^{\infty} dt\, t^{P-1} f(ta_1, ..., ta_P). \tag{14}$$

Applying it to the Schwinger representation (11) and using the fact that $\mathcal{U}$ and $\mathcal{F}$ are homogeneous of degree L and $L-1$ respectively, we get:

$$I = \frac{e^{L\gamma_E\epsilon}}{\prod_{j=1}^{P}(-1)^{\nu_j}\Gamma(\nu_j)} \int_{a_j\geq 0} d^P a \left(\prod_{j=1}^{P} a_j^{\nu_j-1}\right) \delta\left(1-\sum_{j=1}^{P} a_j\right) [\mathcal{U}(a)]^{-D/2} \int_0^\infty dt\, t^{\nu-\frac{lD}{2}-1} e^{-\frac{\mathcal{F}(a;x)}{\mathcal{U}(a)}t} =$$
$$= \frac{e^{L\gamma_E\epsilon}}{\prod_{j=1}^{P}(-1)^{\nu_j}\Gamma(\nu_j)} \int_{a_j\geq 0} d^P a \left(\prod_{j=1}^{P} a_j^{\nu_j-1}\right) \delta\left(1-\sum_{j=1}^{P} a_j\right) \frac{[\mathcal{U}(a)]^{\nu-\frac{(l+1)D}{2}}}{[\mathcal{F}(a;x)]^{\nu-\frac{lD}{2}}} \int_0^\infty du\, u^{\nu-\frac{lD}{2}-1} e^{-u}, \tag{15}$$

where in the last step we use the substitution $u = \frac{\mathcal{F}(a;x)}{\mathcal{U}(a)}t$, so that now the integral over u is the standard definition of $\Gamma(\nu - \frac{lD}{2})$. In this way, we get the final formula for the Feynman parameter representation:

$$I = \frac{e^{L\gamma_E\epsilon}\,\Gamma(\nu-\frac{lD}{2})}{\prod_{j=1}^{P}(-1)^{\nu_j}\Gamma(\nu_j)} \int_{a_j\geq 0} d^P a \Big(\prod_{j=1}^{P} a_j^{\nu_j-1}\Big) \delta\Big(1-\sum_{j=1}^{P} a_j\Big) \frac{[\mathcal{U}(a)]^{\nu-\frac{(l+1)D}{2}}}{[\mathcal{F}(a,x)]^{\nu-\frac{lD}{2}}}. \tag{16}$$

The integration variables a_j are called Feynman parameters.

In addition to its usefulness for computations, this representation also allows us to make an important observation on Feynman integrals: the powers of denominators ν_i and the dimension D have a similar role in (16), in the sense that both appear as exponents of the graph polynomials. This will motivate us to look for relations not only between integrals with different ν_i, but also with different values of D.

2.2.3 Baikov representation

Another important parametric representation is the Baikov representation. In the strict sense, it only applies to a subset of Feynman integrals, where the number P of propagators equals the number N_{sp} of independent scalar products involving loop momenta. The latter for an integral with L loops and E external momenta is given by: $N = L(L+1)/2 + L(E-1)$. This immediately follows from the fact that these scalar products are of the following forms: k_i^2 ($1 \leq i \leq L$), $k_i \cdot k_j$ ($1 \leq i < j \leq L$), $k_i \cdot p_j$ ($1 \leq i \leq L, 1 \leq j \leq E-1$).

Strictly speaking, a Feynman integral has a Baikov representation if $P = N_{sp}$ and each inverse propagator $z_s = q_s^2 - m_s^2$ can be expressed as a linear combination of independent scalar products σ_t:

$$z_s = C_{st}\sigma_t + f_s, \tag{17}$$

where C is a $N_{sp} \times N_{sp}$ invertible matrix and f is a N_{sp}-dimensional vector independent of loop momenta.

However, given an integral I that does not satisfy these conditions, it is always possible to find another one $\tilde{I}$ which does, and define the induced Baikov representation of I from the Baikov representation of $\tilde{I}$. A common situation is the one where $P < N_{sp}$: in this case it is possible to introduce[4] some fictitious extra propagators so that the transformation between the z_s and the σ_t is invertible, and then set the powers ν_s of the extra propagators to zero.

If invertible relations of the form (17) exist, then we can change integration variables in (1) to the z_j, which in this context take the name of Baikov variables. We get the Baikov representation of FIs (see [48] for a detailed derivation):

$$I = \frac{e^{L\gamma_E \epsilon} \left[\det G(p_1, ..., p_{E-1})\right]^{\frac{E-D}{2}}}{\pi^{\frac{N_{sp}-L}{2}} (\det C) \prod_{j=1}^{L} \Gamma\left(\frac{D-E+2-j}{2}\right)} \int_{\mathcal{C}} d^{N_{sp}} z \left[\mathcal{B}(z)\right]^{\frac{D-L-E}{2}} \frac{\mathcal{N}(\{z_k; x\}, D)}{\prod_{s=1}^{N_{sp}} z_s^{-\nu_s}}, \quad (18)$$

where $\det G(q_1, ..., q_n)$ denotes the Gram determinant of momenta $q_1, ..., q_n$ and $\mathcal{B}$ is the Baikov polynomial. The Gram determinants are defined by:

$$\det G(q_1, ..., q_n) = \det\left(q_i \cdot q_j\right)_{1 \leq i,j \leq n} = \begin{vmatrix} q_1 \cdot q_1 & q_1 \cdot q_2 & \cdots & q_1 \cdot q_n \\ q_2 \cdot q_1 & q_2 \cdot q_2 & \cdots & q_2 \cdot q_n \\ \vdots & \vdots & \ddots & \vdots \\ q_n \cdot q_1 & q_n \cdot q_2 & \cdots & q_n \cdot q_n \end{vmatrix}. \quad (19)$$

The Baikov polynomial $\mathcal{B}(z)$ is defined as the Gram determinant involving all loop momenta and independent external momenta, expressed in terms of Baikov variables:

$$\mathcal{B}(z_1, ..., z_P) = \det G(k_1, ..., k_L, p_1, ..., p_{E-1}). \quad (20)$$

The integration contour $\mathcal{C}$ is given by: $\mathcal{C} = \mathcal{C}_1 \cap \mathcal{C}_2 ... \cap \mathcal{C}_{L-1}$, where:

$$\mathcal{C}_j = \left\{ \frac{\det G(k_j, ...k_L, p_1, ..., p_{E-1})}{\det G(k_{j+1}, ...k_L, p_1, ..., p_{E-1})} \geq 0 \right\}. \quad (21)$$

The Baikov representation is very useful to compute cuts of Feynman integrals, which are related to their singularities by Cutkosky rules. In this representation, computing cuts simply corresponds to taking residues where the corresponding z_a are zero. We will say more about that in Section 3.4.

[4] This defines a complete set of Feynman integrals, as we will see in *Section 2.3.1*.

2.3 Linear relations among Feynman integrals

It is often useful to consider Feynman integrals as functions of the propagator exponents $\nu = \{\nu_j\}_{1\leq j\leq P}$ and of the space-time dimension D, for fixed values of the external scales x. This gives rise to the concept of an integral family. In this section, we want to show that the integrals of a family are not independent, but there are linear relations among them, so that the family is spanned by a finite basis: this is a crucial aspect in the development of an efficient method for computing Feynman integrals, as we will see in *Chapter 3*. First, we will focus on linear relations among integrals with different exponents but same space-time dimension, then we will briefly discuss about relations among integrals in different dimensions.

2.3.1 Families, IBPs and Master Integrals

Let us start with some definitions:

Def. 1 A family of F.I. is a (infinite) set of integrals $I(x;\nu;D)$ identified by a common set of invariants x: all integrals in the family share the same topology in terms of propagators and external legs, but differ for the denominator exponents.

Def. 2 A family is said to be complete if all possible scalar products involving loop momenta (e.g. $k_i \cdot k_j$, $k_i \cdot p_j$) can be written as linear combinations of denominators. For a family which is not complete, we call irreducible scalar products (ISPs) the scalar products involving loop momenta that cannot be written as linear combinations of the denominators.

If an integral family is complete, then the numerator of (1) can consequently be rewritten, so that the original integral is a linear combination of integrals with numerators equal to one. Note that every family of FIs can be completed by introducing some "fictitious" denominators corresponding to the ISPs. So from now on we will always assume to deal with complete families.

Now we want to show that the integrals of such a family are not all independent, but there are some linear relations among them, called IBP relations [12, 46], so that each integral of the family can be generated by a finite basis.

Theorem 1 (IBP relations)
Given a Feynman integral in dimensional regularization, $I = \int d^D k_i F(k_i, ...)$, we have:[5]

$$\int d^D k_i \frac{\partial}{\partial k_i^\mu}[v^\mu F(k_i, ...)] = 0, \tag{22}$$

for every D-dimensional vector v^μ; in other words, integrals of total derivatives vanish in dim. reg.

[5] For simplicity we are stating the theorem for a single loop integral, but it is also valid in the multi-loop case for all present loop momenta.

Proof
Using *Prop. 1*, we have that:

- Under an infinitesimal shift, $k_i^\mu \to k_i^\mu + \epsilon v^\mu$:

$$I = \int d^D k_i F(k_i + \epsilon v, ...) = I + \epsilon v^\mu \int d^D k_i \frac{\partial}{\partial k_i^\mu} F(k_i, ...) + o(\epsilon^2). \tag{23}$$

  Therefore: $\int d^D k_i \frac{\partial}{\partial k_i^\mu}[v^\mu F(k_i, ...)] = 0$, for v^μ independent of k_i^μ.

- Under an infinitesimal rescaling, $k_i^\mu \to e^\epsilon k_i^\mu$:

$$I = e^{D\epsilon} \int d^D k_i F(e^\epsilon k_i, ...) = I + \epsilon \left[DI + \int d^D k_i k_i^\mu \frac{\partial}{\partial k_i^\mu} F(k_i, ...) \right] + o(\epsilon^2). \tag{24}$$

  Therefore: $\int d^D k_i \frac{\partial}{\partial k_i^\mu}[k_i^\mu F(k_i, ...)] = 0$.

This completes the proof.

The previous theorem can be used to find linear recursion relations among the integrals of a complete family. In fact, when the differential operator $\frac{\partial}{\partial k_i^\mu} v^\mu$ in the LHS of (22) acts on a propagator, it shifts the value of the exponent by one and produces a numerator, which may not be present in the original integral. However, if v^μ is chosen to be a linear combination of loop and external momenta, then the numerator will be a polynomial in scalar products involving loop momenta and consequently it will be expressible in terms of inverse propagators, being the family complete. Therefore, the vanishing quantity in (22) is nothing but a linear combination of integrals of the same family (same denominators), whose coefficients are in general rational functions of the scales x and the regulator ϵ. These linear recursion relations in the propagator exponents are called IBP relations; they allow us, at least in principle, to express every integral of the family as a linear combination of a basis of integrals, called Master Integrals (MIs).

One can show that the number of MIs for any family is always finite [44] and it is also possible to predict it. However, different bases can be chosen and a clever choice can notably simplify the calculations, as we will see later on.

To better organize the reduction to MIs, it is useful to divide the family into sectors.
Def. 3 A sector is a set including all Feynman integrals of a family sharing the same set of active propagators, where a propagator is said to be active if it is raised to a strictly positive power (ν_i s.t. $\theta(\nu_i) = 1$). Therefore, the sector an integral belongs to can be identified by a vector:

$$S[I(\nu_1, ..., \nu_P)] = (\theta(\nu_1), ..., \theta(\nu_P)) \equiv \theta(\nu), \tag{25}$$

where θ is the Heaviside step-function. There is a natural ordering on sectors: $\theta(\nu) \geq \theta(\nu')$ if $\nu_i \geq \nu'_i$, for all $1 \leq i \leq P$.

From our discussion about IBPs, it is evident that IBPs for a certain integral $I(x;\nu;D)$ will involve integrals from its same sector $\theta(\nu)$ or from lower sectors. This fact significantly simplifies the reduction to MIs: in general, it is not possible to find a solution to IBP relations in closed form; however, since we are typically interested in computing only the specific integrals which appear in our amplitude, we only need to solve IBPs in the subsectors involving the needed denominators.

In practice, the recursion problem can be turned into an algebraic problem: we write down all the IBPs including the integrals we need to reduce, then we solve for the "complicated" integrals in terms of the "simpler"[6] ones. This approach is the basis for the Laporta algorithm [27], which has been implemented in many public codes.

However, for integrals with several loops and external legs, solving the IBP relations is still very challenging and modern techniques have been recently developed: tools from algebraic geometry (Syzygy equations) to get relations with lower powers of denominators; numerical evaluations over finite fields [35] (to avoid complexity of intermediate analytic expressions), followed by a reconstruction of the final analytic result.

2.3.2 Dimension-shift relations

Up to now we only considered linear relations among Feynman integrals with different propagator exponents ν, but same space-time dimension D and invariants x. However, as noted at the end of *Section 2.2.2*, the Feynman representation shows us that there is not a big difference between the dimension D and the exponents ν_i. Therefore, it is reasonable to look for relations among Feynman integrals in different dimensions.

Let us now state two theorems [45, 30] that relate integrals whose space-time dimensions differ by two.

Theorem 1
For Feynman integrals depending on generic non-zero propagator masses, we have:

$$I(x;\nu;D-2) = (-1)^L \mathcal{U}\Big(\frac{\partial}{\partial m_1^2},...,\frac{\partial}{\partial m_p^2}\Big) I(x;\nu;D), \tag{26}$$

where the operator appearing in the rhs is given by the first Symanzik polynomial, with the Schwinger/Feynman parameters replaced by the differential operators $\frac{\partial}{\partial m_i^2}$.

Using this theorem, an integral in $(D-2)$ dimensions can be written as a linear combination of integrals in D dimensions with shifted (because of the action of the

[6] Tipically, we consider as simpler integrals the ones with fewer denominators or smaller exponents.

mass derivatives) exponents. Carrying out the inverse operation requires an additional theorem:

Theorem 2 An integral in $(D+2)$ dimensions can be written as a linear combination of integrals in D dimensions as:

$$I(x;\nu;D+2) = \frac{2^L G(p_1,...,p_{E-1})}{(D-L-E+2)_L}\mathcal{B}(b_1,...,b_{L+E-1})I(x;\nu;D), \tag{27}$$

where $(x)_L$ is the Pochhammer[7] symbol, $\mathcal{B}$ is the Baikov polynomial defined in (20), and the b_i are the operators that lower the value of the exponent ν_i, i.e.:

$$b_i^a I(x;\nu;D) = I(x;\nu_1,...,\nu_i - a,...,\nu_P;D) \tag{28}$$

The relations (26) and (27) are known as dimension-shift relations. They can be very useful when computing Feynman integrals via the method of differential equations, that we will describe in the next section. In fact, for some integral families, it is easier to cast the differential equations in a simple form in $D = 2 - 2\epsilon$ than in the standard $D = 4 - 2\epsilon$ dimensions; then, at the end, one can reconstruct the physical integrals via these relations.

[7]The Pochhammer symbol is defined as: $(a)_n = a(a+1)...(a+n-1) = \frac{\Gamma(a+n)}{\Gamma(a)}$ with $(a)_0 = 1$.

3 The method of differential equations

As discussed previously, the IBP relations allow us to reduce the computation of the infinitely many FIs of a family to that of a finite number of Master Integrals. There are different techniques to compute MIs, but the most successful one is the method of differential equations [25, 39, 26], based on the fact that MIs satisfy systems of differential equations in the invariants. In this section, we present the main steps of the method, which are the following: obtaining the differential equations, finding a basis where they take a simpler form (canonical basis), and then solving them with the appropriate boundary conditions. For this review chapter, we mainly follow [2, 22, 4].

3.1 Obtaining the differential equations

For a complete family of FIs depending on the scales $x = (x_1, ..., x_s)$, let us fix a basis of MIs, represented as a vector $\vec{I}(x, \epsilon) = (I_1(x; \nu^1; \epsilon), ..., I_N(x; \nu^N; \epsilon))^T$, where $\nu^i = \{\nu^i_j\}_{1 \leq j \leq P}$ is the set of exponents appearing in the denominators of the i-th integral and we assume that the integrals are ordered in the vector from lower to higher sectors, i.e. $\theta(\nu^1) \leq \theta(\nu^2) \leq ... \leq \theta(\nu^N)$.

We can argue that the derivatives of MIs w.r.t. an external scale are still integrals of the same family. In fact, when computing the derivative of $\vec{I}(x, \epsilon)$ with respect to an external scale x_i, it is possible to take the derivative under the sign of integral, so that it acts directly on the integrand. If $x_i = m_j^2$, the operator ∂_{x_i} will simply shift by one the exponents of all denominators containing m_j. If x_i is a scalar product between external momenta, $x_i = p_j \cdot p_k$, then we need to express ∂_{x_i} in terms of the differential operators $O_{jk} = p_j^\mu \frac{\partial}{\partial p_k^\mu}$; this is done by employing the chain rule: $O_{jk} = p_j^\mu \frac{\partial}{\partial p_k^\mu} = \sum_l p_j^\mu \frac{\partial x_l}{\partial p_k^\mu} \frac{\partial}{\partial x_l}$, and then inverting the system to find $\frac{\partial}{\partial x_l}$. The operators O_{jk} act on the integrand in a similar way as discussed (see *Section 2.3.1*) for the operators on the LHS of (22), i.e. without producing new denominators. Therefore, at the end, for the derivatives of MIs, we get linear combinations of integrals of the same family, which can be reduced to MIs using IBP identities.

This means that the derivative of a master integral with respect to an external invariant x_i gives a linear combination of master integrals, so we can write:

$$\partial_{x_i} \vec{I}(x, \epsilon) = A_{x_i}(x, \epsilon) \vec{I}(x, \epsilon), \tag{29}$$

where $A_{x_i}(x, \epsilon)$ is a $N \times N$ matrix. This is a system of linear first-order differential equations in the invariant x_i satisfied by the MIs. Since IBPs only involve rational coefficients, then the entries of $A_{x_i}(x, \epsilon)$ are rational functions in x and ϵ. Moreover, if, as we assumed, the integrals in $\vec{I}(x, \epsilon)$ are ordered from the lowest to the top level sec-

tor, then[8] the matrix will be in block lower-triangular form: every block on the diagonal corresponds to the homogeneous part of the corresponding sector.

Repeating this procedure for all the scales x_i we get a system of differential equations for each of them; we can rewrite these systems in a more compact form in terms of a total differential $d = \sum_{i=1}^{s} \partial_{x_i} dx_i$:

$$d\vec{I}(x,\epsilon) = A(x,\epsilon)\vec{I}(x,\epsilon), \tag{30}$$

where $A(x,\epsilon) = \sum_{i=1}^{s} A_{x_i}(x,\epsilon)dx_i$ is a matrix of one-forms, whose coefficients are rational functions in x and ϵ.

3.2 Some properties of the differential equations

Let us now discuss the main properties of the differential equations satisfied by the MIs.

1. *Integrability condition*
The total differential satisfies the condition $d^2 = 0$, in fact:

$$d^2 = d\Big(\sum_j \frac{\partial}{\partial x_j} dx_j\Big) = \sum_{i,j} \frac{\partial^2}{\partial x_i \partial x_j} dx_i \wedge dx_j = 0, \tag{31}$$

where we used the fact that the wedge product between differential forms is antisymmetric, while second partial derivatives are symmetric. This gives a constraint on $A(x,\epsilon)$:

$$0 = d^2\vec{I} = d\big(A\vec{I}\big) = \big(dA\big)\vec{I} - A \wedge d\vec{I} = \big(dA - A \wedge A\big)\vec{I}, \tag{32}$$

where we used (30) to express $d\vec{I}$. Therefore, the matrix $A(x,\epsilon)$ must satisfy the integrability condition:

$$dA(x,\epsilon) - A(x,\epsilon) \wedge A(x,\epsilon) = 0. \tag{33}$$

Using the definition of the differential operator d and the antisymmetry of the wedge product, this can be rewritten as a set of differential relations among the matrices $A_{x_i}(x,\epsilon)$:

$$\partial_{x_i} A_{x_j} - \partial_{x_j} A_{x_i} - A_{x_i} A_{x_j} + A_{x_j} A_{x_i} = 0 \qquad \forall i,j \quad , \tag{34}$$

which can be used to check the correctness of the differential equations.

2. *Euler scaling relation*
Since Feynman integrals are homogeneous functions in the external scales x_i (see *Prop. 3* of *Section 2.1*), then the derivatives $\partial_{x_i} I(x;\nu;\epsilon)$ will not be independent, even if the

[8] Recall that an integral can only couple to integrals with the same or smaller number of propagators, since derivatives cannot produce new denominators.

scales x_i are independent. In fact, by Euler's theorem for homogeneous functions, we can write for a generic Feynman integral:

$$\sum_{i=1}^{s} x_i \frac{\partial}{\partial x_i} I(x;\nu;\epsilon) = \frac{\alpha}{2} I(x;\nu;\epsilon). \tag{35}$$

If we now change variables $(x_1, ..., x_s) \to (y_1, ..., y_s) = (x_1/x_s, ..., x_{s-1}/x_s, x_s)$, we have:

$$\sum_{i=1}^{s} x_i \frac{\partial}{\partial x_i} = \sum_{i=1}^{s-1} x_i \frac{\partial}{\partial x_i} + x_s \frac{\partial}{\partial x_s} = \sum_{i=1}^{s-1} y_i \frac{\partial}{\partial y_i} + y_s \Big(\frac{\partial y_s}{\partial x_s} \frac{\partial}{\partial y_s} + \sum_{i=1}^{s-1} \frac{\partial y_i}{\partial x_s} \frac{\partial}{\partial y_i} \Big) = y_s \frac{\partial}{\partial y_s}. \tag{36}$$

Plugging in eq. (35) and solving the resulting differential equation, we get:

$$I(x;\nu;\epsilon) = y_s^{\alpha/2} \hat{I}(y_1, ..., y_{s-1};\nu;\epsilon) = x_s^{\alpha/2} \hat{I}(x_1/x_s, ..., x_{s-1}/x_s;\nu;\epsilon). \tag{37}$$

This means that the non trivial functional dependence of $I(x;\nu;\epsilon)$ is only in the ratios x_i/x_s ($1 \leq i \leq s-1$), or equivalently we can always set one scale (e.g. x_s) to one and take derivatives only with respect to the other $(s-1)$ scales. This also tells us that a one-scale integral has a trivial scale dependence, so it cannot be computed with the method of differential equations, but we need to employ other techniques, e.g. direct integration using Feynman parameters.

Eq. (35) can be rewritten for a basis of master integrals as:

$$\sum_{i=1}^{s} x_i \frac{\partial}{\partial x_i} \vec{I}(x,\epsilon) = \frac{1}{2} \big[\vec{I}(x,\epsilon)\big] \vec{I}(x,\epsilon), \tag{38}$$

where $\big[\vec{I}(x,\epsilon)\big] = diag\Big(\big[I_1(x,\nu^1,\epsilon)\big], ..., \big[I_N(x,\nu^N,\epsilon)\big] \Big)$ is the diagonal matrix made up of the mass dimensions of the MIs. This is known as the Euler scaling relation and provides another check for the correctness of the differential equations.

3. *Change of basis*
As already said, the basis of MIs is not unique; in fact we can always perform a change of basis from $\vec{I}(x,\epsilon)$ to $\vec{J}(x,\epsilon)$ by setting:

$$\vec{J}(x,\epsilon) = R(x,\epsilon)\vec{I}(x,\epsilon), \tag{39}$$

where $R(x,\epsilon)$ is some invertible matrix. We assume it to be rational in ϵ, and we call the transformation rational/ algebraic/ transcendental depending on whether the matrix entries of $R(x,\epsilon)$ are rational/ algebraic/ transcendental in x. We want to see how our differential equations (30) behave under a change of basis; plugging (39) in them we get:

$$d\vec{J}(x,\epsilon) = A'(x,\epsilon)\vec{J}(x,\epsilon), \tag{40}$$

where:

$$A'(x,\epsilon) = R(x,\epsilon)\big[A(x,\epsilon)R^{-1}(x,\epsilon) - dR^{-1}(x,\epsilon)\big]. \tag{41}$$

We can see that the new basis satisfies differential equations of the same form as (30), whose matrix $A'(x,\epsilon)$ is related to the original matrix $A(x,\epsilon)$ by the transformation (41). Equivalently, the single differential equations (29) will now take the form:

$$\partial_{x_i}\vec{J}(x,\epsilon) = A'_{x_i}(x,\epsilon)\vec{J}(x,\epsilon), \tag{42}$$

where:

$$A'_{x_i}(x,\epsilon) = R(x,\epsilon)A_{x_i}(x,\epsilon)R^{-1}(x,\epsilon) + [\partial_{x_i}R(x,\epsilon)]R^{-1}(x,\epsilon). \tag{43}$$

It is interesting to notice that this transformation is similar to the gauge transformation for a non-abelian gauge potential: $A_\mu \to A'_\mu = UA_\mu U^{-1} - (\partial_\mu U)U^{-1}$.

Note also that, while $A(x,\epsilon)$ is a matrix of rational one-forms (as a consequence of IBPs), if the transformation (39) is not rational, then the matrix entries of $A'(x,\epsilon)$ will not be rational. Thus, it is useful to give the following definition: an IBP-basis is a basis related to the original basis of integrals in which we solved IBPs by a rational transformation; in such a basis, the differential equations will still involve rational coefficients.

3.3 Canonical form of differential equations

We want to perform a change of the basis of MIs, so that the differential equations take a form which is as simple as possible. Let us state the following conjecture [23], which has been supported by all multi-loop computations performed up to now:

Conjecture 1
For every IBP-basis $\vec{I}(x,\epsilon)$, satisfying the differential equation (30), there exists a (possibly transcendental) transformation to a new basis $\vec{J}(x,\epsilon)$, described by (39), such that:

$$d\vec{J}(x,\epsilon) = A'(x,\epsilon)\vec{J}(x,\epsilon) \qquad \text{with} \quad A'(x,\epsilon) = \epsilon\tilde{A}(x), \tag{44}$$

where $\tilde{A}(x)$ is a matrix of one-forms with at most logarithmic singularities.[9]

Such a basis, where the ϵ-dependence factorizes in the differential equations, is called a canonical basis and the corresponding differential equations (44) are said to be in canonical form.

The simplest possibility is to have a canonical dlog-form:

$$\tilde{A}(x) = \sum_i A_i \, d\log p_i(x), \tag{45}$$

[9] Equivalently, we can say that the matrices $A'_{x_i}(x,\epsilon)$ have at most single poles.

where A_i are constant matrices and $p_i(x)$ are algebraic functions. However, it is not always possible to cast differential equations in this form.

Now we want to describe how canonical differential equations can be solved. Let's consider a system of differential equations in canonical form:

$$d\vec{J}(x,\epsilon) = \epsilon \tilde{A}(x)\vec{J}(x,\epsilon) \tag{46}$$

and suppose that we already know the value of $\vec{J}(x_0,\epsilon)$ at a certain point $x = x_0$, which provides a valid boundary condition for our problem. The value of $\vec{J}(x,\epsilon)$ at point x can be obtained by parallel transporting the solution from x_0 to x along a path γ connecting the two points; the independence of the result on the specific chosen path (homotopy invariance) is guaranteed by the integrability condition (33), which for systems in canonical form reduces to the simpler conditions:

$$d\tilde{A}(x) = 0 \qquad , \qquad \tilde{A}(x) \wedge \tilde{A}(x) = 0, \tag{47}$$

showing in particular that $\tilde{A}(x)$ must be a matrix of closed one-forms.
The precise criterion for homotopy invariance will be discussed in *Section 4.1.2*.

The solution of (46) can be formally written in terms of a path-ordered exponential:

$$\vec{J}(x,\epsilon) = \mathbb{P}\exp\left[\epsilon \int_\gamma \tilde{A}(x')\right]\vec{J}(x_0,\epsilon). \tag{48}$$

In particular, the path-ordered exponential provides a matrix-valued general solution to the system of differential equations, the value of $\vec{J}(x_0,\epsilon)$ fixes the boundary conditions.

Coming back to our analogy with gauge theories, if we think of the matrix $\tilde{A}(x)$ as the analogous of a gauge potential, then the path-ordered exponential represents a Wilson line connecting points x_0 and x along γ; the independence on the path is a consequence of having a vanishing curvature tensor, as we can read from the integrability condition written in the form of (34).

However, as previously mentioned, we are never interested in finding a global solution in ϵ, but we just want to compute the first coefficients of its Laurent expansion around $\epsilon = 0$: the main advantage of the canonical form is that it makes this task particularly easy. Indeed, plugging the ansatz:[10] $\vec{J}(x,\epsilon) = \sum_{k\geq k_0} \vec{J}^{(k)}(x)\epsilon^k$ in the canonical DEs (46) and solving it order by order in ϵ, we can easily see that the lowest order (nonzero) coefficient $\vec{J}^{(k_0)}$ is a constant vector, which can be fixed by using the boundary conditions; each new order is determined from the previous one by an additional integration (together with the boundary conditions):

$$\begin{cases} \vec{J}^{(k_0)}(x) = const \\ \vec{J}^{(k)}(x) = \vec{J}^{(k)}(x_0) + \int_{x_0}^{x} \tilde{A}(x)\vec{J}^{(k-1)}(x) \qquad k > k_0 \end{cases} . \tag{49}$$

[10] Here we are assuming the expansion to start from a certain index k_0, whose value is determined from the boundary conditions.

This tells us that, at every order in ϵ, the Laurent coefficients can be expressed in terms of "iterated integrals", whose precise mathematical definition will be given in the next chapter.

Note that the same conclusion could have been obtained by expanding the path-ordered exponential appearing in the formal solution (48). Moreover, one can exploit the homotopy invariance to choose a path which makes the iterated integrals easy to evaluate in terms of known classes of special functions: typically one chooses a piecewise-constant path, i.e. a composition of segments where all variables except one are constant, producing in this way iterated integrals in one variable.

3.4 Cuts and differential equations

Cuts of Feynman integrals play a crucial role in understanding their analytic structure and revealing physical discontinuities associated with unitarity. In this section, we first explain how they can be easily computed using Baikov representation; then we discuss their relations with differential equations: cuts satisfy the same DEs as the original MIs, maximal cuts give a solution of homogeneous equations and contain the leading singularities. We mainly follow [48].

Cuts of a Feynman integral are defined as the integrals obtained from it by putting a subset of its propagators on-shell. In the momentum representation, cutting the j-th propagator clearly corresponds to performing the replacement:

$$\frac{1}{q_j^2 - m_j^2} \to 2\pi i\, \delta\big(q_j^2 - m_j^2\big), \tag{50}$$

then one has to compute the remaining momentum-space integral. Particularly important is the maximal cut, where we cut all the propagators whose exponents ν_j are positive.

The computation of cuts becomes much easier in the Baikov representation (18), as the integration variables z_j are the inverse propagators; therefore, cutting propagators turns the original integral into a lower-dimensional one. In fact, in this representation, the replacement (50) reads:

$$\frac{1}{z_j} \to 2\pi i\, \delta(z_j). \tag{51}$$

For $\nu_j = 1$, this corresponds to removing the integration over z_j, setting $z_j = 0$ in the Baikov polynomial. In formulas:

$$I = A \int_{\mathcal{C}} \Big(\prod_{i=1}^{P} dz_i \Big) \frac{\big[\mathcal{B}(z_1, ..., z_j, ..., z_P)\big]^{\frac{D-L-E}{2}}}{\prod_{i=1}^{P} z_i^{\nu_i}}, \tag{52}$$

$$Cut_{e_j} I = (2\pi i) A \int_{\mathcal{C}} \Big(\prod_{\substack{i=1 \\ i\neq j}}^{P} dz_i \Big) \frac{\big[\mathcal{B}(z_1, ..., z_{j-1}, 0, z_{j+1}, ..., z_P)\big]^{\frac{D-L-E}{2}}}{\prod_{\substack{i=1 \\ i\neq j}}^{P} z_i^{\nu_i}}, \tag{53}$$

where I is the original integral, $Cut_{e_j} I$ is the one with cut j-th propagator, A is the usual prefactor appearing in the Baikov representation formula (18).

We can also interpret the result of the integration over the variable z_j, corresponding to the cut propagator, as the residue of the original integrand at $z_j = 0$, or equivalently as its integral along a small[11] anti-clockwise γ_j around $z_j = 0$. In fact, writing the original Feynman integral as $I = \int_{\mathcal{C}} (\prod_i dz_i) \frac{f(z)}{z_j}$, where $f(z)$ is regular at $z_j = 0$, we have for the integral over z_j:

$$2\pi i \int dz_j f(z) \delta(z_j) = 2\pi i f(z)\big|_{z_j=0} = 2\pi i \, Res\Big(\frac{f(z_j)}{z_j}\Big)\Big|_{z_j=0} = \oint_{\gamma_j} dz_j \frac{f(z)}{z_j}, \tag{54}$$

where we treated f as a function of only z_j and in the last step we used the residue theorem.

This implies that a cut Feynman integral in the Baikov representation can be interpreted as the original Feynman integral with a modified integration domain.[12] This observation has an important consequence connected to the differential equations. One can argue that the cut master integrals satisfy the same differential equations as the original master integrals [38], based on the following:

Theorem 1
Let $\vec{I}$ denote a basis of Feynman master integrals satisfying the differential equations $d\vec{I} = A\vec{I}$. Suppose $\vec{I}'$ is another set of integrals, defined by the same integrands as $\vec{I}$ in Baikov representation, but integrated over a different contour $\mathcal{C}'$ in Baikov space. The deformed integrals $\vec{I}'$ will satisfy the same differential equations as $\vec{I}$, i.e. $d\vec{I}' = A\vec{I}'$, provided that the new integration contour $\mathcal{C}'$ satisfies the following requirements:

1. IBPs still hold, i.e. $\int_{\mathcal{C}'} d\omega = \int_{\partial\mathcal{C}'} \omega = 0$;
2. the variation of the integral with respect to the kinematic variables comes entirely from the integrand, i.e. $\frac{\partial}{\partial x} \int_{\mathcal{C}'} \omega = \int_{\mathcal{C}'} \frac{\partial \omega}{\partial x}$;
3. the symmetries among the integrals are preserved.[13]

[11] By "small", here we mean that it must not enclose any singularities other than $z_j = 0$.

[12] This is the intersection of the original domain $\mathcal{C}$ with the hyperplane $z_j = 0$.

[13] For example, for the bubble integral with equal internal masses we have the symmetry $I_{\nu_1\nu_2} = I_{\nu_2\nu_1}$; we require the new integration contour $\mathcal{C}'$ to be such that $I'_{\nu_1\nu_2} = I'_{\nu_2\nu_1}$.

Another consequence of (54) is that the cut of the j-th propagator of a Feynman integral with $\nu_j \leq 0$ vanishes, since $z_j = 0$ is not a singularity of the integrand, so the corresponding residue vanishes. On the other side, a Feynman integral with $\nu_j \leq 0$ belongs to a sub-sector of the family where the j-th propagator is pinched. Therefore, we can say that cutting the j-th propagator has the effect of setting all sub-sectors where this propagator is pinched to zero. In particular, the maximal cut will set all the subsectors to zero.

This implies that the differential equations are still valid for the maximal cuts, but they restrict to their homogeneous part. We can say that the maximal cut integrals are a solution of the homogeneous equations for the top sector integrals.

On the other side, from what we said, it is clear that in Baikov representation the maximal cut can be computed as the residue of the Feynman integral at the global pole, where all the denominators vanish; therefore, at $o(\epsilon^0)$, it gives the leading singular behavior of the integral, often referred to as the leading singularity. Extracting the leading singularities is a key step of the procedure to find a canonical basis, as we will explain in the next section.

3.5 How to find a canonical form

From the discussion in *Section 3.3*, the great usefulness of working in a canonical basis should be clear. Despite the existence of a canonical basis for a general problem is still conjectural, a systematic procedure to cast differential equations in canonical form has been recently proposed [16, 22]. This procedure, that we will largely employ in this work, is based on five main steps, whose basic ideas are reviewed in the following paragraphs.

3.5.1 Choice of a good initial basis

Assuming that for a given family a canonical basis exists, it will always be possible, in principle, to reach it starting from any other basis, by performing a proper rotation. However, for this procedure to work, the initial basis must be chosen carefully, according to the following criteria:

- Avoid integrals with power-like UV or IR divergencies or such to generate differential equations whose coefficients have poles in ϵ.
- For sectors with one master integral, try to select a candidate with unit leading singularities.
- For sectors with more masters, first focus on the homogeneous equation at $\epsilon = 0$, in order to determine the underlying geometry, which also tells us how many masters can be decoupled.

- If all the integrals are decoupled, try to choose them with unit leading singularities. If n of the m masters in the sector are coupled, first choose the remaining $m-n$, such to make the decoupling manifest.

- Regarding the coupled masters, the first is chosen to be a series of dlog forms corresponding to the holomorphic differential of the first kind of that geometry. The remaining masters in the coupled block are chosen to be linear combinations of derivatives of the first one with respect to the internal masses.

3.5.2 Rotation by the inverse of W^{ss}

Now the crucial step of the procedure comes. We know that, in the polylogarithmic case, the canonical integrals at $\epsilon = 0$ are iterated integrals of pure (see *Section 4.4*) dlog forms, i.e. with constant leading singularities. Therefore, for a polylogarithmic geometry and decoupled masters in the top sector, a canonical basis can be simply found by dividing the original masters by their leading singularities.[14]

The idea is to generalize this procedure for coupled masters and more complicated geometries. In the previous section, we have seen that the leading singularity is contained in the maximal cuts or equivalently in the solution of the homogeneous equations in the top sector at $\epsilon = 0$.

Therefore, in our initial basis, we have to compute the matrix W of solutions of the homogeneous equations at $\epsilon = 0$ for every coupled block in the top sector: this matrix W is called Wronskian matrix or period matrix. Then, we split W into a semi-simple part W^{ss} and a unipotent part W^u:

$$W = W^{ss} \cdot W^u. \tag{55}$$

The only requirements are that the semi-simple part is invertible and the unipotent one satisfies a unipotent system of differential equations, i.e.:

$$dW^u = \Big(\sum_i U_i(x) dx_i \Big) W^u, \tag{56}$$

where $U_i(x)$ are nilpotent matrices. This splitting is not unique in general: we perform it in such a way that W^{ss} is lower-triangular, while W^u is upper-triangular with constant diagonal entries normalized to one.

The semi-simple part W_{ss} can be seen as a "matrix version" of the leading singularity; therefore, by analogy with the decoupled case, we have to rotate the basis in the coupled block with the inverse of W^{ss}.

[14] This is also what we did in the previous step to find a good initial basis.

3.5.3 Going to an upper triangular ϵ-form

Now, we can easily cast the matrix of the DEs in an upper triangular ϵ-form, which means that the non ϵ-factorized terms will only appear below the diagonal of the new matrix. We can reach this form by simply adjusting some ϵ factors and swapping the positions of some master integrals in the basis.

3.5.4 Cleaning up the homogeneous blocks

The next step achieves full ϵ-factorization within each homogeneous block. This is done by shifting the master integrals which generate non ϵ-factorized homogeneous equations, by other masters in the same sector. In the simplest cases, this procedure amounts to removing total derivatives of the functions introduced in the rotation with the inverse of W^{ss}. In more involved situations, however, it becomes necessary to introduce new functions in terms of iterated integrals built from the same set of objects appearing in the inverse rotation.

3.5.5 Cleaning up the inhomogeneous blocks

As a last step, we need to ϵ-factorize the inhomogeneous blocks of the matrix of DEs. This is achieved by shifting the MIs of a given sector by integrals in lower sectors. As for the previous step, also here, the introduction of new functions might be required.

3.6 Boundary conditions

Fixing the boundary conditions is a fundamental step in the computation of Feynman integrals via the method of differential equations. It is well known that in order to fix all integration constants for a system of n first-order DEs (or equivalently for an nth-order DE), we need to impose n boundary conditions.

A possibility is to compute analytically the master integrals at some specific kinematic point where they take a simple form; however, in many cases, one can obtain the boundary information simply by imposing some physical consistency conditions without any need of performing a separate calculation. For this latter approach, we need to look at the behavior of the integrals near the singular points of the DEs: in fact, it is well known that the solutions of a DE can have at most (but not necessarily) the singularities of the DE. We know that singularities for an amplitude come from cuts,[15] i.e. internal propagators going on shell. It may happen that a singular point for the differential equation is not singular for a specific MI; in that case the boundary condition is simply provided by the regularity condition at that point: in practice, we can fix some

[15] In particular, one can show that an amplitude can develop a pole when a single-particle goes on shell, a branch-cut when two or more particles go on-shell.

integration constants by requiring the singular part of the general solution to vanish. This is just an example, there are other physical conditions one can exploit to fix the boundaries even at a singular point. Another possibility is to compute numerically the MIs at one point.

4 Special numbers and functions in FIs

In this chapter, we review the mathematical structures — special numbers and functions — that appear in the analytic expressions of Feynman integrals. We begin with a detailed overview of iterated integrals and their properties, then state a theorem that constrains the types of transcendental structures admissible in such integrals. Finally, we focus on two key classes of iterated integrals relevant to Feynman integrals: multiple polylogarithms (MPLs) and integrals over elliptic curves. We follow mainly [14], [2] and [50].

4.1 Iterated integrals

As noted in the previous chapter, the Laurent expansion of Feynman integrals naturally gives rise to iterated integrals. In this section, we want to study their mathematical properties in detail.

4.1.1 Definition and basic properties

Def. 1 (Iterated integral)
Consider a geometric space X with local coordinates $\xi = (\xi_1, ..., \xi_s)$. Let $\gamma : [0, 1] \to X$ be a curve on X, and $\omega_1, ..., \omega_n$ be one-forms on X. We define the iterated integral of $\omega_1 ... \omega_n$ on γ as:

$$\begin{aligned} \int_\gamma \omega_1 ... \omega_n = \int_{0 \le t_1 \le ... \le t_n \le 1} f_1(t_1) dt_1 ... f_n(t_n) dt_n = \\ = \int_0^1 dt_n f_n(t_n) \int_0^{t_n} dt_{n-1} f_{n-1}(t_{n-1}) ... \int_0^{t_2} dt_1 f_1(t_1), \end{aligned} \tag{57}$$

with $\int_\gamma () = 1$, and $f_i : \mathbb{C} \to \mathbb{C}$ defined as the pull-back of ω_i along γ, i.e. $\gamma^* \omega_i = \omega_i \circ \gamma = f_i(t_i) dt_i$. We refer to the one-forms ω_i as letters and to $\omega_1 ... \omega_n$ as a word of length n; the set of all independent letters is called an alphabet.

Let us now enumerate without proofs the main properties of iterated integrals:

- Independence on the parametrization of the path;
- Linearity:

$$\int_\gamma (\alpha \omega_1 ... \omega_n + \beta \omega'_1 ... \omega'_m) = \alpha \int_\gamma \omega_1 ... \omega_n + \beta \int_\gamma \omega'_1 ... \omega'_m; \tag{58}$$

- Path composition:
  If $\gamma_1, \gamma_2 : [0,1] \to X$ are two paths s.t. $\gamma_1(1) = \gamma_2(0)$, then we have:

$$\int_{\gamma_1 \circ \gamma_2} \omega_1 ... \omega_n = \sum_{k=0}^{n} \int_{\gamma_1} \omega_1 ... \omega_k \cdot \int_{\gamma_2} \omega_{k+1} ... \omega_n; \tag{59}$$

- Path reversal:

$$\int_{\gamma^{-1}} \omega_1 ... \omega_n = (-1)^n \int_{\gamma} \omega_n ... \omega_1, \tag{60}$$

  where $\gamma^{-1}(t) = \gamma(1-t)$ is the reversal of path γ;

- Shuffle product:

$$\int_{\gamma} \omega_1 ... \omega_n \cdot \int_{\gamma} \omega'_1 ... \omega'_m = \int_{\gamma} \omega_1 ... \omega_n \sqcup\!\sqcup \omega'_1 ... \omega'_m, \tag{61}$$

  where the shuffle product $\sqcup\!\sqcup$ is defined recursively as:

$$\begin{aligned} &(\omega_1 ... \omega_n) \sqcup\!\sqcup (\omega'_1 ... \omega'_m) = \\ &= \omega_1 \big[(\omega_2 ... \omega_n) \sqcup\!\sqcup (\omega'_1 ... \omega'_m)\big] + \omega'_1 \big[(\omega_1 ... \omega_n) \sqcup\!\sqcup (\omega'_2 ... \omega'_m)\big] \\ &\text{with} \qquad (\omega_1 ... \omega_n) \sqcup\!\sqcup () = () \sqcup\!\sqcup (\omega_1 ... \omega_n) = (\omega_1 ... \omega_n). \end{aligned} \tag{62}$$

  One can easily see from this definition that the shuffle product of two words gives the sum of all possible permutations of the letters preserving the internal ordering of each word, e.g.:

$$\begin{aligned} \omega_1\omega_2 \sqcup\!\sqcup \omega_3\omega_4 = \omega_1\omega_2\omega_3\omega_4 + \omega_1\omega_3\omega_2\omega_4 + \omega_1\omega_3\omega_4\omega_2 + \\ + \omega_3\omega_1\omega_2\omega_4 + \omega_3\omega_1\omega_4\omega_2 + \omega_3\omega_4\omega_1\omega_2. \end{aligned} \tag{63}$$

4.1.2 Homotopy invariance

In *Section 3.3*, we claimed that the solution of differential equations for MIs are homotopy invariant functions as a consequence of the integrability condition. Here, we want to give a precise mathematical definition of homotopy invariance for iterated integrals and a necessary and sufficient condition for it, which we will find to be equivalent to the integrability condition.

Def. 1 (Homotopic paths)
Two paths $\gamma_1, \gamma_2 : [0,1] \to X$, having the same extrema $\gamma_1(0) = \gamma_2(0) = x_0$, $\gamma_1(1) = \gamma_2(1) = x_1$, are said to be homotopic if there exists a map $\phi : [0,1] \times [0,1] \to X$ suh that:
(i) $\phi(0,t) = \gamma_1(t), \quad \phi(1,t) = \gamma_2(t) \qquad \forall\, 0 \leq t \leq 1;$

(ii) $\phi(s,0) = x_0, \qquad \phi(s,1) = x_1 \qquad \forall\, 0 \leq s \leq 1.$

Def. 2 (Homotopy invariant function)
A function $f(\gamma)$ is said to be homotopy invariant if, $\forall \gamma_1 \sim \gamma_2$, we have: $f(\gamma_1) = f(\gamma_2)$. In other words, the function does not depend on the details of the path, but only on its endpoints.

Iterated integrals are in general NOT homotopy invariant, as we can see from the following example.

Example
Consider $X = \mathbb{R}^2$ and the family of paths $\gamma_{r,s} : [0,1] \to X$ defined by: $\gamma_{r,s}(t) = (t^r, t^s)$ for $r, s > 0$. All of them have endpoints $(0,0)$ and $(1,1)$. Let us compute the iterated integral of $\omega_1\omega_2$, with $\omega_1 = dx$ and $\omega_2 = dy$, along a generic path of the family:

$$\int_{\gamma_{r,s}} \omega_1\omega_2 = \int_{0\leq t_1\leq t_2\leq 1} r t_1^{r-1} s t_2^{s-1} dt_1 dt_2 = rs \int_0^1 dt_2 t_2^{s-1} \int_0^{t_2} dt_1 t_1^{r-1} = \frac{s}{r+s}. \quad (64)$$

The result depends on the path (it depends on the specific values of r and s), hence the integral is not homotopy invariant.

Now let us give an homotopy invariance condition for iterated integrals. We first start from the simple case of an iterated integral of length $n = 1$; let ω be a one-form and γ_1, γ_2 be two homotopic paths. We have:[16]

$$\int_{\gamma_1} \omega = \int_{\gamma_2} \omega \iff \int_{\gamma_1\gamma_2^{-1}} \omega = 0. \quad (65)$$

Note that $\gamma_1\gamma_2^{-1}$ is a closed path, so if we consider a domain D such that $\partial D = \gamma_1\gamma_2^{-1}$, by Stokes' theorem:

$$\int_{\gamma_1\gamma_2^{-1}} \omega = \int_{\partial D} \omega = \int_D d\omega_1. \quad (66)$$

For the iterated integral of ω to be homotopy invariant, this last integral must vanish for all paths γ_1 and γ_2, which happens if and only if ω_1 is closed, i.e. $d\omega_1 = 0$. So, for n=1, the necessary and sufficient condition for homotopy invariance is that the one-form is closed. This result can be generalized to higher lengths: the iterated integral of a linear combination ω of words is homotopy invariant iff $D\omega = 0$, where the action of the differential D on a word of one-forms is defined by:

$$D(\omega_1...\omega_n) = \sum_{i=1}^{n} \omega_1...(d\omega_i)...\omega_n + \sum_{i=1}^{n} \omega_1...(\omega_i \wedge \omega_{i+1})...\omega_n. \quad (67)$$

[16] The equivalence follows from path composition and path reversal properties.

This is equivalent to the integrability condition (33) for the differential equations.[17]

Moreover, if all one-forms appearing in the word are closed (as for dlogs), then on the rhs of (67) we are left only with the second term. This is the case for iterated integrals arising from differential equations in canonical form: the first of the integrability conditions (47) requires closure, the second one guarantees homotopy invariance.

4.1.3 Regularization

As previously said, when solving the differential equations for Feynman integrals, it is often convenient to fix the boundary condition at a singular point of the DEs. However, if an end-point of the path is singular, the iterated integrals arising from the DEs will typically be divergent. Therefore, we need to define a regularized version, that removes divergencies, but preserves the properties of iterated integrals and coincides with the standard definition when the integral is convergent.

For simplicity, we only consider the case in which all singularities are logarithmic and the space X is one-dimensional. Note that this assumptions are not so restrictive: in fact for a system of differential equations in the canonical form all singularities are logarithmic; moreover, if the space X is not one-dimensional, we can always split it into piece-wise constant paths, so that on each of them the problem becomes one-dimensional. For example, let us assume that $\gamma : [0,1] \to [0,x]$ and that some one-forms ω_i have a logarithmic singularity at the origin ($\omega_i = a_i \, dlog\xi + ...$), with no other singularities in the integration contour. The regularized version of $\int_\gamma \omega_1 ... \omega_n = \int_0^x \omega_1 ... \omega_n$ is defined via the following steps:

1. Introduce a small cut-off ε and replace:

$$\int_0^x \omega_1 ... \omega_n \longrightarrow \int_\varepsilon^x \omega_1 ... \omega_n. \tag{68}$$

2. Having only logarithmic singularities, in the limit $\varepsilon \to 0$:

$$\lim_{\varepsilon \to 0} \int_\varepsilon^x \omega_1 ... \omega_n = \sum_{k=0}^{n} I_k(x) \log^k \varepsilon + o(\varepsilon). \tag{69}$$

3. The regularized version is defined by throwing away all logs:

$$\int_\gamma^{[reg]} \omega_1 ... \omega_n = I_0(x). \tag{70}$$

[17] This shows that iterated integrals appearing in the solution are homotopy invariant.

This procedure is called shuffle-regularization, it is easy to check that it satisfies all our requirements. The simplest example of application is the following:

Example

$$\int_0^x \frac{d\xi}{\xi} \longrightarrow \int_\varepsilon^x \frac{d\xi}{\xi} = \log x - \log \varepsilon \longrightarrow \log x. \tag{71}$$

Therefore: $\int_\gamma^{[reg]} \frac{d\xi}{\xi} = \log x$.

Already from this simple example, it is clear that the result depends on our choice of "regularization scheme"; indeed, if we rescale the cut-off, i.e. $\varepsilon \to v\varepsilon$, we get a different result: $\int_\gamma^{[reg]} \frac{d\xi}{\xi} = \log x - \log v$. However, when solving the DEs, the boundary conditions will also depend on the choice of v in such a way that this dependence cancels in the final result for the integral, as it has to be.

4.1.4 Linear independence

An important property of iterated integrals is that, under some assumptions, they are linearly independent functions. This is particularly useful in the context of Feynman integrals, because it leads to shorter analytic expressions that are free of hidden cancellations.

Let us first define linear (in)dependence for one-forms:

Def

The one-forms ω_i are said to be linearly dependent over an algebra of functions $\mathcal{C}$, if there exists a function $f \in \mathcal{C}$ and some constants $\alpha_i \neq 0$ such that:

$$\sum_i \alpha_i \omega_i = df. \tag{72}$$

They are said linearly independent if instead (72) holds only for $\alpha_i = 0 \quad \forall i$.

It is possible to prove that iterated integrals are linearly independent over $\mathcal{C}$ as functions, if and only if they involve one-forms that are linearly independent over $\mathcal{C}$.

4.2 Transcendentality and periods

Before stating a general theorem that answers our question about the kind of numbers and functions appearing in the results of Feynman integrals, we need to recall some basic definitions.

Def. 1 (Algebraic and transcendental numbers/functions)
A complex number is called algebraic over $\mathbb{Q}$, if it is a zero of some polynomial with rational coefficients; the set of algebraic numbers is denoted by $\overline{\mathbb{Q}}$. A complex number that is not algebraic is called transcendental. These definitions can be naturally extended to functions.

To prove that a number is transcendental we can use the following:

Lemma (Hermite-Lindelmann)
Let z be a nonzero complex number. Then either z or e^z is transcendental.

This implies in particular that: e, π, π^n ($n \in \mathbb{N}$), ζ_{2n}, $\log q$ ($q \in \overline{\mathbb{Q}}$) are transcendental numbers.

We can define a class of numbers, called periods, that lie in between algebraic and transcendental numbers:

Def. 2 (Periods)
A complex number is called a period if both its real and imaginary parts can be written as integrals of an algebraic function with algebraic coefficients over a domain defined by polynomial inequalities with algebraic coefficients.

e.g.: $q \in \overline{\mathbb{Q}}$, π, $\log z$ ($z \in \overline{\mathbb{Q}}$), $Li_2(z)$ ($z \in \overline{\mathbb{Q}}$) are periods.
Numbers that are conjectured not to be periods are: e, γ_E, $1/\pi$, $\log \pi$,...

Now we can state the following important theorem [5]:

Theorem (Bogner, Weinzierl)
Under suitable assumptions,[18] the coefficients of the Laurent expansion of a Feynman integral, normalized[19] as in (1), are periods.

We saw previously that the Laurent coefficients of FIs are expressed in terms of iterated integrals. The previous theorem motivates us to consider integrals which produce periods, therefore we have to start from an algebraic integrand: the simplest possibility is to start from a rational function. By integration, we can produce other rational functions, or a logarithm, when we integrate over a single pole. Iterating integrations, we can obtain rational functions, logarithms, but also new functions when we integrate

[18] All scalar products $p_i \cdot p_j$ have to be negative or zero, all internal masses positive and all ratios of invariants algebraic.

[19] We stress the fact that this normalization for FIs is chosen so that, when expanding in ϵ, the transcendental numbers which are not periods (like γ_E) exactly cancel.

over a single pole. These generalizations of the logarithm function are called multiple polylogarithms (MPLs), we will study them in detail in the next section.

4.3 Multiple Polylogarithms (MPLs)

As anticipated in the previous section, the simplest and most important class of iterated integrals that appears in the computation of Feynman integrals is that of Multiple Polylogarithms (MPLs). In this section, we want to study in details their properties.

4.3.1 Basic definitions and properties

MPLs are defined recursively as:

$$G(a_1,...,a_n;z)=\int_0^z \frac{dt}{t-a_1}G(a_2,...,a_n;t) \qquad with \quad G(;z)=1. \tag{73}$$

The vector $\vec{a}=(a_1,...,a_n)$ is called vector of singularities (or indices) of the MPL and the number of its elements is called transcendental weight of the MPL. By their definition, it is clear that MPLs are periods for algebraic arguments.

Note that, for $a_n=0$, the integral in (73) is divergent; we can regularize it as described in *Section 4.1.3*. In particular, this is equivalent to define in the case where all the a_i are vanishing:

$$G(\vec{0}_n;z)=\frac{1}{n!}\log^n z, \tag{74}$$

and then find regularized versions of the other MPLs with $a_n=0$ by using shuffle product, as explicitly shown in an example at the end of this paragraph.

We can see that MPLs contain logarithms and classical polylogarithms as special cases, in particular we have:

$$\begin{aligned} &i) \quad G(\vec{a}_n;z)=\frac{1}{n!}log^n\Big(1-\frac{z}{a}\Big),\\ &ii) \quad G(\vec{0}_{n-1},1;z)=-Li_n(z) \qquad \text{where} \quad \begin{cases} Li_1(z)=\int_0^z \frac{dt}{1-t}=-\log(1-z)\\ Li_n(z)=\int_0^z \frac{dt}{t}Li_{n-1}(z)=\sum_{k=1}^{\infty}\frac{z^k}{k^n} \end{cases}, \end{aligned} \tag{75}$$

which can be easily proved by induction.

As iterated integrals, MPLs satisfy all properties discussed in *Section 4.1*, including shuffle product:

$$G(a_1,...,a_{n_1};z)G(a_{n_1+1},...,a_{n_1+n_2};z)=\sum_{\sigma\in\Sigma(n_1,n_2)} G(a_{\sigma(1)},...,a_{\sigma(n_1+n_2)};z), \tag{76}$$

where $\Sigma(n_1, n_2)$ is the set of all shuffles of the $n_1 + n_2$ indices, i.e. the set of all permutations of these indices preserving the internal ordering of the vectors $(a_1, ..., a_{n_1})$ and $(a_{n_1+1}, ..., a_{n_1+n_2})$.
It is important to notice that shuffle product preserves the weight of MPLs: from a product of two MPLs (evaluated at the same point) with respective weights n_1 and n_2, we get a linear combination of MPLs of weight $n_1 + n_2$. We can say that MPLs with the shuffle product form a graded algebra, called shuffle algebra.

As mentioned above, we can use shuffle product for regularization; we can write MPLs with trailing zeroes in terms of others which have either rightmost index non-zero or all indices zeroes: the former are regular, the latter are regularized by (74). For example:

$$\begin{aligned} G(a,0,0;z) &= G(a;z)G(0,0;z) - G(0,0,a;z) - G(0,a,0;z) = \\ &= G(a;z)G(0,0;z) - G(0,0,a;z) - [G(0,a;z)G(0;z) - 2G(0,0,a;z)] = \\ &= G(0,0;z)G(a;z) + G(0,0,a;z) - G(0,a;z)G(0;z). \end{aligned} \tag{77}$$

4.3.2 Some other properties of MPLs

In the following, we will enumerate the main other properties satisfied by MPLs:

1. $G(a_1, ..., a_n; z)$ is logarithmically divergent when $z \to a_1$.

2. $G(a_1, ..., a_n; z)$ is analytic at $z = 0$ for $a_n \neq 0$, with $G(a_1, ..., a_n; 0) = 0$.

3. $G(a_1, ..., a_n; z)$, as a function of $z \in \mathbb{C}$, has brunch cuts at most for $Re(z) > Re(a_i) \quad \forall i$, but not necessarily.
   e.g.: $G(a, z) = \log\left(1 - \frac{z}{a}\right)$ has a branch cut from $z = Re(a)$ to $z = \infty$;
   $G(0, 1; z) = \int_0^z \frac{dt}{t} \int_0^t \frac{du}{u-1} = -Li_2(z)$ has a branch cut starting at $z = 1$, but there is no branch cut starting at $z = 0$.

4. For $a_n \neq 0$, there is a rescaling invariance:

$$G(a_1, ..., a_n; z) = G(\lambda a_1, ..., \lambda a_n; \lambda z), \qquad \text{for} \quad a_n \neq 0, \quad \lambda \in \mathbb{R}^*. \tag{78}$$

5. For $a_i \in \{-1, 0, 1\}$ MPLs reduce to harmonic polylogarithms (HPLs):

$$H(\vec{a}, z) = (-1)^p G(\vec{a}, z), \tag{79}$$

   where p is the number of elements in $\vec{a}$ that are equal to $(+1)$.

4.3.3 Functional relations and linear independence

It is conjectured that all functional relations among MPLs preserve the transcendental weight.

As already seen, we can find relations among MPLs in the same variable z by using shuffle product. However, if all the indices a_i in two MPLs are different, then no relations among them can be written, so they result to be linearly independent. In fact, if we think of MPLs as iterated integrals of linear combinations of words with letters $\omega_i = dlog(x - a_i)$, then it is clear that, for all a_i's different, these one-forms will be linearly independent over $\mathcal{C} = \mathbb{Q}$, according to the definition given in *Section 4.1.4*. Therefore, the iterated integrals (MPLs) constructed from them will also be linearly independent as functions.

This is true only if the MPLs are functions of the same variable z and this variable does not appear in the indices. Instead, if we consider MPLs of the same weight depending on different (but related) variables, it is possible to find some non-trivial relations among them. As an example, let us discuss the relation among MPLs with variables $x > 0$ and $-x$, which is very useful when performing analytical continuation of these functions.

We want to relate $G(...; y)$, where $y = -x + i\varepsilon$ (ε small positive real number), to $G(...; x)$. Restricting for simplicity the indices to only 1 and 0, we can proceed recursively on the weight. At weight $n = 1$, we have:

$$\begin{aligned} G(0; y) &= \log y = \log(-x + i\varepsilon) = \log x + i\pi = G(0; x) + i\pi, \\ G(1; y) &= \log(1 - y) = \log(1 + x) = G(-1; x). \end{aligned} \tag{80}$$

At weight $n = 2$ we have 4 different MPLs, two of them are very easy to compute:

$$\begin{aligned} G(0, 0; y) &= \frac{1}{2}\log^2 y = \frac{1}{2}(\log x + i\pi)^2 = G(0, 0; x) + i\pi G(0; x) - \frac{\pi^2}{2}, \\ G(1, 1; y) &= \frac{1}{2}\log^2(1 - y) = \frac{1}{2}\log^2(1 + x) = G(-1, -1; x). \end{aligned} \tag{81}$$

$G(0, 1; y)$ can be computed using the expression for $G(1; y)$. Indeed:

$$G(0, 1; y) = \int_0^{y=-x+i\varepsilon} \frac{dt}{t} G(1; t) \Longrightarrow \frac{\partial}{\partial x} G(0, 1; y) = \frac{1}{x} G(1; y) = \frac{1}{x} G(-1; x). \tag{82}$$

Integrating back:

$$G(0, 1; y) = \int_0^x \frac{dx'}{x'} G(-1; x') + c, \tag{83}$$

where c is fixed knowing that $G(0, 1; 0) = G(0, -1; 0) = 0$; therefore we get:

$$G(0, 1; y) = G(0, -1; x). \tag{84}$$

The last function $G(1,0;y)$ can be computed from $G(0,1;y)$ using the shuffle product:

$$\begin{aligned} &G(1,0;y) = G(1;y)G(0;y) - G(0,1;y) = \\ &= G(-1;x)[G(0;x) + i\pi] - G(0,-1;x) = i\pi G(-1;x) + G(-1,0;x). \end{aligned} \tag{85}$$

Repeating the same approach, it is possible to find relations among higher weight functions.

Thus, already from this simple example, a very important point emerges: when dealing with MPLs, if we understand functional relations for weight one functions (logs), then we can derive all functional relations at any weight iteratively.

4.4 Transcendental weight and canonical form

Now, we are going to introduce the important concept of transcendental weight, which is connected to the canonical form of differential equations.

Def. 1 Given a function f, which is a linear combination of iterated integrals of *dlog* forms, its transcendental weight $\mathcal{T}(f)$ is defined as the number of iterated integrations. Clearly, $\mathcal{T}(f_1 \cdot f_2) = \mathcal{T}(f_1) + \mathcal{T}(f_2)$.
E.g. : $\mathcal{T}(\log z) = 1, \qquad \mathcal{T}(Li_n(z)) = n, \qquad \mathcal{T}\big(G(a_1,...,a_n;z)\big) = n.$

This definition can be generalized to constants expressible as iterated integrals of *dlog* forms,
e.g.: $\mathcal{T}(\log c) = 1$ (for $c \neq 0,1$), $\mathcal{T}(\pi) = 1$ since $\log(-1) = \pm i\pi$, $\mathcal{T}\big(\zeta(n)\big) = n$.

In order to see the connection with the canonical form, we need to give two more definitions.

Def. 2 A function f is said to have uniform transcendental weight (UT function), if it is a sum of terms with the same transcendental weights.

A stronger property is that of purity.

Def. 3 A function f is pure if it has uniform transcendental weight and its transcendental weight is lowered by one via differentiation, i.e. $\mathcal{T}(df) = \mathcal{T}(f) - 1$.

For simplicity, let us focus on a case where the differential equations are in canonical dlog form. If the lowest-order Laurent coefficients of the MIs are (UT) constants of the same transcendental weight, then the higher-order ones, which are obtained by iterated integrations, will also have uniform transcendental weight. We can also make the canonical basis integrals pure functions by associating weight -1 to the dimensional regulator ϵ. In fact, from the canonical DEs (46), we have: $\mathcal{T}(d\vec{J}) = \mathcal{T}(\epsilon) + \mathcal{T}(\tilde{A}) + \mathcal{T}(\vec{J})$. Since $\mathcal{T}(\epsilon) = -1$ and $\mathcal{T}(\tilde{A}) = 0$ being $\tilde{A}$ a matrix of *dlog* forms, we get: $\mathcal{T}(d\vec{J}) = \mathcal{T}(\vec{J}) - 1$, as claimed.

4.5 Beyond Polylogarithms

In *Section 4.3* we studied MPLs, which are the most general[20] functions one can obtain by iterating integrations of rational differential forms $R(x)dx$ with a finite set of poles $\{a_1, ..., a_n, \infty\}$ on the punctured Riemann sphere, $\mathbb{CP}^1/\{a_1, ..., a_n, \infty\}$. We can extend this construction to more general geometries. In particular, a case that is relevant for physics is that of iterated integrals over an elliptic curve, that can be identified, as we will see, with a torus. In this section, we first introduce the concept of elliptic functions and elliptic curve and explore the connection between them; then we come back to the problem of defining iterated integrals on elliptic curves.

4.5.1 Elliptic functions

Let us start from some basic definitions [49].

Def. 1 An elliptic function $f(z)$ is a complex function which is:

(a) meromorphic, i.e. it has finitely many poles, but no branch-cuts;

(b) doubly periodic, i.e.: $f(z) = f(z + \omega_1) = f(z + \omega_2) \quad \forall z$, where $\omega_1, \omega_2 \in \mathbb{C}$ are two complex numbers linearly independent over $\mathbb{R}$ (i.e. $\tau = \frac{\omega_2}{\omega_1} \notin \mathbb{R}$) , called the two fundamental periods of f.

Def. 2 Let f be an elliptic function with fundamental periods $\omega_1, \omega_2 \in \mathbb{C}$. The set of points in the complex plane given by:

$$\Lambda(\omega_1, \omega_2) = \{m\omega_1 + n\omega_2 | m, n \in \mathbb{Z}\} \tag{86}$$

is called the period lattice. Clearly, all the points of this lattice are still periods of f. The parallelogram P of vertices $\{0, \omega_1, \omega_2, \omega_1 + \omega_2\}$ is called the period parallelogram of f.

Note that, due to its periodicity, an elliptic function is fully determined on $\mathbb{C}$ by specifying its values on the period parallelogram P. Moreover, identifying opposite sides of P yields a torus, denoted as $\mathbb{C}/\Lambda$, which is the natural domain for elliptic functions. In this sense, an elliptic function on $\mathbb{C}$ descends to a well-defined meromorphic function on the torus $\mathbb{C}/\Lambda$. Another important observation is that the shape of this torus does not depend on the specific values of ω_1 and ω_2, but only on their ratio $\tau = \frac{\omega_2}{\omega_1}$, called modulus. Therefore, we can always decide to rescale periods and define the period lattice of an elliptic function as: $\Lambda(1, \tau) \equiv \Lambda(\tau)$.

In the following, we state the main basic properties [49] of elliptic functions:

[20] More precisely, given any rational function $R(x)$, we can decompose it into partial fractions and express its iterated integrals in terms of MPLs.

Prop.1 For an elliptic function, the number of poles inside the period parallelogram equals the number of zeroes.

Prop.2 An elliptic function with no poles (or equivalently no zeroes) inside the period parallelogram is a constant.

Prop.3 Given an elliptic function f with period parallelogram P, the contour integral of f over ∂P vanishes: $\int_{\partial P} f(z)dz = 0$.

Cor. 1 The sum of residues of an elliptic f inside the period parallelogram P vanishes: $\sum_{z_0 \in P} Res\big[f(z)\big]\Big|_{z=z_0} = 0$.

Cor. 2 An elliptic function has at least 2 simple poles or a double pole inside the period parallelogram.

The simplest (and most important) example of an elliptic function is given by the Weierstrass $\wp$-function:
e.g.

$$\wp(z;\tau) := \wp(z) = \frac{1}{z^2} + \sum_{\lambda \in \Lambda(\tau)\setminus\{0\}} \left(\frac{1}{(z-\lambda)^2} - \frac{1}{\lambda^2} \right). \tag{87}$$

One can easily check that it satisfies the requirements of *Def. 1.* In fact, this function has only double poles at the lattice points, therefore is meromorphic. The second term in the sum guarantees uniform convergence; this property allows us to shift terms in the sum, which is crucial for proving periodicity.

An important property of this function, that we will use later on, is that it satisfies the following differential equation:

$$(\wp'(z;\tau))^2 = 4\wp^3(z;\tau) - g_2\wp(z;\tau) - g_3, \tag{88}$$

where $g_2, g_3 \in \mathbb{C}$ are determined by the periods of the Weierstrass $\wp$-function.

Another important result, which we will not prove, is that every elliptic function can be written as a rational function in $\wp(z;\tau)$ and $\wp'(z;\tau)$. This explains the central role of Weierstrass $\wp$-function in the theory of elliptic functions.

4.5.2 Elliptic curves

Now we want to introduce the concept of elliptic curve [43] and construct the corresponding Riemann surface; explore intuitively its relation with the elliptic functions previously introduced; in particular, we want to show how the Weierstrass $\wp$-function can be useful to parametrize an elliptic curve.

Let us start from the definition of an elliptic curve:
Def. An elliptic curve is an algebraic curve in $\mathbb{C}^2$ defined by:

$$E : \big\{(x,y) \in \mathbb{C}^2 : y^2 = P_4(x)\big\}, \tag{89}$$

where $P_4(x)$ is a polynomial of degree three or four in the complex variable x.
For example, let us assume for simplicity:

$$P_4(x) = \sqrt{(x-a_1)(x-a_2)(x-a_3)(x-a_4)} \quad with \quad a_i \in \mathbb{R}, \quad a_1 < a_2 < a_3 < a_4. \tag{90}$$

The function $y(x) = \sqrt{P_4(x)}$ is multivalued on the complex plane; our goal is to introduce a Riemann surface on which $y(x)$ becomes single-valued. We note that going aroung a single a_i results in a change of sign of the square root, while going around two of them returns the function to its original value. This motivates us to introduce two branch cuts: one between a_1 and a_2, the other between a_3 and a_4.
We then take two copies of the Riemann sphere (with these branch cuts), denoted $\mathcal{R}_+$ and $\mathcal{R}_-$, corresponding to the two possible values of $y(x) = \pm\sqrt{P_4(x)}$. Along each of the branch cuts, we "open" the slits in both sheets and glue them together crosswise: the upper edge of the cut on $\mathcal{R}_+$ is glued to the lower edge of the cut on $\mathcal{R}_-$, and vice versa. This gluing identifies points in such a way that the resulting surface accommodates a well-defined single-valued function. The resulting topological surface is a torus, i.e., a compact Riemann surface of genus one. This is the Riemann surface associated with the elliptic curve.

One can show that it is always possible to find a change of coordinates that puts the elliptic curve into the so called Weierstrass form [43]:

$$y^2 = 4x^3 - g_2 x - g_3, \qquad \text{with} \quad g_2, g_3 \in \mathbb{C}. \tag{91}$$

Note that this equation has the same form as the differential equation (88) for the Weierstrass $\wp$-function; in particular from the values of g_2 and g_3, we can reconstruct the periods of the corresponding function, that we can also rename as the periods of the elliptic curve E.

As prevously discussed, due to its periodicity, the function $\wp(z;\tau)$ can be interpreted as a function defined on the torus $\mathbb{C}/\Lambda(\tau)$. We can therefore create a correspondence between the points on this torus and the ones on the elliptic curve E via the mapping:

$$\phi : \mathbb{C}/\Lambda(\tau) \to E, \quad z \in \mathbb{C}/\Lambda(\tau) \to (x,y) = (\wp(z;\tau), \wp'(z,\tau)) \in E, \tag{92}$$

where we exploited the fact that the equation of the curve in the form (91) corresponds to the differential equation (88) satisfied by Weierstrass $\wp$-function.

The mapping (92) is invertible; in particular, the point z_0 of the torus, corresponding to the point $(x_0, y_0) \in E$, is given by the elliptic integral of the first kind:

$$z_0 = \int_\infty^{x_0} \frac{dx}{y(x)} = -\int_{x_0}^{\infty} \frac{dx}{\sqrt{4x^3 - g_2 x - g_3}}. \tag{93}$$

In fact: $\int_\infty^{x_0} \frac{dx}{y(x)} = \int_0^{z_0} \frac{\wp'(z;\tau)dz}{\wp'(z;\tau)} = z_0$, where we used that $x = \wp(z;\tau)$ has a pole at $z = 0$ and that $x_0 = \wp(z_0;\tau)$ from (92).

4.5.3 Integrals on elliptic curves

As discussed, iterated integrals of rational functions on the punctured Riemann sphere produce MPLs: in this case, the integrand is a meromorphic function on the punctured Riemann sphere, $\mathbb{CP}^1/\{a_1, ..., a_n, \infty\}$. On an elliptic curve, instead, the meromorphic functions are rational functions in (x, y) subject to the constraint (89), which defines the elliptic curve. The most general function with this property has the form:

$$f(x) = \frac{P_1(x) + P_2(x)y(x)}{Q_1(x) + Q_2(x)y(x)} = R_1(x) + \frac{1}{y(x)}R_2(x), \tag{94}$$

where $R_1(x)$ and $R_2(x)$ are rational functions in x, while $y(x) = \sqrt{P_4(x)}$. By integrating the first term over x, we get rational functions and logarithms as usual; by integrating the second one, we can get new functions. By partial fractioning this term, we can only get terms of the form: $\frac{x^m}{y}$ and $\frac{1}{y(x-c)^m}$, with $m \in \mathbb{N}$. The (infinitely many) integrals of all these expressions can be reduced to integrals of the following differential forms:

$$\omega_1 = \frac{dx}{y}, \quad \omega_2 = \frac{xdx}{y}, \quad \omega_3 = \frac{dx}{y(x-c)}, \quad \omega_4 = \frac{dx}{x-c}. \tag{95}$$

Let us analyze them in detail:

- ω_4 is just a *dlog* form, whose integral gives $\log(x - c)$.
- ω_1 is called elliptic differential of the first kind, or holomorphic differential, because it has no poles. Its integral can be expressed in terms of elliptic integrals of the first kind:
$$K(\lambda) = \int_0^1 \frac{dx}{\sqrt{(1-x^2)(1-\lambda x^2)}}. \tag{96}$$
- ω_2 is called elliptic differential of the second kind, it has a double pole with vanishing residue. Its integral can be expressed in terms of elliptic integrals of the second kind:
$$E(\lambda) = \int_0^1 dx \sqrt{\frac{1-\lambda x^2}{1-x^2}}. \tag{97}$$
- ω_3 is called elliptic differential of the third kind, it has a pole with non-vanishing residue. Its integral can be expressed in terms of elliptic integrals of the third kind:
$$\Pi(n|\lambda) = \int_0^1 \frac{dx}{(1-nx^2)\sqrt{(1-x^2)(1-\lambda x^2)}}. \tag{98}$$

Summarizing, from a single integration of meromorphic functions over an elliptic curve, we can get rational functions, logarithms and elliptic integrals of the three kinds. Iterating integrations, we obtain a new class of iterated integrals, called elliptic multiple polylogarithms (eMPLs) [40]: these are iterated integrals of differential forms which are products of one-forms of the four types seen above. Note that MPLs are a special instance of eMPLs, obtained including only one-forms of type ω_4.

One can show [17] that eMPLs can be written more compactly as:

$$\mathcal{E}(n_1,\ldots,n_k;a_1,\ldots,a_k;z;\tau) = \int_0^z dt\; g^{(n_1)}(t-a_1,\tau)\,\mathcal{E}(n_2,\ldots,n_k;a_2,\ldots,a_k;t;\tau). \tag{99}$$

This has the same form as the definition (73) for MPLs, but now the integration kernels $g^{(n)}(z;\tau)$, with $n \in \mathbb{N}_0$, are some more complicated special functions.[21]

[21] They are defined as the coefficients in the expansion of the Kronecker elliptic function $F(z,\alpha;\tau)$ in the variable α: $F(z,\alpha;\tau) = \frac{1}{\alpha}\sum_{n=0}^{\infty} g^{(n)}(z,\tau)\alpha^n$.

5 Series expansions of DEs for FIs

We have previously seen that, when the differential equations (DEs) for the master integrals (MIs) are cast in canonical form, they can, in principle, be solved order by order in ϵ, allowing one to compute the full Laurent expansion to any desired order. However, it is not always possible to find global analytic solutions in the external kinematic variables. Even when such solutions exist, they are often expressed in terms of complicated special functions that are difficult to evaluate in practice.

However, as we will see in the first section of this chapter, it is always possible to find local generalized series solutions around a given point using Frobenius method, provided that the point is not an essential singularity of the DEs. These series are guaranteed to converge at least up to the nearest singularity.

The good news is that the DEs governing Feynman integrals are expected to have only regular singular points [33]. This means that, at least in principle, one can construct a basis of solutions around each singularity and analytically continue them by matching across overlapping regions of convergence, thereby reconstructing a global solution.

However, this approach comes with a practical challenge: for problems involving many singularities or multiple scales, the series expansions tend to converge slowly, especially near the boundary of their circle of convergence. We will address this issue in *Section 5.2*, introducing a change of variables that has the effect of improving convergence.

5.1 Series solutions of DEs: Frobenius method

There is a systematic method for finding series solutions to linear differential equations, known as Frobenius method, which will be the focus of this section. We will follow mainly [41] and [7].

Consider a linear homogeneous n-th-order differential equation, written in normal form:[22]

$$u^{(n)}(z) + p_1(z)u^{(n-1)}(z) + ... + p_{n-1}(z)u'(z) + p_n(z)u(z) = 0, \tag{100}$$

where $z \in \mathbb{C}$ and $\{p_m(z)\}_{1\leq m\leq n}$ are rational functions of z.
Suppose that z_0 is a regular singular point of (100), i.e. $(z - z_0)^m p_m(z)$ is analytic at $z = z_0$, or equivalently $p_m(z)$ has expansion:

$$p_m(z) = \frac{1}{(z - z_0)^m} \sum_{l=0}^{\infty} p_m^{(l)} (z - z_0)^l \qquad \forall m. \tag{101}$$

[22] By normal form, we mean that the coefficient of the highest derivative is normalized to one.

According to Fuchs's theorem, around such a point z_0, there exists at least a solution of the form of a generalized power series:

$$u(z) = (z - z_0)^\rho \sum_{n=0}^{\infty} c_n (z - z_0)^n, \tag{102}$$

where $\rho \in \mathbb{R}$ is called the indicial exponent.

Plugging the ansatz (102) and the expansion (101) for coefficients $p_m(z)$ in the differential equation (100), we get:

$$\begin{aligned}\sum_{k=0}^{\infty} c_k (z - z_0)^k \Big\{ &(k+\rho)(k+\rho-1)...[k+\rho-(n-1)] + \\ &+ (k+\rho)(k+\rho-1)...[k+\rho-(n-2)] \sum_{l=0}^{\infty} p_1^{(l)} (z - z_0)^l + ... \\ &..... + (k+\rho) \sum_{l=0}^{\infty} p_{n-1}^{(l)} (z - z_0)^l + \sum_{l=0}^{\infty} p_n^{(l)} (z - z_0)^l \Big\} = 0.\end{aligned} \tag{103}$$

With some algebraic manipulations,[23] it can be rewritten as:

$$\begin{aligned}\sum_{k=0}^{\infty} \Bigg\{ &(k+\rho)...[k+\rho-(n-1)] c_k + \sum_{l=0}^{k} \Big[(k-l+\rho)...[k-l+\rho-(n-2)] p_1^{(l)} + ... \\ &..... + (k-l+\rho) p_{n-1}^{(l)} + p_n^{(l)} \Big] c_{k-l} \Bigg\} (z - z_0)^k = 0.\end{aligned} \tag{104}$$

For this equality to be satisfied, all the coefficients of the various powers of $(z - z_0)$ must vanish. In particular, setting to zero the lowest order coefficient, we get (excluding the case $c_0 = 0$, corresponding to the trivial solution) the indicial equation:

$$\rho(\rho-1)...[\rho-(n-1)] + \rho(\rho-1)...[\rho-(n-2)] p_1^{(0)} + ... + \rho p_{n-1}^{(0)} + p_n^{(0)} = 0. \tag{105}$$

This is an algebraic equation of degree n, from which we can determine the possible values for the indicial exponent ρ, each of them producing a different solution of (100). By

[23] There are double sums of the form: $\sum_{k=0}^{\infty} \alpha_k (z - z_0)^k \sum_{l=0}^{\infty} \beta_l (z - z_0)^l$, which can be rewritten (taking $k' = k + l$) as: $\sum_{k'=0}^{\infty} (z - z_0)^{k'} \sum_{l=0}^{k'} \alpha_{k'-l} \beta_l$.

setting to zero the higher-order coefficients of (104), we get recursive relations among the coefficients c_m, which can be solved recursively, determining all of them from the knowledge of c_0.

For an n-th-order differential equation, we expect n independent solutions; however, it may happen that the individual equation (105) does not give n dinstinct solutions for ρ. In that case,[24] we can find the remaining solutions of (100) starting from a more general ansatz, that takes into account the possibility of having logarithmic singularities at $z = z_0$:

$$u(z) = (z - z_0)^\rho \sum_{m=0}^{m_{max}} \sum_{k=0}^{\infty} c_{k,m} (z - z_0)^k \log^m (z - z_0). \tag{106}$$

In practice, we first try to solve the system using ansatz (106) for $m_{max} = 0$, which corresponds to (102). If we obtain n linearly independent solutions, we are done; otherwise we increase the value of m_{max}, eventually up to $(n - 1)$. The general solution is a linear combination of all linearly independent solutions obtained in this way. To find a particular solution, we need to fix the n coefficients of the linear combination by imposing proper boundary conditions.

5.2 Convergence and Bernoulli-like variables

From the theory of differential equations, it is well known that the radius of convergence of a series solution is at least the distance from the expansion point to the nearest singularity of the equation. However, from a numerical perspective, convergence tends to slow down significantly as one approaches the boundary of the circle of convergence: increasingly higher orders in the expansion are required to maintain a fixed level of precision.

A common strategy to improve convergence and effectively extend the radius of convergence involves performing a change of variables that maps the singularities to infinity. In simple, one-scale problems it is possible to push away one singularity through a logarithmic change of variables [1, 18], introducing what are known as Bernoulli-like variables. However, in the presence of multiple scales and several singularities, situations frequently encountered when computing scattering amplitudes, the structure of the problem becomes substantially more involved. Understanding and optimizing convergence in these settings is still an open challenge. We will focus on these cases in the next chapters, for the moment we just present the standard Bernoulli-like variables, aiming to shed light on why they appear to work so well.

[24] We must proceed in this way also when some indicial exponents differ by an integer number; in fact, in that case, they produce solutions of (100) that are not independent.

5.2.1 The standard Bernoulli variable

The Bernoulli change of variable was introduced in [1] by 't Hooft and Veltman in order to find a series representation for the dilogarithm function with better convergence properties. Recalling the integral definition of the dilogarithm:

$$Li_2(x) = \int_0^x dt \frac{\log(1-t)}{t}, \tag{107}$$

it is natural to think at the following change of variable:

$$u = -\log(1-t), \tag{108}$$

which gives:

$$\begin{aligned} Li_2(x) &= -\int_0^x dt \frac{\log(1-t)}{t} = \int_0^z du \frac{u}{e^u - 1} = \\ &= \int_0^z \sum_{n=0}^{\infty} B_n \frac{u^n}{n!} = \sum_{n=0}^{\infty} B_n \frac{z^{n+1}}{(n+1)!}, \qquad with \quad z = -\log(1-x), \end{aligned} \tag{109}$$

where we used the definition of Bernoulli numbers B_n in terms of their generating function:

$$\frac{u}{e^u - 1} = \sum_{n=0}^{\infty} B_n \frac{u^n}{n!}. \tag{110}$$

These numbers have interesting mathematical properties [29]. Here, we highlight those that are most relevant for numerical applications:

1. Odd-indexed Bernoulli numbers, except B_1, are vanishing;
2. Even-indexed Bernoulli numbers alternate in sign;
3. Their magnitude grows rapidly. Asymptotically: $\left|B_{2k}\right| \approx 4\left(\frac{k}{\pi e}\right)^{2k}\sqrt{\pi k}$.

The new series representation (109) for the dilogarithm in the variable z, called the Bernoulli variable, has some advantages compared to the standard one:

$$Li_2(x) = \sum_{n=1}^{\infty} \frac{x^n}{n^2}. \tag{111}$$

The fact that the branching point $x = 1$ is pushed to $z = +\infty$ guarantees convergence in the new variable even in regions where the original series was not convergent; moreover, the new series representation converges much more rapidly to the function's value, likely due to the alternating signs of Bernoulli numbers.

5.2.2 Bernoulli-like variables: a new perspective

It is possible to define generalized Bernoulli-like variables in order to improve convergence of the series expansions for a generic function having only one finite singularity (excluding eventually the expansion point). This type of variable transformation has been already employed in the physics literature, particularly in the context of Feynman integrals [18, 37, 10], as a form of experimental mathematics, whose only justification is its empirical success. Here, we want to revisit this technique from a different perspective, giving a general definition of this change of variable and trying to provide a deeper understanding of why it is so effective, even if our justification remains heuristic rather than fully rigorous.

Consider a generic function $f(z)$ in the complex plane, having singularities at $z = z_1$ and $z = \infty$, and focus on its expansion around a point $z = z_0$:

$$f(z) = \sum_{n=0}^{\infty} a_n (z - z_0)^n. \tag{112}$$

We can define the Bernoulli-like variable:

$$t = -\log\left(\frac{z - z_1}{z_0 - z_1}\right) \quad \Longleftrightarrow \quad z = z_1 - (z_1 - z_0)e^{-t}. \tag{113}$$

This change of variable sends the expansion point $z = z_0$ to $t = 0$, while the singular points $z = z_1$ and $z = \infty$ are mapped respectively to $t = \pm\infty$. This clearly extends the region of convergence; moreover, from some numerical tests, it seems that the rapidity of convergence is also significantly improved for a general $f(z)$ with the above properties.

In order to try to understand the reason for this nice numerical behavior, we can rewrite the series (112) in terms of the Bernoulli-like variable t. We have:

$$f(z) = \sum_{n=0}^{\infty} a_n (z - z_0)^n = \sum_{n=0}^{\infty} a_n (z_1 - z_0)^n (1 - e^{-t})^n. \tag{114}$$

Using Taylor expansion formula and the binomial theorem, we can write:

$$\begin{aligned}(1 - e^{-t})^n &= \sum_{k=0}^{\infty} \frac{1}{k!} \Big[\frac{\partial^k}{\partial t^k}(1 - e^{-t})^n\Big]\Big|_{t=0} t^k = \sum_{k=0}^{\infty} \frac{1}{k!} \Big[\sum_{j=0}^{n} \binom{n}{j} (-1)^j e^{-tj}\Big]\Big|_{t=0} t^k = \\ &= \sum_{k=0}^{\infty} \sum_{j=0}^{n} \binom{n}{j} (-1)^{j+k} \frac{j^k}{k!} t^k = \sum_{k=0}^{\infty} (-1)^{n+k} \frac{n!}{k!} S(k, n) t^k,\end{aligned} \tag{115}$$

where in the last step we recognized the definition of Stirling numbers[25] of the second kind [29]:

$$S(k,n) = \frac{1}{n!}\sum_{j=0}^{n}(-1)^{n+j}\binom{n}{j}j^k. \tag{116}$$

Plugging (115) in (114), our function is rewritten as a power series in t:

$$f(t) = \sum_{k=0}^{\infty}\frac{(-1)^k}{k!}\left(\sum_{n=0}^{k}a_n(z_0-z_1)^n n! S(k,n)\right)t^k. \tag{117}$$

This can be thought of as an analytical continuation of the series representation (112) for the function f, since it is valid in a larger domain.

Moreover, in analogy with the dilogarithm case, the rapid convergence of the series can be reasonably attributed to two structural features of the coefficients. First, the coefficients exhibit an alternation of signs, which naturally leads to partial cancellations between successive terms. Second, each coefficient contains a sum of terms already appearing in the previous orders. This structure effectively acts as a "resummation" of earlier terms, but with partial cancellations. The combination of these two aspects is expected to play a crucial role in accelerating convergence.

This alternating character also has practical implications for numerical computations: from standard calculus, it is well known that in alternating series with decreasing term magnitudes, the truncation error is bounded by the absolute value of the first neglected term. This provides a simple and effective estimate of the numerical error, that we will largely employ in the following.

[25] It is interesting to notice that these special numbers are related to Bernoulli numbers, in fact: $B_k = \sum_{n=0}^{k}(-1)^{n+k}\frac{n!}{n+1}S(k,n)$.

6 A simple case: the 1-loop bubble

In this chapter, we apply the machinery previously described to the simplest nontrivial case: the equal-mass bubble integral. Thanks to the simplicity of the problem, much of the analysis can be carried out analytically. We begin by deriving the IBP relations, selecting a basis of master integrals, and obtaining the corresponding differential equations. After identifying a canonical basis, we solve the system exactly in terms of multiple polylogarithms (MPLs). Then, we construct (analytically) series solutions around $s = 0$ and $s = 4m^2$. Finally, we use Mathematica to evaluate both the exact and the series solutions, compare them numerically, and accelerate convergence by introducing a Bernoulli-like variable for each expansion.

6.1 IBPs and MIs

In this section, we derive the IBP relations for the bubble integral family in the equal mass case and choose a basis of master integrals for it.

The bubble integral family with equal internal masses is characterized by two denominators:

$$\begin{cases} D_1 = k^2 - m^2 \\ D_2 = (k+p)^2 - m^2 \end{cases}, \tag{118}$$

where k and p are respectively the loop and the external momenta, m is the mass of internal lines.

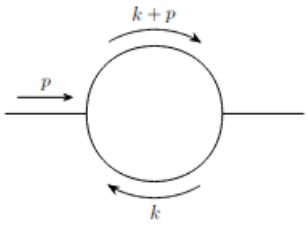

Figure 1: General bubble integral with labeled momenta.

The generic integral of this family looks like:

$$I_{a_1,a_2} = \int \frac{1}{D_1^{a_1} D_2^{a_2}}, \qquad where \quad \int \equiv e^{\gamma_E \epsilon} \int \frac{d^D k}{i\pi^{D/2}}. \tag{119}$$

There are two invariants: $x = \{p^2 \equiv s, m^2\}$, of which only one is independent, as we will check explicitly. The family is complete, since there are two denominators and two

scalar products involving the loop momentum k: $\{k^2, k \cdot p\}$, so that we can write from (118):

$$\begin{cases} k^2 = D_1 + m^2 \\ k \cdot p = \frac{D_2 - D_1 - s}{2} \end{cases} . \tag{120}$$

Note also that, being the internal masses equal, the family has an additional simmetry:

$$I_{a_1,a_2} = I_{a_2,a_1}, \tag{121}$$

as one can easily check by performing the shift: $k \to -k - p$.
The IBP relations can be derived from:

$$\int \frac{\partial}{\partial k^\mu} \frac{v^\mu}{D_1^{a_1} D_2^{a_2}} = 0 \qquad with \quad v^\mu = \{k^\mu, p^\mu\}. \tag{122}$$

Using (120) to express the scalar products appearing in the numerator, we get:

$$\begin{cases} (D - 2a_1 - a_2) I_{a_1,a_2} - 2a_1 m^2 I_{a_1+1,a_2} - a_2(2m^2 - s) I_{a_1,a_2+1} - a_2 I_{a_1-1,a_2+1} = 0 \\ (a_1 - a_2) I_{a_1,a_2} + a_1 s I_{a_1+1,a_2} - a_2 s I_{a_1,a_2+1} - a_1 I_{a_1+1,a_2-1} + a_2 I_{a_1-1,a_2+1} = 0 \end{cases} . \tag{123}$$

These are the IBPs for the bubble integral family with equal internal masses. We find that there are two MIs, which we can choose to be $I_{1,0}$ and $I_{1,1}$, to which any other integral of the family can be related. Note that the first MI is a tadpole, so it belongs to a subsector; the second one is in the top[26] sector. They are showed in the following Figure 2:

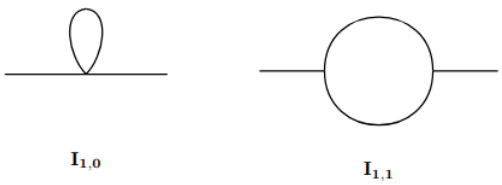

Figure 2: Our choice of masters for the equal-mass bubble integral family.

6.2 Differential equations

Let us derive the differential equations for the chosen basis of MIs.

[26] By top sector, we mean the sector having the largest number of active denominators.

We can easily rewrite $\frac{\partial}{\partial s}$ in terms of $\frac{\partial}{\partial p^\mu}$:

$$\frac{\partial}{\partial s} = \frac{1}{2s} p^\mu \frac{\partial}{\partial p^\mu}. \tag{124}$$

We have:

$$\begin{aligned}
&\partial_{m^2} I_{1,0} = \partial_{m^2} \int \frac{1}{D_1} = \int \frac{1}{D_1^2} = I_{2,0}, \qquad \partial_s I_{1,0} = 0, \\
&\partial_{m^2} I_{1,1} = \partial_{m^2} \int \frac{1}{D_1 D_2} = \int \frac{1}{D_1^2 D_2} + \int \frac{1}{D_1 D_2^2} = I_{2,1} + I_{1,2} = 2I_{2,1}, \\
&\partial_s I_{1,1} = \partial_s \int \frac{1}{D_1 D_2} = -\frac{\partial_s D_2}{D_1 D_2^2} = -\frac{1}{2s} \int \frac{D_2 - D_1 + s}{D_1 D_2^2} = -\frac{1}{2s}(I_{1,1} - I_{2,0} + s I_{2,1}).
\end{aligned} \tag{125}$$

Using IBPs (123), we can rewrite $I_{2,0}$ and $I_{2,1}$ in terms of the MIs, getting the systems of differential equations in the two invariants:

$$\frac{\partial}{\partial m^2} \begin{pmatrix} I_{1,0} \\ I_{1,1} \end{pmatrix} = \begin{pmatrix} \frac{D-2}{2m^2} & 0 \\ -\frac{D-2}{m^2(4m^2-s)} & \frac{2(D-3)}{4m^2-s} \end{pmatrix} \begin{pmatrix} I_{1,0} \\ I_{1,1} \end{pmatrix}, \tag{126}$$

$$\frac{\partial}{\partial s} \begin{pmatrix} I_{1,0} \\ I_{1,1} \end{pmatrix} = \begin{pmatrix} 0 & 0 \\ \frac{D-2}{s(4m^2-s)} & -\frac{1}{2}\left(\frac{1}{s} + \frac{D-3}{4m^2-s}\right) \end{pmatrix} \begin{pmatrix} I_{1,0} \\ I_{1,1} \end{pmatrix}. \tag{127}$$

One can easily check that these DEs satisfy the integrability condition as well as the Euler scaling relation. We can also check that only one scale is independent, by performing the change of variable:

$$\begin{cases} \tilde{m}^2(m^2, s) = m^2 \\ \tilde{s}(m^2, s) = \frac{s}{m^2} \end{cases}. \tag{128}$$

We get:

$$\begin{aligned}
\tilde{m}^2 \frac{\partial}{\partial \tilde{m}^2} \begin{pmatrix} I_{1,0} \\ I_{1,1} \end{pmatrix} &= \begin{pmatrix} \frac{D-2}{2} & 0 \\ 0 & \frac{D-4}{2} \end{pmatrix} \begin{pmatrix} I_{1,0} \\ I_{1,1} \end{pmatrix}, \\
\frac{\partial}{\partial \tilde{s}} \begin{pmatrix} I_{1,0} \\ I_{1,1} \end{pmatrix} &= \begin{pmatrix} 0 & 0 \\ \frac{D-2}{\tilde{m}^2 \tilde{s}(4-\tilde{s})} & -\frac{1}{2}\left(\frac{1}{\tilde{s}} + \frac{D-3}{4-\tilde{s}}\right) \end{pmatrix} \begin{pmatrix} I_{1,0} \\ I_{1,1} \end{pmatrix}.
\end{aligned} \tag{129}$$

The first equation gives the trivial mass dependence, the second is the non-trivial one. Note that the latter is equivalent to (127) for $m^2 = \tilde{m}^2 = 1$, so we could directly set $m = 1$ from the beginning and derive only the system in s:

$$\frac{\partial}{\partial s} \begin{pmatrix} I_{1,0} \\ I_{1,1} \end{pmatrix} = \begin{pmatrix} 0 & 0 \\ \frac{D-2}{s(4-s)} & -\frac{1}{2}\left(\frac{1}{s} + \frac{D-3}{4-s}\right) \end{pmatrix} \begin{pmatrix} I_{1,0} \\ I_{1,1} \end{pmatrix}. \tag{130}$$

6.3 Canonical form

For this simple case, we could directly solve the non-canonical equation (130). However, to anticipate what we will do in more complicated cases, we decide to work in a canonical basis:

$$\begin{cases} J_1 = I_{2,0} \\ J_2 = \sqrt{s(s-4)} I_{2,1} \end{cases} . \tag{131}$$

Note that we construct the canonical basis starting from integrals with the first denominator squared[27] and normalizing the second master by its leading singularity. Now we want to write the differential equations in this basis.

Taking derivatives with respect to s, we get:

$$\begin{aligned} &\partial_s J_1 = \partial_s \int \frac{1}{D_1^2} = 0, \\ &\partial_s J_2 = \partial_s \Big[\sqrt{s(s-4)} \int \frac{1}{D_1^2 D_2} \Big] = \frac{s-2}{\sqrt{s(s-4)}} I_{2,1} + \frac{\sqrt{s(s-4)}}{2} I_{2,2}. \end{aligned} \tag{132}$$

Using IBP relations (123), we can rewrite:

$$I_{2,2} = \frac{D-4}{s(s-4)} I_{2,0} + \frac{(6-D)s-4}{s(s-4)} I_{2,1}. \tag{133}$$

Therefore, the differential equations in the new basis take the form:

$$\frac{\partial}{\partial s} \begin{pmatrix} J_1 \\ J_2 \end{pmatrix} = \epsilon \begin{pmatrix} 0 & 0 \\ \frac{1}{\sqrt{s(s-4)}} & -\frac{1}{s-4} \end{pmatrix} \begin{pmatrix} J_1 \\ J_2 \end{pmatrix}. \tag{134}$$

As expected, the system is now in canonical form (ϵ-dependence factorizes); however, in this basis the matrix entries are no longer rational functions in s. For this simple case, it is possible to rationalize them by performing the change of variable:

$$s = -\frac{(1-y)^2}{y}, \tag{135}$$

where y is called the *Landau variable*. Now the canonical DEs take the form:

$$\frac{\partial}{\partial y} \begin{pmatrix} J_1 \\ J_2 \end{pmatrix} = \epsilon \begin{pmatrix} 0 & 0 \\ -\frac{1}{y} & \frac{1}{y} - \frac{2}{y+1} \end{pmatrix} \begin{pmatrix} J_1 \\ J_2 \end{pmatrix}. \tag{136}$$

It is important to notice that, while the DEs in s have singular points at $s = 0$, $s = 4$ and $s = \infty$, (136) is singular only for $y = -1$ (corresponding to $s = 4$), $y = 0$ and $y = \infty$ (both corresponding to $s = \infty$). This will be important when imposing boundary conditions: we cannot use regularity at $y = 1$ $(s = 0)$ as a BC, since this information is already encoded in the DEs (136).

[27] We choose $I_{2,1}$ since it is UV finite in $D = 4 - 2\epsilon$, so it is a good initial integral according to the criteria in *Section 3.5.1*.

6.4 Solving the canonical equations

We want to solve the canonical DEs (136). The only non-trivial equation is the second one, since the first one simply tells us that the tadpole J_1 does not depend on s. Therefore, J_1 has to be computed by direct integration, getting:

$$J_1 = I_{2,0} = e^{\gamma_E \epsilon}\Gamma(\epsilon) = \frac{1}{\epsilon} + \epsilon\frac{\pi^2}{12} - \epsilon^2\frac{\zeta(3)}{3} + o(\epsilon^3). \tag{137}$$

Expanding the second of (136) in ϵ, we get:

$$\frac{\partial}{\partial y}J_2^{(n)}(y) = \Big(\frac{1}{y} - \frac{2}{y+1}\Big)J_2^{(n-1)}(y) - \frac{1}{y}J_1^{(n-1)}, \tag{138}$$

where $J_1^{(n)}$ (already known from (137)) and $J_2^{(n)}$ are the order n coefficients of the Laurent expansions in ϵ, respectively for J_1 and J_2. Therefore, we can write:

$$J_2^{(n)}(y) = \int dy\Big[\Big(\frac{1}{y} - \frac{2}{y+1}\Big)J_2^{(n-1)}(y)\Big] - J_1^{(n-1)}\log(y) + c^{(n)}, \tag{139}$$

where the coefficients $c^{(n)}$ are fixed order by order in ϵ by imposing a suitable boundary condition (BC). In particular, we know that the physical integral $I_{2,1}(s)$ has a branch cut for $s > 4$, but is regular at s=0; therefore the canonical integral $J_2(s) = \sqrt{s(s-4)}I_{2,1}(s)$ will satisfy $J_2(s=0) = 0$, or equivalently:

$$J_2(y=1) = 0. \tag{140}$$

This is our boundary condition.

From (137), (138) and (140), it is evident that $J_2^{(n)} = 0\ \forall n < 0$; using (139), we can compute recursively the Laurent coefficients for $n \geq 0$.
Since (139) (or equivalently (136)) only contains $dlogs$ of rational functions ($dlog(y)$, $dlog(y+1)$), then the solution at any order can be expressed in terms of MPLs. For example, at second order in ϵ, we get:

$$\begin{aligned} J_2(y) = &- G(0;y) + \epsilon\Big[\frac{\pi^2}{6} + 2G(-1,0;y) - G(0,0;y)\Big] + \epsilon^2\Big[-\frac{\pi^2}{3}G(-1;y) + \\ &+ \frac{\pi^2}{12}G(0;y) - 4G(-1,-1,0;y) + 2G(-1,0,0;y) + 2G(0,-1,0;y) + \\ &- G(0,0,0;y) + 2\zeta(3)\Big] + o(\epsilon^3). \end{aligned} \tag{141}$$

Note that this solution has a branch cut for $y < 0$, which corresponds to $s > 4$. To express the solution in this region, we need to perform an analytical continuation[28] for MPLs.

[28] The procedure is the one described in *Section 4.3.3*. As usual, the correct sign for the imaginary part is given by Feynman prescription: $s \to s + i\varepsilon$, or equivalently $y \to y + i\varepsilon \equiv -x + i\varepsilon \quad (\varepsilon > 0, x > 0)$.

6.5 Series expansions around s=0 and s=4

For this problem, we have been able to rationalize the canonical DEs and to find a global solution in the external scale s. However, as previously mentioned, in more complicated situations, it is only possible to find local series solutions around specific points. It is instructive to try these techniques already for this simple case. In particular, in this section, we will look for series solutions around $s = 0$ and $s = 4$.

Consider the second of the canonical DEs (134), which can be rewritten in the form:

$$(s-4)\sqrt{s}\frac{\partial J_2(\epsilon,s)}{\partial s} = \epsilon\big[\sqrt{s-4}J_1(\epsilon) - \sqrt{s}J_2(\epsilon,s)\big], \tag{142}$$

with $J_1(\epsilon)$ given by (137). As a solution around $s = 0$, we take the ansatz:

$$J_2(\epsilon,s) = \sum_{n=0}^{\infty} b_n(\epsilon)s^{n+\frac{1}{2}}, \tag{143}$$

where the coefficients $b_n(\epsilon)$ are functions of ϵ, which can be expanded around $\epsilon = 0$ up to the needed order. Note also that this ansatz automatically satisfies the boundary condition $J_2(\epsilon, s = 0) = 0$. Plugging (143) in (142), using the expansion for $\sqrt{s-4}$ around $s = 0$, and equating the coefficients of the same powers, we get the recursion relations:

$$\begin{cases} b_0(\epsilon) = -i\epsilon J_1(\epsilon) \\ b_n(\epsilon) = \frac{1}{4n+2}\Big[(n-\frac{1}{2}+\epsilon)b_{n-1}(\epsilon) - \epsilon J_1(\epsilon)\frac{(-4)^{1/2-n}}{n!}\frac{\Gamma(3/2)}{\Gamma(3/2-n)}\Big] \end{cases} . \tag{144}$$

For the expansion around $s = 4$, we can proceed in a similar way, but we need a more general ansatz, which takes into account the presence of a logarithmic singularity:

$$J_2(\epsilon,s) = \sum_{n=0}^{\infty}\alpha_n(\epsilon)\cdot(s-4)^n + \sum_{m=0}^{\infty}\beta_m(\epsilon)\cdot\log^m(s-4). \tag{145}$$

Plugging in the differential equation (142), we find:

$$\begin{cases} \alpha_n(\epsilon) = \frac{\epsilon J_1(\epsilon)}{n+1/2+\epsilon}\frac{(-4)^{1/2-n}}{n!}\frac{\Gamma(3/2)}{\Gamma(3/2-n)} \\ \beta_m(\epsilon) = -\frac{\epsilon}{m}\beta_{m-1}(\epsilon) \end{cases} , \tag{146}$$

where $\beta_0(\epsilon) = \sum_{k=k_0}^{\infty}\epsilon^k\beta_0^{(k)}$ has to be determined by imposing suitable boundary conditions. We can observe that, since $\beta_0^{(k)} = 0 \quad \forall k < k_0$, then (146) implies that:

$\beta_m^{(k)} = 0 \quad \forall k < k_0 + m$; in other words, at order ϵ^k, (145) only contains coefficients $b_m^{(k)}$ with $m \leq k - k_0$:

$$J_2^{(k)} = \sum_{n=0}^{\infty} \alpha_n^{(k)} \cdot (s-4)^n + \sum_{m=0}^{k} \beta_m^{(k)} \cdot \log^m(s-4), \tag{147}$$

where we used the fact that in this case $k_0 = 0$.

As a boundary condition, we can impose, order by order in ϵ, the matching between (147) and the series solution around s=0 when both are evaluated at s=2: at order $k_0 = 0$ we determine $\beta_0^{(0)}$, from (146) we compute $\beta_1^{(1)}$, then from matching at order 1 we determine $\beta_0^{(1)}$, etc...

6.6 Study of convergence and Bernoulli-like variables

Now we want to study the numerical convergence of the series solutions found in the previous section, comparing results with the analytical expectations. Then, we will introduce Bernoulli-like variables to improve convergence, as discussed in *Section 5.2.2*.

The expansion around $s = 0$ is expected to have radius of convergence $r_0 = 4$, since the nearest singularity lies at $s = 4$. This is confirmed by our numerical results shown in the plots on the left of Figure 3. The relative difference between the series expansions (truncated to 10 orders) and the exact values of the first three Laurent coefficients of J_2 is below 10^{-4} throughout most of the interval $s \in [-4, 4]$, with larger deviations only near the endpoints. Increasing the expansion to 100 orders allows us to reach this accuracy across the entire interval; however, in the remaining part of the real s-axis, the series still fails to provide even a single digit of precision.

Regarding the expansion around $s = 4$, the nearest singularity of the differential equation is at $s = 0$; however, this is not a singular point of the particular solution corresponding to J_2. It is therefore interesting to investigate whether this "spurious"[29] singularity still affects the radius of convergence.

Our numerical results, shown in the plots on the left of Figure 4, indicate that the radius of convergence is $R_{4,\text{num}} = 4$: this suggests that the coefficients of the series solution "remember" that $s = 0$ was a singular point of the differential equation. This behavior is consistent with the general theory of linear differential equations and is further confirmed by analitically computing the radius of convergence directly from the closed-form expression for the coefficients α_n, derived in (146). For large n, the

[29] By spurious we mean that this is a singularity of the differential equations, but not of the physical solution (it disappears when imposing the boundaries).

coefficients $\alpha_n^{(k)}$, where k is the (fixed) order in ϵ, are given by:

$$\alpha_n^{(k)} \sim \frac{J_1^{(k)}}{n+1/2} \frac{(-4)^{1/2-n}}{n!} \frac{\Gamma(3/2)}{\Gamma(3/2-n)}. \tag{148}$$

By applying the ratio test, we find:

$$R_{4,th} = \lim_{n\to\infty} \left| \frac{\alpha_{n+1}^{(k)}}{\alpha_n^{(k)}} \right| = 4 \qquad \forall k\,. \tag{149}$$

Therefore, it is evident that in this case the radius of convergence is limited by the nearest singular point of the differential equation, even though this point is regular for the particular solution under consideration. There are also special cases for which such spurious singularities do not affect the radius of convergence: we will see some examples of this behavior later on.

As previously mentioned, for the expansion around $s = 0$, the convergence is slow near the extrema of the interval $[-4, 4]$ and totally absent in the external region of the real s-axis. We can define a Bernoulli-like variable of the form proposed in (113):

$$t = -\log\left(1 - \frac{s}{4}\right) \Longleftrightarrow s = 4(1 - e^{-t}). \tag{150}$$

This transformation maps $s = 0$ to $t = 0$, $s = 4$ and $s = \infty$ to $t = \infty$. In practice, we perform this change of variable in our series solution and re-expand up to the same order; then we estimate the accuracy of our results by computing the relative error with respect to the exact solution, previously found.

The advantage of using this new variable is twofold:

1. The convergence of the series for $|s| < 4$ is much faster than before. In fact, including only 10 orders we can get a similar precision to the one obtained with 100 orders when using the variable s. Another interesting observation is that, including more than 50 orders, the relative precision stabilizes around 10^{-16}.

2. There is convergence also for points of the complex s-plane that lie outside the original circle of convergence. In particular, as showed in the plots on the right of Figure 3, for all values of t corresponding to $s \in \mathbb{R}$ the series is now convergent. However, it is interesting to notice that convergence is a bit slower in a small region around the singularity $s = 4$, that was pushed away.

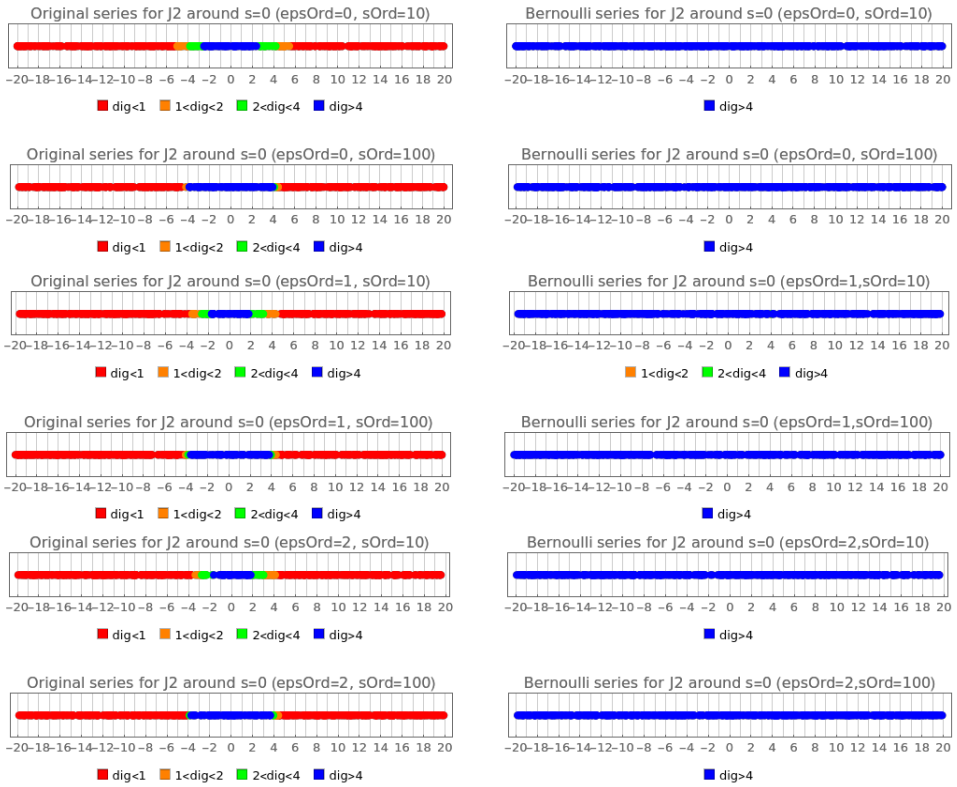

Figure 3: Relative truncation errors along the real s-axis in the expansions around $s = 0$ of J_2 up to $o(\epsilon^2)$. Different colors indicate the error at each point. Left: original series; right: Bernoulli-like variable series. For each case, two plots are shown, corresponding to truncation at 10 and 100 orders, respectively.

Summarizing, using this Bernoulli-like variable, we are able to cover the entire real s-axis with high accuracy (> 4 digits) using only one expansion point ($s = 0$) and including few orders ($\simeq$10 orders) in the expansion.

In alternative, one can choose $s = 4$ as expansion point. In this case, the proper Bernoulli-like variable is defined by:

$$t = -\log\left(\frac{s}{4}\right) \Longleftrightarrow s = 4e^{-t}. \tag{151}$$

This transformation maps $s = 4$ to $t = 0$, $s = 0$ and $s = \infty$ to $t = \infty$. The effect on convergence is analogous to the previous case, as showed in Figure 4.

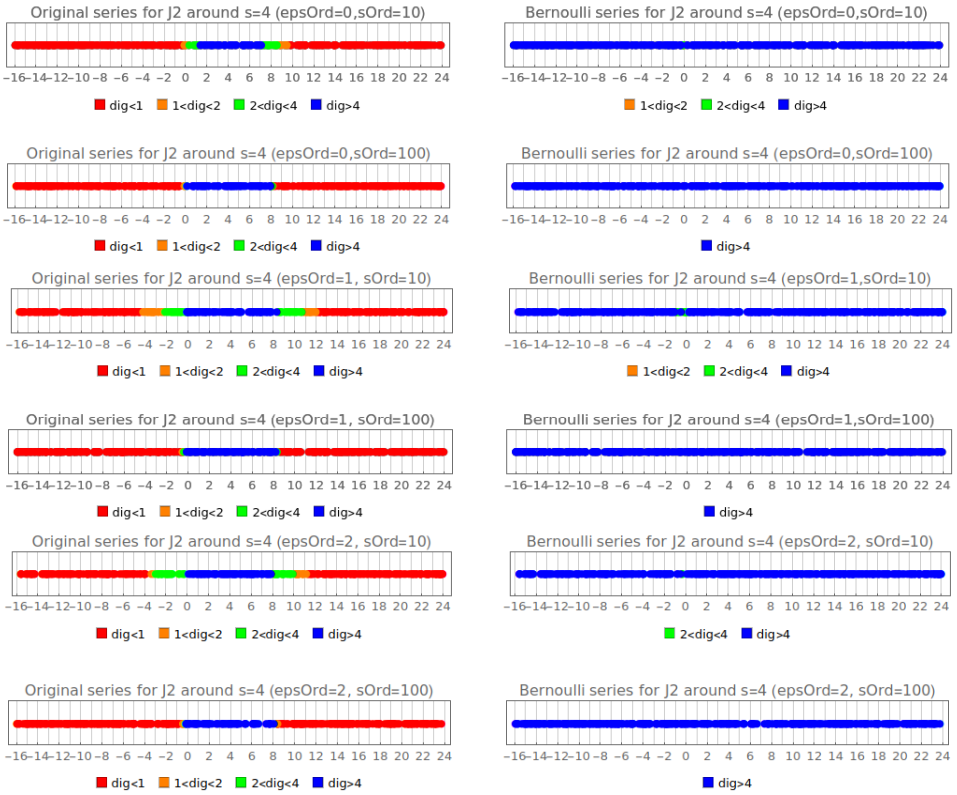

Figure 4: Relative truncation errors along the real s-axis in the expansions around $s = 4$ of J_2 up to $o(\epsilon^2)$. Different colors indicate the error at each point. Left: original series; right: Bernoulli-variable series. For each case, two plots are shown, corresponding to truncation at 10 and 100 orders, respectively.

7 The equal-mass sunrise

This chapter focuses on the equal-mass sunrise integral, which is the simplest example featuring an elliptic geometry. Full analytic and full series expansion treatments of the problem can be found in [28] and [37], respectively. Here, instead, we combine an iterative method, facilitated by working in a canonical basis, with a series expansion approach.

The IBP reduction and derivation of the differential equations are carried out using dedicated computational tools [32]. We then construct a canonical basis following the procedure outlined in Section 3.5, which includes solving the homogeneous block via the Frobenius method. The canonical system is solved iteratively in ϵ, constructing at each order series expansions in s around its singular points, with boundary conditions fixed numerically. Finally, we analyze the convergence of the series solutions and study the effect of Bernoulli-like changes of variables on their behavior.

7.1 MIs and differential equations

Let us introduce the sunrise integral family with equal masses and derive the differential equations.

The sunrise integral family is a two-loop family, associated to Feynman diagrams with two external and three internal lines, as shown in the following figure:

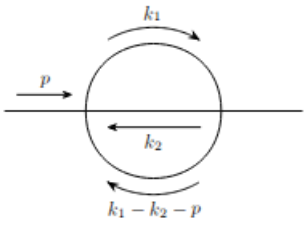

Figure 5: General sunrise integral with labeled momenta.

This topology involves two loop momenta, k_1 and k_2, and one external momentum, p. For simplicity, in this chapter we consider the case where all three internal lines carry the same mass m. Thus, the generic integral of this family reads:

$$I_{\nu_1,\nu_2,\nu_3} = \frac{e^{2\gamma_E \epsilon}}{i\pi^D} \int \frac{d^D k_1 d^D k_2}{(k_1^2 - m^2)^{\nu_1} (k_2^2 - m^2)^{\nu_2} \left[(k_1 - k_2 - p)^2 - m^2\right]^{\nu_3}}. \tag{152}$$

There are five possible scalar products involving loop momenta, but only three denominators; therefore, we need to introduce two fictitious denominators to complete the family. In particular, we choose: $D_4 = (k_1 - p)^2$, $D_5 = (k_2 - p)^2$.

Differently from the previous chapter, the IBP reduction and the derivation of the differential equations for this family are performed using computer algebra systems, in particular we used the software *Reduze* [32]. The reduction reveals that there are three master integrals (MIs): in particular, we choose as masters the two-loops tadpole $I_{1,1,0}$ and the two sunrises $I_{1,1,1}$ and $I_{2,1,1}$. They are showed in the following Figure 6:

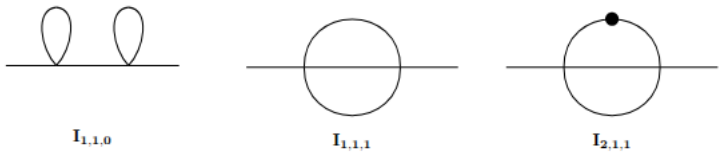

Figure 6: Our choice of masters for the equal-mass sunrise integral family.

There is only one independent kinematic scale in the problem, which we take to be $s \equiv p^2$. Setting $m = 1$, the differential equations for the master integrals in $d = 2 - 2\epsilon$ dimensions take the form:

$$\frac{\partial}{\partial s}\begin{pmatrix} I_{1,1,0} \\ I_{1,1,1} \\ I_{2,1,1} \end{pmatrix} = \begin{pmatrix} 0 & 0 & 0 \\ 0 & -\frac{1+2\epsilon}{s} & -\frac{3}{s} \\ -\frac{2\epsilon^2}{(s-1)(s-9)} & -\frac{(s-3)(1+5\epsilon+6\epsilon^2)}{s(s-1)(s-9)} & \frac{9+27\epsilon-10s\epsilon-s^2(1+\epsilon)}{s(s-1)(s-9)} \end{pmatrix} \begin{pmatrix} I_{1,1,0} \\ I_{1,1,1} \\ I_{2,1,1} \end{pmatrix}, \tag{153}$$

where the first equation simply tells us that the tadpole does not depend on s, as we already knew.

The advantage of working around $d_0 = 2$ dimensions is that the two integrals in the top sectors are both UV (and IR) finite. This makes the original basis a convenient starting point for constructing a canonical basis. The physical results in $d = 4$ space-time dimensions can then be recovered using dimensional shift relations.

7.2 Finding a canonical form

Now we want to write the DEs (153) in canonical form, so that it is easier to solve them. As discussed, this corresponds to performing a particular rotation of our basis $\vec{I}$ of MIs to a new basis $\vec{J} = R\vec{I}$; the corresponding transformation for the matrix A of the system is given by (43), that in our case becomes:

$$A' = RAR^{-1} + \frac{\partial R}{\partial s}R^{-1}, \qquad with \quad A'(\epsilon, s) = \epsilon\tilde{A}(s). \tag{154}$$

To construct the rotation matrix, we follow the procedure described in *Section 3.5*.

1. As previously observed, the two masters in the top sector are finite in $d_0 = 2$ dimensions. First, we rotate them to a derivative basis, where we take as third master the derivative of the second one w.r.t the scale s. This is a good initial basis, which makes the following steps easier. This rotation is described by the matrix:

$$R_1 = \begin{pmatrix} 1 & 0 & 0 \\ 0 & 1 & 0 \\ 0 & -\frac{1+2\epsilon}{s} & -\frac{3}{s} \end{pmatrix}. \tag{155}$$

2. Then, we compute the Wronskian[30] matrix of the homogeneous equations for the top sector integrals at $\epsilon = 0$:

$$W(s) = \begin{pmatrix} \omega_0(s) & \omega_1(s) \\ \omega_0'(s) & \omega_1'(s) \end{pmatrix}. \tag{156}$$

The functions appearing in the matrix W are complicated transcendental functions, which can be interpreted as the periods on an elliptic curve. However they can be computed explicitly through series expansions. Specifically, ω_0 is represented by a regular power series, while ω_1 includes logarithmic terms. The details of this computation are provided in the next section.

Then we split W into a unipotent part W_u and a semi-simple part W_{ss}, as described in *Section 3.5*. In particular, we take:

$$W_u = \begin{pmatrix} 1 & \frac{\omega_1}{\omega_0} \\ 0 & 1 \end{pmatrix} \qquad W_{ss} = \begin{pmatrix} \omega_0 & 0 \\ \omega_0' & \frac{\det W}{\omega_0} \end{pmatrix}, \tag{157}$$

where we do not need the explicit form of the matrix W to compute its determinant. In fact, it is known that the Wronskian matrix satisfies a matrix version of the original differential equations:

$$W'(s) = \hat{A}(s)W(s), \tag{158}$$

where $\hat{A}(x)$ denotes the 2×2 top-sector block of the full differential equation matrix $A(x)$. Its general solution is given by:

$$W(s) = \exp\left[\int \hat{A}(s)ds\right]. \tag{159}$$

[30] We recall that this is the matrix whose columns contain the independent solutions of the homogeneous 2x2 system for the integrals in the top sector ($I_{1,1,1}$, $\partial_s I_{1,1,1}$).

Therefore, using the matrix identity $\det\left(e^{M}\right) = e^{trM}$, valid for a generic square matrix M, we have :[31]

$$\det W(s) = \exp\left[\int \hat{A}(s)ds\right]. \tag{160}$$

Note also that, by performing the splitting according to (157), the unipotent part contains a pure logarithm (i.e. with constant coefficient normalized to one), while the semi-simple part has uniform transcendental weight zero. This semi-simple component can be viewed as analogous to the leading singularity in the decoupled case. This observation justifies the procedure of rotating the basis in the top sector by the inverse of the semi-simple part. The rotation matrix is given by:

$$R_2 = \begin{pmatrix} 1 & 0 & 0 \\ 0 & & \\ 0 & & W_{ss}^{-1} \end{pmatrix}. \tag{161}$$

This is the crucial step; however, after applying this rotation, the matrix of the system is not yet fully ϵ-factorized.

3. We also have to rescale the third integral by a factor $\frac{1}{\epsilon}$, to account for the fact that it involves one fewer integration compared to the second one.[32] In addition, we multiply all the 3 masters by a factor ϵ^2: this is just our choice to obtain an ϵ expansion beginning at order zero. Therefore:

$$R_3 = \begin{pmatrix} \epsilon^2 & 0 & 0 \\ 0 & \epsilon^2 & 0 \\ 0 & 0 & \epsilon \end{pmatrix}. \tag{162}$$

At this stage, only the matrix entry A_{32} is not yet ϵ-factorized.

4. To achieve a full ϵ-factorization, our last step is to shift the third master by a term proportional to the second one. This corresponds to performing an additional rotation of the form:

$$R_4 = \begin{pmatrix} 1 & 0 & 0 \\ 0 & 1 & 0 \\ 0 & f(s)\omega_0^2(s) & 1 \end{pmatrix}, \tag{163}$$

[31] Note that this determines $\det W$ up to a prefactor (on the rhs there is an indefinite integral) depending on our choice for the normalization of ω_0 and ω_1.

[32] This ensures that the resulting basis satisfies the uniform transcendentality (UT) property.

where $f(s)$ is chosen in such a way that the unwanted terms vanish. In our case, we must take $f(s) = \frac{3}{2}s^2 - 5s - \frac{9}{2}$, in order to obtain the canonical form of the differential equations:

$$\frac{\partial}{\partial s}\begin{pmatrix} J_1 \\ J_2 \\ J_3 \end{pmatrix} = \epsilon \begin{pmatrix} 0 & 0 & 0 \\ 0 & -\frac{3s^2-10s-9}{2s(s-1)(s-9)} & \frac{1}{\omega_0^2(s)s(s-1)(s-9)} \\ 6\omega_0(s) & \frac{(s+3)^4\omega_0^2(s)}{4s(s-1)(s-9)} & -\frac{3s^2-10s-9}{2s(s-1)(s-9)} \end{pmatrix} \begin{pmatrix} J_1 \\ J_2 \\ J_3 \end{pmatrix}. \tag{164}$$

It is important to stress that the rotation matrix $R = R_4R_3R_2R_1$ and the resulting canonical equations depend on the function $\omega_0(s)$, for which we have not found a global analytical form, but just some series expansions. Therefore, using these expansions for $\omega_0(s)$ in the rotation, we can only construct some (different) "local" canonical bases, each of them valid in a neighborhood of the corresponding expansion point.

7.3 How to solve the homogeneous system

In this section, we describe how to find two fundamental solutions to the homogeneous system in the top sector at $\epsilon = 0$, which define the Wronskian matrix (156). The system consists of two coupled first-order linear differential equations; however, having performed a rotation to the derivative basis by using (155), we can immediately rewrite them as a unique linear second-order differential equation:

$$I''(s) = -\frac{3s^2 - 20s + 9}{s(s-1)(s-9)}I'(s) - \frac{s-3}{s(s-1)(s-9)}I(s). \tag{165}$$

This differential equation has only regular singular points at: $s = 0$, $s = 1$, $s = 9$ and $s = \infty$. We can find local series solutions around them via Frobenius method. In particular, for all singular points, the indicial equation gives two coincident solutions ($\rho_1 = \rho_2 = 0$); this implies that the two independent solutions of the DE around one of these points, say s_0, will be a regular solution $\omega_0^{(s_0)}$ and a logarithmic divergent solution $\omega_1^{(s_0)}$. In particular, for the finite singularities $s = 0, 1, 9$ we have:

$$\begin{aligned} \omega_0^{(s_0)}(s) &= \sum_{n=0}^{\infty} a_n^{(s_0)}(s-s_0)^n, \\ \omega_1^{(s_0)}(s) &= \sum_{n=0}^{\infty} b_n^{(s_0)}(s-s_0)^n + \log(s-s_0)\omega_0^{(s_0)}(s). \end{aligned} \tag{166}$$

By plugging (166) in the differential equation (165), we get recursion relations for the coefficients $a_n^{(s_0)}$ and $b_n^{(s_0)}$; the recursion is initialized by imposing some initial conditions, in our case we simply choose:[33] $a_0^{(s_0)} = 1$, $b_0^{(s_0)} = 0$.

[33] It is understood that $a_n = 0 \quad \forall n < 0$, $b_n = 0 \quad \forall n < 0$.

Note that, while it is possible to obtain series solutions to (165) using built-in functions in Mathematica, this numerical approach becomes inefficient when many terms in the series expansion are required. To overcome this, we implement a symbolic procedure based on the Frobenius method: we first define a function that extracts the recursion relations analytically, and then use these relations to compute the series coefficients up to the desired order.

In particular, for the recursion relations, we get:

$$\begin{cases} a_n^{(0)} = \dfrac{1}{9n^2}\Big[-(n-1)^2 a_{n-2}^{(0)} + (10n^2-10n+3)a_{n-1}^{(0)}\Big], \\ b_n^{(0)} = \dfrac{1}{9n^3}\Big[-n(n-1)^2 b_{n-2}^{(0)} + n(10n^2-10n+3)b_{n-1}^{(0)} + \\ \qquad\qquad -2(n-1)a_{n-2}^{(0)} + 2(5n-3)a_{n-1}^{(0)}\Big]. \end{cases} \tag{167}$$

$$\begin{cases} a_n^{(1)} = \dfrac{1}{8n^2}\Big[(n-1)^2 a_{n-2}^{(1)} - (7n^2-7n+2)a_{n-1}^{(1)}\Big], \\ b_n^{(1)} = \dfrac{1}{8n^3}\Big[n(n-1)^2 b_{n-2}^{(1)} - n(7n^2-7n+2)b_{n-1}^{(1)} + \\ \qquad\qquad -2(n-1)a_{n-2}^{(1)} - (7n-4)a_{n-1}^{(1)}\Big]. \end{cases} \tag{168}$$

$$\begin{cases} a_n^{(9)} = \dfrac{1}{72n^2}\Big[-(n-1)^2 a_{n-2}^{(9)} - (17n^2-17n+6)a_{n-1}^{(9)}\Big], \\ b_n^{(9)} = \dfrac{1}{72n^3}\Big[-n(n-1)^2 b_{n-2}^{(9)} - n(17n^2-17n+6)b_{n-1}^{(9)} + \\ \qquad\qquad -2(n-1)a_{n-2}^{(9)} - (17n-12)a_{n-1}^{(9)}\Big]. \end{cases} \tag{169}$$

To find solutions around $s = \infty$, we rewrite (165) setting $y = 1/s$ and look for solutions around $y_0 = 0$ of the form:

$$\begin{aligned} \omega_0^{(\infty)}(y) &= y\sum_{n=0}^{\infty} a_n^{(\infty)} y^n, \\ \omega_1^{(\infty)}(y) &= y\sum_{n=0}^{\infty} b_n^{(\infty)} y^n + \log(y)\,\omega_0^{(\infty)}(y). \end{aligned} \tag{170}$$

We find:

$$\begin{cases} a_n^{(\infty)} = \dfrac{1}{n}\Big[-9(n-1)^2 a_{n-2}^{(\infty)} + (10n^2-10n+3)a_{n-1}^{(\infty)}\Big], \\ b_n^{(\infty)} = \dfrac{1}{n^2}\Big[-9n(n-1)^2 b_{n-2}^{(\infty)} + n(10n^2-10n+3)b_{n-1}^{(\infty)} + \\ \qquad\qquad -18(n-1)a_{n-2}^{(\infty)} + 2(5n-3)a_{n-1}^{(\infty)}\Big]. \end{cases} \tag{171}$$

7.4 Solving the canonical DEs via series expansions

Let us describe the procedure used to find series solutions to the canonical differential equations and fix the boundary conditions.

The canonical DEs (164) can be solved order by order in ϵ, as discussed in *Section 3.3*:

$$\partial_s \vec{J}^{(n)}(s) = \tilde{A}(s)\vec{J}^{(n-1)}(s) \qquad \Longrightarrow \qquad \begin{cases} \vec{J}^{(n_0)} = \text{const} \qquad (n_0 = 0) \\ \vec{J}^{(n)}(s) = \int ds \tilde{A}(s)\vec{J}^{(n-1)}(s) + c^{(n)} \end{cases} . \tag{172}$$

However, unlike the simpler case of the bubble integral, here the matrix entries of $\tilde{A}(s)$ contain more complicated functions of s, including $\omega_0(s)$, which is an elliptic period associated with the underlying geometry of the problem. Although a full analytic solution to the system is known in terms of elliptic functions [9], this representation is often cumbersome and less suitable for numerical evaluations. A more efficient and flexible approach is to work with series expansions.

We therefore construct local solutions around the singular points of the differential equations, using a more systematic method than the one used for the bubble, where we relied on an ansatz. Specifically, we expand the matrix $\tilde{A}(s)$ around the point of interest, using for $\omega_0(s)$ the series representations previously found; then, we integrate the system iteratively, starting from the lowest nontrivial order in ϵ, according to (172). The integration constants at each order are fixed by imposing suitable boundary conditions.

Clearly, the precision of the resulting Laurent coefficients $J^{(n)}$ improves as more terms are included in the s-expansion. The main limitation, however, is that integrating expressions with many terms can become computationally expensive when using standard Mathematica integration routines. Fortunately, the integrands that appear in each step are structurally simple, usually consisting of combinations of powers, logarithms, and products of the two. Therefore, it is convenient to implement a custom integration function that integrates them through direct pattern-based replacements: this significantly improves performance.

As previously mentioned, the leading-order coefficients $\vec{J}^{(n_0)}$, along with the integration constants at higher orders in ϵ, are fixed by imposing boundary conditions. In total, three boundary conditions are required. The simplest way to fix them is by evaluating the three master integrals numerically at a specific point, which can be done efficiently using the package *AMFlow*[31], and then matching these values to the corresponding truncated series solution evaluated at the same point: in this way, the numerical values of the integration constants can be determined order by order in ϵ. These numerical values are then matched[34] to an appropriate set of known analytical con-

[34]The matching is carried out numerically using the Mathematica function *FindIntegerNullVector*, by

stants. The uniform transcendentality (UT) property of the canonical basis plays a crucial role in this process, as it constrains the transcendental weight of the constants that can appear at each order in ϵ, significantly narrowing down the possible combinations.

From unitarity, we know that the sunrise integral develops a branch cut starting at $s = 9$, corresponding to the physical threshold where all three internal lines go on-shell. In contrast, the points $s = 0$ and $s = 1$, while being singularities of the associated differential equations, are not physical singularities of the integrals themselves: that particular solution remains regular at these points.

As a result, when expanding the differential equations around the spurious singularities ($s = 0$, $s = 1$), the boundary values can be computed directly at the expansion point. Conversely, when working around the physical singularities ($s = 9$, $s = \infty$), the numerical evaluation must be performed at a nearby (non-singular) point.

Note that, when expanding around the spurious singularities $s = 0$ and $s = 1$, we can also use regularity as a boundary condition, imposing the coefficient of the logarithms in the general solution to vanish. However, other two BCs have to be imposed in order to fix all the constants.

An important remark is that the expansions for the canonical integrals around different points are not expected to match in the common regions of convergence since each of them is referred to a different canonical basis (see also the observation at the end of *Section 7.2*), the one constructed around the specific expansion point. However, by rotating the various series solutions back to the pre-canonical basis, one can easily check that they match, as expected.

7.5 Study of convergence and Bernoulli-like variables

In this section, we want to study convergence of the series expansions found for the master integrals of the sunrise family. To avoid confusion, it is convenient to perform this analysis after rotating the series back to the pre-canonical basis;[35] moreover we only focus on the leading-order (order 0) in ϵ for the two integrals in the top sector. Then we introduce Bernoulli-like variables and study their effect on convergence. This analysis is inspired by [37], though it includes several original observations and developments.

Here, differently from the case of the bubble integral, in estimating the error of our series solution, we avoid relying on analytic results, as for more complicated problems such expressions will be either unavailable or impractical to evaluate (this is precisely

comparing the high-precision numerical values with a predefined set of transcendental constants.

[35] In principle one can also do this analysis directly for the solutions in the canonical basis, however the radius of convergence will be influenced by that of the expansion for ω_0.

where series expansion methods prove especially effective). Instead, we assess convergence by defining the truncation error as the relative variation between two successive partial sums upon including one more order. Specifically, we define the numerical interval of convergence of a series as the region along the real s-axis where the truncation error after summing 100 orders is less than 10^{-4} (except eventually near the endpoints).

The results for the master[36] $I_{1,1,1}$ are shown in the following figure:

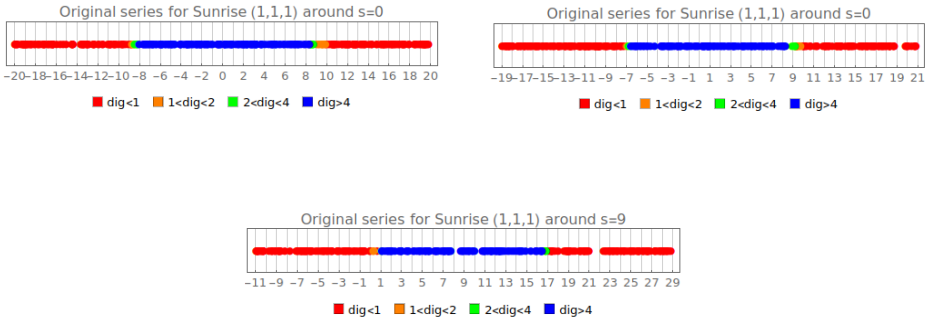

Figure 7: Relative truncation errors along real s-axis of the series for $I_{1,1,1}$ respectively around $s = 0,\ 1,\ 9$ when including 100 orders. Each color corresponds to a certain precision, expressed in digits. From these plots, we can estimate the convergence radius.

According to our numerical results and the criterion above, the expansion around $s = 0$ has radius of convergence $r_0 = 9$. This is one of the special cases, mentioned previously, where a spurious singularity ($s = 1$ in this case) does not affect the convergence of the series. This behavior is consistent with Fuchs theorem on series solutions of differential equations, since it only gives a lower bound for the radius of convergence.

In contrast, the expansion around $s = 9$ turns out to have a radius of convergence $r_9 = 8$, indicating that the spurious singularity at $s = 1$ does influence the convergence of the series in this case. This is analogous to what we observed in the expansion of the bubble integral around its physical singularity at $s = 4$.
Regarding the expansion around $s = 1$, the radius of convergence is $r_1 = 8$: the spurious singularity at $s = 0$ is not seen by the series coefficients, but the physical one at $s = 9$ is.

Using the variable s, we are able to cover the entire real s-axis using three expansion points: the expansion around $s = 0$ covers the region $-9 < s < 9$, the one around $s = 9$ covers $1 < s < 17$, the one around $s = \infty$ covers $17 < s < +\infty$ and $-\infty < s < 0$.

[36] For the other master $I_{2,1,1}$, the convergence plots are roughly the same.

Also in this case, we can improve convergence by rewriting the series in terms of Bernoulli-like variables. For the expansion around $s = 0$, we can define the variable:

$$t = -\log\left(1 - \frac{s}{9}\right) \Longleftrightarrow s = 9(1 - e^{-t}), \tag{173}$$

which maps $s = 0$ to $t = 0$, $s = 9$ and $s = \infty$ to $t = \infty$.

This change of variable works quite well. Including only 20 orders in the expansion, we get a similar precision to the one obtained with 70 terms in the original series in the variable s. Moreover, there is convergence also for points in the complex plane outside the original circle of convergence: in particular, we are able to cover (the corresponding of) the entire[37] real s-axis with a precision better than 4 digits, by including only 16 orders in the accelerated expansion, as shown in the following figure:

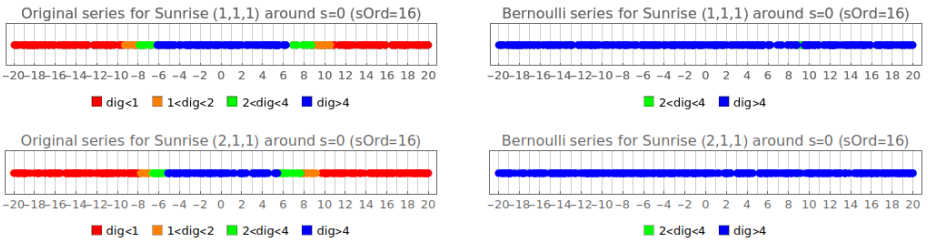

Figure 8: Relative truncation error for expansions of $I_{1,1,1}$ and $I_{2,1,1}$ with 16 terms. Left: original series; right: series in Bernoulli variable. Each color corresponds to a certain error, as indicated by the legend.

Even if the accelerated expansion around $s = 0$ is enough for numerical evaluations, it is still interesting to study the effect of a Bernoulli-like change of variable on the other expansions. Particularly interesting is the case of the expansion around $s = 9$. The corresponding Benoulli-like variable is defined by:

$$t = -\log\left(\frac{s-1}{8}\right) \Longleftrightarrow s = 1 + 8e^{-t}, \tag{174}$$

so that the expansion point $s = 9$ is mapped to $t = 0$, while $s = 1$ and $s = \infty$ are sent to $t = \infty$.

The results for the expansion of $I_{1,1,1}$ are reported in the following Figure 9.

[37] To be precise, near the singularity $s = 9$ that we pushed away, the convergence is a bit slower. This seems to be a general feature of the Bernoulli variable.

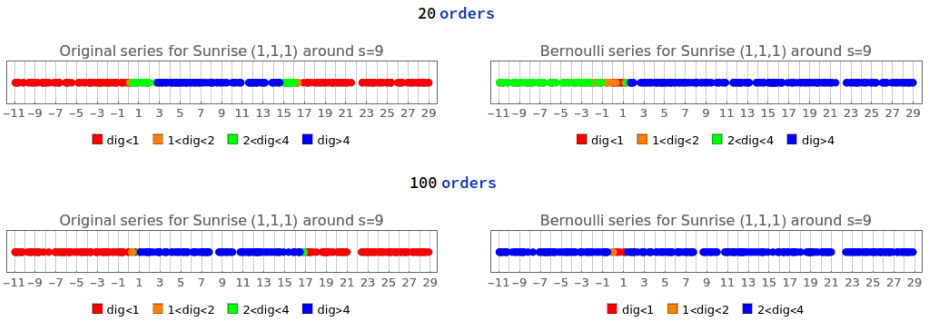

Figure 9: Relative truncation errors along the real s-axis in the expansions around $s = 9$ of $I_{1,1,1}$. Different colors indicate the error at each point. Left: original series; right: Bernoulli-variable series. In the first row both series are truncated at 20 orders, in the second one at 100 orders.

This expansion has an interesting feature. The series in the Bernoulli variable converges rapidly along most of the positive real s-axis, and more slowly on the negative side. However, there is a small region, roughly corresponding to the interval $[-1, 1]$, where the series fails to converge entirely. In this region, even after including 100 terms, the relative truncation error remains of order one, yielding no meaningful digits of precision.

This behavior is caused by the spurious singularity at $s = 0$, which affects convergence. Naively, one might expect the radius of convergence to be 9, since the expansion is centered at $s = 9$ and the closest singularity is now at $s = 0$. However, because the expansion is performed in the Bernoulli-like variable t, convergence is not limited by the actual singularities of the original function in the complex s-plane, but rather by how those singularities are mapped into the complex t-plane. Specifically, $s = 0$ is mapped to $t_0 = 3\log 2 - i\pi$, so the series is guaranteed to converge only inside a circle of radius $r = |t_0| = \sqrt{(3\log 2)^2 + \pi^2}$ in the complex t-plane.

The exterior of this disk, when mapped back into the s-plane, identifies[38] a region whose intersection with the real axis lies mostly within $[-1, 1]$. Therefore, the Bernoulli change of variable (174) effectively compresses the divergent behavior into a narrow region, enabling rapid convergence almost everywhere else. This explains the observed behavior.

More generally when there are many singularities, pushing one of them away also changes the relative positions of the others with respect to the expansion point and this could also have bad effects on convergence. Therefore, for problems with many

[38] Note, however, that we are not claiming *all* points in the excluded region map to $s \in [-1, 1]$, only that most of them do. Conversely, using (174), one finds that the condition $-1 \leq s \leq 1$ corresponds to $t = u + i(2k + 1)\pi$, with $u \geq 2\log 2$, $k \in \mathbb{Z}$. Thus, all such points satisfy $|t| \geq \sqrt{(2\log 2)^2 + \pi^2}$, so most of them lie outside the circle of convergence in t-plane.

singularities, a naive Bernoulli-like change of variable is not guaranteed to work. In the next section, we will discuss an attempt of generalization for integrals with multiple singularities.

7.6 An attempt of generalizing Bernoulli-like transformations

We ask whether it is possible to generalize the standard Bernoulli-like change of variables in the presence of multiple singularities, in such a way that more than one finite singularity is mapped to infinity, potentially leading to improved convergence.

For simplicity, we consider a problem with two finite singularities (excluding the expansion point) and a third singularity at infinity. One possible approach in order to simultaneously send both finite singularities to infinity, while preserving the singularity at infinity, is to apply two consecutive Bernoulli-like transformations.

Let us now analyze this procedure in a general setting.
We consider a complex function $f(s)$, with singularities at $s = s_1$, $s = s_2$, and at infinity, and focus on its expansion around a point $s = s_0$. The singularity at $s = s_1$ can be pushed to infinity by performing a first Bernoulli-like change of variable:

$$t = -\log\left(\frac{s - s_1}{s_0 - s_1}\right) \quad \Longleftrightarrow \quad s = s_1 + (s_0 - s_1)e^{-t}. \tag{175}$$

Under this transformation, the location of the second singularity, $s = s_2$, in the complex t-plane becomes:

$$t_2 = -\log\left(\frac{s_2 - s_1}{s_0 - s_1}\right). \tag{176}$$

To push this second singularity further away, we introduce a second Bernoulli-like variable:

$$z = -\log\left(\frac{t - t_2}{-t_2}\right) = -\log\left(1 - \frac{t}{t_2}\right), \tag{177}$$

where we used the fact that the original expansion point $s = s_0$ corresponds to $t_0 = 0$.

The resulting double Bernoulli-like variable z is thus given by:

$$z = -\log\left[1 - \frac{1}{a}\log\left(\frac{s - s_1}{s_0 - s_1}\right)\right] \quad \Longleftrightarrow \quad s = s_1 + (s_0 - s_1)e^{a(1-e^{-z})}, \tag{178}$$

where we defined $a = \log\left(\frac{s_2 - s_1}{s_0 - s_1}\right)$.
This transformation maps the expansion point $s = s_0$ to $z = 0$, and sends the singularities $s = s_1$, $s = s_2$, and $s = \infty$ to infinity, but along three distinct directions in the complex z-plane.

At first glance, this appears to be a promising change of variable for improving convergence. However, numerical tests show that this transformation does *not* yield an infinite radius of convergence in the z-plane, as one might hope.

The reason becomes clear upon inspecting the expression for $s(z)$ in Eq. (178). The singularity at $s = s_2$ arises not only in the limit $z \to +\infty$, but also at an infinite set of complex points:

$$z_n = -\log\left(\frac{2\pi i n}{a}\right). \tag{179}$$

The one closest to the origin dictates the radius of convergence, which remains finite.

Therefore, while this generalized change of variable seems to push multiple singularities to infinity along different directions, it does *not* lead to convergence everywhere in the complex z -plane. Depending on the specific configuration of singularities, the resulting convergence properties may be better or worse than those obtained using the standard Bernoulli-like transformation.

We leave a more systematic investigation of such generalizations and their convergence behavior to future work. In the following chapters, we will instead focus on expansion techniques for problems characterized by multiple scales, and explore whether it is possible to use Bernoulli-like changes of variable to accelerate convergence and extend the region of convergence. This question is particularly relevant, as expansions involving two or more variables typically come with significant computational costs, both in terms of time and memory. Therefore, achieving faster convergence could offer substantial practical advantages.

8 Accelerate series expansions for multi-scale problems

In this chapter, we propose a heuristic method to extend the region of convergence and accelerate the convergence rate of multi-variable series expansions, by introducing several Bernoulli-like variables. This approach is not a fully algorithmic or general prescription, but rather a set of guiding principles and practical steps to be mindful of when dealing with multi-dimensional problems with a complicated singularity structure. Our approach is inspired by the work of [19].

To test the effectiveness of this approach, we apply it to two different amplitudes: one [20] describing the decay of a Higgs boson into three gluons, and the other [21] describing the similar process for a Z boson. Both amplitudes are expressed in terms of two-dimensional multiple polylogarithms (2D MPLs), offering a well-controlled setting for our analysis.

8.1 Bernoulli-like variables for 2D series expansions

Let us illustrate the procedure in the case of a two-dimensional problem.

Consider a function $f(x, y)$, with singularities that typically form curves in the (x, y) plane. Our goal is to construct series expansions for f with improved convergence properties covering a desired region. The main steps are the following:

1. **Define the target region and analyze singularities**
   Identify the portion of the (x, y) plane to be covered. The method works better when this region is bounded and the singularities are straight lines.

2. **Choose the expansion points**
   The most critical points for expansions are the intersections of singular curves; therefore, it is reasonable to choose one of them as the expansion point. However, unlike the one-dimensional case, a naive expansion around such a point may fail if more than two singular curves intersect at that point or if even two curves are tangent there.

3. **Apply blow-ups when necessary**
   In cases of complicated intersections or tangencies at the expansion point, perform a suitable change of variables (a "blow-up") to resolve overlapping singularities, effectively separating them to produce well-defined expansions.
   In practice, after the blow-up, the original expansion point is mapped to an entire

line, and one must choose a specific point of it as the new expansion point. This corresponds to expanding around the original point in a particular direction.

4. **Analyze singularities**

   Carefully examine the geometry of singularities and identify the ones which most limit convergence. Typically these are the ones closest to the expansion point, but not necessarily: in fact, even singularities outside the region of interest can affect convergence within it.

   If a blow-up was performed in the previous step, this analysis must be performed directly in the new variables, as the transformation changes the shape and relative position of the singularities and the region of interest.

5. **Introduce the first Bernoulli-like variable**

   Starting from the series expansion in the original (or blown-up) variables, replace one variable by performing a Bernoulli-like transformation designed to push the nearest problematic singularity to infinity. Re-expand in the new variables up to the same order.

6. **Introduce the second Bernoulli-like variable**

   Perform a similar transformation for the second variable, removing another limiting singularity, and then re-expand. There is no universal rule for which singularities to remove; intuition based on the transformed geometry of the singularities and the region of interest guides this choice, as we will better see in the examples.

7. **Cover the entire region with multiple expansions if needed**

   If one expansion cannot cover the full region of interest, select additional expansion points following the criteria above and patch together their respective expansions.

8.2 Higgs decay into three gluons at two-loops

The first amplitude used for testing our procedure is a two-loops helicity amplitude for the decay of an Higgs boson into three gluons, computed in [20].

In the Standard Model (SM), the Higgs boson only interacts with massive particles, therefore it cannot couple directly to gluons. However, starting at one loop, it can interact with gluons through loops of massive quarks. Since the process starts at one loop, computing higher order corrections in the full theory is complicated. However, since the most important contributions come from loops involving the top quark, which is the heaviest particle in the Standard Model, the computation can be performed in an

Effective Field Theory (EFT),[39] where the top quark is integrated out ($m_t = \infty$). The effective Lagrangian is:

$$\mathcal{L}_{int} = -\frac{\lambda}{4} H G_a^{\mu\nu} G_{a,\mu\nu}, \tag{180}$$

where $G_a^{\mu\nu}$ is the field strength tensor of the gluons and H is the Higgs field. In this theory, the calculation already starts at tree-level, having an Hgg vertex in addition to the QCD vertices.

8.2.1 Kinematics

Let us describe the kinematics of our process:

$$H(p_4) \longrightarrow g_1(p_1) + g_2(p_2) + g_3(p_3). \tag{181}$$

The Mandelstam invariants are given by:

$$s_{12} = (p_1 + p_2)^2, \qquad s_{13} = (p_1 + p_3)^2, \qquad s_{23} = (p_2 + p_3)^2, \tag{182}$$

and satisfy:

$$s_{12} + s_{13} + s_{23} = M_H^2, \tag{183}$$

where M_H is the Higgs mass. We define the dimensionless ratios:

$$x = \frac{s_{12}}{M_H^2}, \qquad y = \frac{s_{13}}{M_H^2}, \qquad z = \frac{s_{23}}{M_H^2}. \tag{184}$$

In terms of them, (183) is rewritten as:

$$x + y + z = 1. \tag{185}$$

In the decay region the invariants are non-negative, e.g. for s_{12} we have:

$$s_{12} = (p_1 + p_2)^2 = 2p_1 \cdot p_2 = 2(E_1 E_2 - \vec{p_1} \cdot \vec{p_2}) = 2E_1 E_2 (1 - \cos\theta_{12}) > 0, \tag{186}$$

where we used that for massless on-shell particles $p^2 = 0$, $|\vec{p}| = p^0 \equiv E$.
This, together with (185), defines the kinematic region:

$$z \geq 0, \qquad 0 \leq y \leq 1 - z, \qquad x = 1 - y - z. \tag{187}$$

Therefore, there are two independent scales that will appear in the amplitude (in (187) we chose y and z, but any other choice could have been made) and the physical region is a triangle in the plane of these two variables.

[39] Note that the ratio m_H/m_t is not that small, so it is not entirely obvious that this is a good approximation, but it often is, in practice.

8.2.2 The amplitude

In this section, we just want to briefly describe how the amplitude was computed in reference [20].

1) The first step is the tensor reduction. The amplitude has the form:

$$\mathcal{M} = S_{\mu\nu\rho}(p_1, p_2, p_3)\epsilon_1^\mu \epsilon_2^\nu \epsilon_3^\rho, \tag{188}$$

where ϵ_i denote the polarization vectors of external gluons; $S_{\mu\nu\rho}$ can contain only a limited number of tensor structures, built out of the gluons four-momenta and the metric tensor. One can find such a tensor basis and project the amplitude on it, so that he has to work only with the scalar coefficients of the amplitude with respect to this basis, known as form factors. In particular, in the reference paper, they show that there are four independent[40] tensor structures, so the amplitude can be decomposed as:

$$\mathcal{M} = \sum_{i=1}^{4} \mathcal{G}_i T_i, \tag{189}$$

where $\{T_i\}$ is the basis of tensor structures, already contracted with gluon polarizations, and $\mathcal{G}_i$ are the form factors. The latter can be obtained by applying suitable projector operators $\mathcal{P}_i$ on the full amplitude expanded in Feynman diagrams:

$$\mathcal{G}_i = \sum_{pol} \mathcal{P}_i \mathcal{M}, \qquad \text{with} \quad \mathcal{P}_i = \sum_{j=1}^{4} c_i^{(j)} T_j^\dagger, \quad c_i^{(j)} = (T_j^\dagger T_i)^{-1}. \tag{190}$$

This tensor basis is useful to obtain compact expressions for the helicity amplitudes, where the external gluon polarizations are fixed:

$$\mathcal{M}^{\lambda_1\lambda_2\lambda_3} = S_{\mu\nu\rho}(p_1, p_2, p_3)\epsilon_{1,\lambda_1}^\mu(p_1)\epsilon_{2,\lambda_2}^\nu(p_2)\epsilon_{3,\lambda_3}^\rho(p_3). \tag{191}$$

In particular, there are only due independent helicity amplitudes for this process, which are chosen to be $\mathcal{M}^{+++}$ and $\mathcal{M}^{++-}$: all the others can be obtained from them by parity conjugation and relabeling of gluon momenta.

Using the tensor decomposition (189) in the found basis $\{T_i\}$, the helicity amplitudes can be written compactly in terms[41] of spinor products:

$$\mathcal{M}^{+++} = \alpha \frac{M_H^4}{\sqrt{2}\langle 12\rangle\langle 23\rangle\langle 31\rangle}, \qquad \mathcal{M}^{++-} = \beta \frac{[12]^3}{\sqrt{2}[23][13]}, \tag{192}$$

[40] In particular, they restrict the number of tensor structures using the transversality conditions $\epsilon_i \cdot p_i = 0$, $i = 1, 2, 3$ and the cyclic gauge choice: $\epsilon_1 \cdot p_2 = \epsilon_2 \cdot p_3 = \epsilon_3 \cdot p_1 = 0$.

[41] One simply has to compute the basis elements T_i using the specific gluon polarizations, expressed in the spinor-helicity formalism.

where the new form factors α and β are linear combinations of the original form factors $\mathcal{G}_i$; they can also be computed directly by defining some helicity projectors[42] $\mathcal{P}_\alpha$ and $\mathcal{P}_\beta$, so that:

$$\alpha = \sum_{pol} P_\alpha M, \qquad \beta = \sum_{pol} P_\beta M. \tag{193}$$

2) At each order in the perturbative expansion, the contribution of Feynman diagrams to the form factors can be written as a combination of scalar Feynman integrals. These integrals are computed with the usual machinery: reduction to MIs, derivation of DEs for MIs in the variables y and z, rotation to a canonical basis and solution of the canonical equations.

3) The last step, which we will not describe in detail, consists in the UV renormalization and the IR regularization of the amplitude.

The final expressions for the form factors α and β, computed up to $o(\epsilon^2)$, involve 2D MPLs [19] with the following alphabet:

$$\{y, z, 1-y, 1-z, y+z, 1-y-z\}, \tag{194}$$

where the letters correspond to the singularities of the differential equations for the relevant master integrals.

However, as showed in literature [13], this result can be written entirely in terms of classical polylogarithms.

8.2.3 Improving the convergence

We focus on the two-loop contribution to the form factor β, which has the largest expression. Our goal is to obtain series expansions for it valid within the physical region and to improve their convergence using the method described in *Section 8.1*.

The expression that we have to expand involves two-dimensional multiple polylogarithms (2D MPLs) in variables y and z, with alphabet given by (194). Note that only $x = 0$, $y = 0$ and $z = 0$ correspond to true[43] singularities of the amplitude, associated respectively to the physical thresholds $s_{12} = 0$, $s_{13} = 0$, $s_{23} = 0$. The other three letters correspond to spurious singularities inherited from the differential equations. The amplitude is not singular at those lines and they are also outside the physical region; however, they can still limit convergence of the series expansions.

As previously said, the physical region is the triangle defined by (187). This is showed in Figure 10, together with the various singular lines.

[42] They are built by replacing in the expressions for α and β the $\mathcal{G}_i$ with the corresponding projectors $\mathcal{P}_i$; so, in the end, they will be expressed in terms of the basis elements T_i.

[43] One can also check that these are the only singularities of the expression for β by decomposing it in a basis of rational functions and computing the symbol for the combinations of MPLs that appear as coefficients of the expression with respect to this basis.

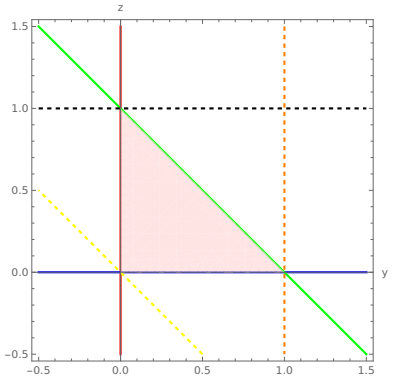

Figure 10: The figure shows the physical region (highlighted) in the variables (y,z) and the singularities of the involved MPLs: the solid lines are singularities for the full expression, the dashed ones are spurious singularities.

Our aim is to obtain expansions with at least four-digit precision over the entire region. We choose $(y, z) = (0, 0)$ as the first expansion point. We note that there are three singular lines passing through this point, therefore we need to perform a blow-up. In particular, we set:

$$\begin{cases} y = t \\ z = vt \end{cases} . \tag{195}$$

The following plot shows how the singularities are remapped in the blown-up space:

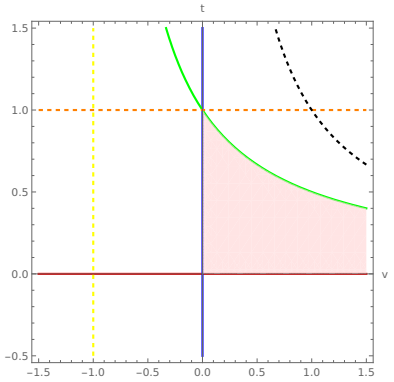

Figure 11: The figure shows the physical region (highlighted) in the variables (t,v) of the blow-up and the singularities of the involved MPLs: the solid lines are singularities for the full expression, the dashed ones are spurious singularities. Note that the blow-up has changed the relative position of singularities.

Now there are only two singularities passing trough the point $(t, v) = (0, 0)$; therefore the expression can be expanded in t and v around that point, which corresponds in

the original space to expanding around the origin $(x, y) = (0, 0)$, approaching it along the direction[44] of the y axis. Equivalently, we are requiring y to go to zero faster then z; therefore we can expect the expansion to work better in the region where $y < z$.

In practice, using the Mathematica package *PolyLogTools* [15], we fiber our expression involving 2D MPLs of t and v with respect to a chosen ordering of the two variables: this means that, after fixing an ordering of the two variables, the expression is rewritten as a linear combination of MPLs in the first variable, whose singularities may depend on the second one, multiplied by MPLs in the second variable whose singularities are constant. This decomposition is performed automatically by using the function *ToFibrationBasis*. Then we can expand[45] in these variables following the specified order. In this way, we get a well-defined series expansion for the two-loop contribution to the form factor β. In the following, we will refer to it as the "original" expansion.

The convergence of this expansion can be improved by introducing two Bernoulli-like variables, with the method previously presented. In particular, there are four singular curves we can move: one corresponds to the original physical singularity $y+z-1 = 0$, the other three are the spurious singularities.

Naively, one might consider choosing the physical singularity, which is also the closest to the expansion point, as the first to be pushed away. However, this is not a good choice: in fact, its effect is to extend the physical region up to infinity in such a way that some other singularities, previously outside, may now fall within it. This can lead to a deterioration in convergence, potentially making the situation worse than before.

Instead, a good solution is to push away the curves corresponding to the original (spurious) singularities $y = 1$ and $z = 1$. In particular, we proceed in the following way. Starting from the expression fibrated in v, we expand in that variable and then replace it by setting:

$$v = \frac{1 - e^{-s}}{t} \Longleftrightarrow s = -\log(1 - vt), \tag{196}$$

where we introduced the first Bernoulli-like variable s, such to map the singularity $vt = 1$ (or equivalently $z = 1$) to infinity.
After re-expanding in s, we then expand the resulting expression in t and introduce a second Bernoulli-like variable pushing away $t = 1$ (or equivalently $y = 1$), by setting:

$$t = 1 - e^{-u} \Longleftrightarrow u = -\log(1 - t). \tag{197}$$

Finally, we re-expand in u, getting a series in the two variables (u, s).

The following figure shows the physical region and the relative positions of singularities in the (u, s) plane:

[44] Recall that $v = v_0$ identifies the direction of the line $z = v_0 y$.
[45] This is done by using the function *ExpandPolyLogs* of *PolyLogTools*.

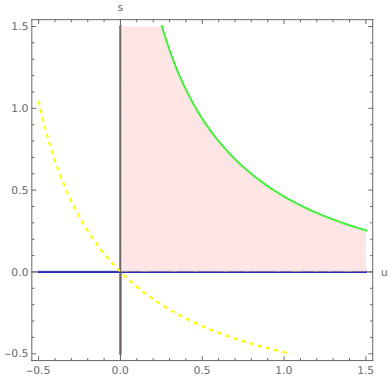

Figure 12: The figure shows the remapping of physical region (highlighted) and singularities of the involved MPLs in the space of Bernoulli variables (u, s) : the solid lines are singularities for the full expression, the dashed ones are spurious singularities. Note that two singularities have disappeared.

Note that the previous changes of variables reintroduce a third singular line crossing the origin. In principle, this should be eliminated by performing again a blow-up; however, for this particular case, one can realize[46] that these variables already produce a well-defined expansion.

At this stage, we numerically evaluate both the original series and the one in Bernoulli variables at random points within the kinematic region. These values are then compared with the corresponding evaluations of the full original [47] expression. This allows us to estimate the accuracy of both expansions as the relative difference with the corresponding exact values, testing in this way the effectiveness of our procedure. The results are showed in Figure 13 where the local accuracy, computed by including 20 orders in both variables, is represented by the color of each point.

[46]The only terms in the expansion where s and u are not separated are of the form $\log(s/u)$, so they can be directly replaced by $\log(s) - \log(u)$, producing a well-defined two-variables expansion.

[47]In fact, in this case, it is possible to evaluate the original expression in MPLs by using the function *Ginsh* of PolyLogTools.

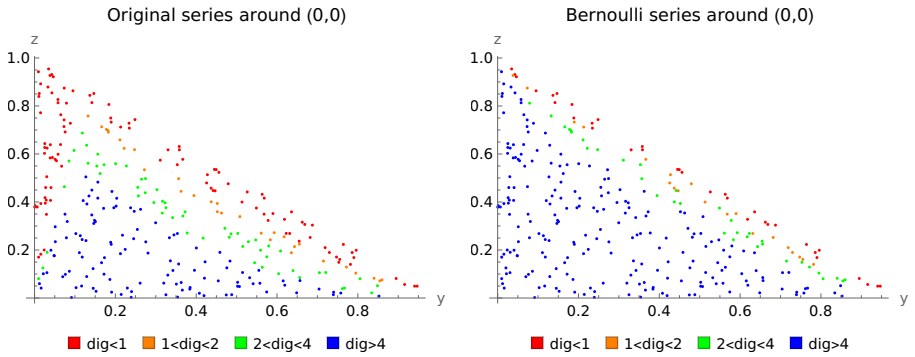

Figure 13: Numerical errors for expansions of β around $(y, z) = (0, 0)$ including 20 orders. On the left there is the expansion in the original variables, on the right the one in Bernoulli variables. Each color corresponds to a certain relative error with respect to the Ginsh evaluation, expressed in terms of digits.

It is evident that the introduction of Bernoulli-like variables via the described procedure has notably improved the convergence: for a fixed number of orders, we are able to get a precision larger than four-digits in a much wider region. However, twenty orders are not enough to cover the entire physical region with the required accuracy. One possibility could be to increase the number of orders, but this is unpractical for a huge expansion like this. However, as suggested in *Step 7*, we can repeat the same procedure for the other two corners of the triangle defining the kinematic region, and then combine the three accelerated expansions.

In particular, exploiting the symmetry of the alphabet under the exchange of y, z, and $x = 1 - y - z$ (due to the fact that the final states involves three particles of the same kind), one can use for blowing up the same position as (195), up to relabeling of x, y and z. In particular, choosing as expansion point $(y, z) = (1, 0)$, corresponding to $(x, z) = (0, 0)$, we set:

$$\begin{cases} y = 1 - (v+1)t \\ z = vt \end{cases} . \tag{198}$$

For the expansion around $(y, z) = (0, 1)$, corresponding to $(y, x) = (0, 0)$, we set:

$$\begin{cases} y = vt \\ z = 1 - (v+1)t \end{cases} . \tag{199}$$

The subsequent definitions of Bernoulli-like variables are identical to (196) and (197). The following plots in Figure 14 and Figure 15 show the results for these last two expansions, that are analogous to the first one.

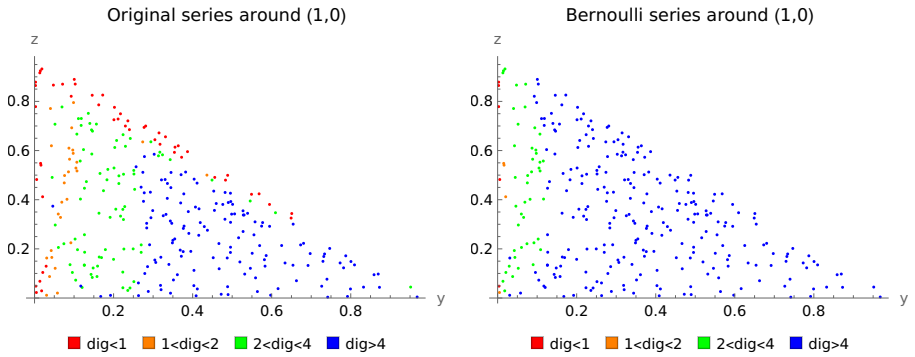

Figure 14: Numerical errors for expansions of β around $(y, z) = (1, 0)$ including 20 orders. On the left there is the expansion in the original variables, on the right the one in Bernoulli variables. Each color corresponds to a certain relative error with respect to the Ginsh evaluation, expressed in terms of digits.

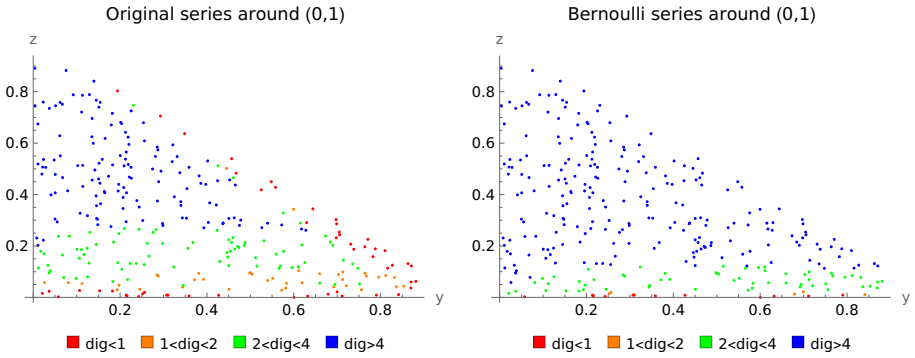

Figure 15: Numerical errors for expansions of β around $(y, z) = (0, 1)$ including 20 orders. On the left there is the expansion in the original variables, on the right the one in Bernoulli variables. Each color corresponds to a certain relative error with respect to the Ginsh evaluation, expressed in terms of digits.

By combining the three expansions, we can obtain high-accuracy evaluations in the entire physical region. An interesting aspect is that, as shown in Figure 16, the required accuracy can be obtained including only 10 orders in both Bernoulli-like variables, while at least 20 were needed in the original variables. This is a big advantage from the point of view of computation time and memory.

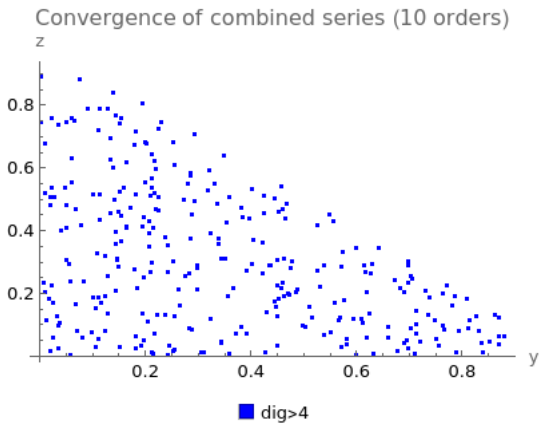

Figure 16: Numerical errors for an optimal combination of the three expansions around the corners of the triangle. Including only 10 orders in both variables, we get an accuracy of more than four digits in the entire physical region.

8.3 Z decay into three gluons at two-loops

Now, we want to apply our method to the amplitude for another process, namely the decay of a Z boson into three gluons:

$$Z(p_4) \longrightarrow g(p_1) + g(p_2) + g(p_3). \tag{200}$$

This amplitude was computed in [21], with the same[48] procedure described in *Section 9.2.2*. The kinematics is also the same and the results, up to two loops, are expressed in terms of MPLs with the same alphabet as (194). The only difference is that this amplitude is intrinsically more involved, as it is not known to admit a representation in terms of classical polylogarithms, unlike the previous case.

There are two independent helicity amplitudes for this process: $\mathcal{M}_{+++}$ and $\mathcal{M}_{+--}$. In particular, we focus on $\mathcal{M}_{+++}$, which depends on six form factors: $\{\alpha_i\}_{i=1,2,3}$ and $\{\beta_i\}_{i=1,2,3}$, whose expressions are reported in the ancillary files of the reference paper [21].

Being the physical region and the relative positions of singularities the same as for the amplitude in the previous section, we expect to obtain accelerated series expansions by using identical definitions for the blow-ups and the Bernoulli-like changes of variables.

In the following, we report the results for the expansions of the form factor α_1 around the three corners; the plots on the left are referred to the original series ex-

[48] Apart from the complications coming from having a massive vector boson in the initial state, instead of a scalar particle.

pansions (the ones in the blow-up variables), those on the right are referred to the corresponding series in Bernoulli-like variables.

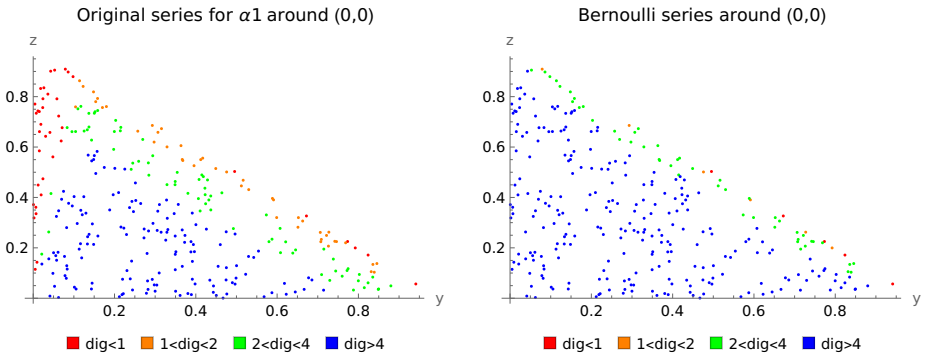

Figure 17: Numerical errors for expansions of α_1 around $(y, z) = (0, 0)$ including 20 orders. On the left there is the expansion in the original variables, on the right the one in Bernoulli variables. Each color corresponds to a certain relative error with respect to the Ginsh evaluation, expressed in terms of digits.

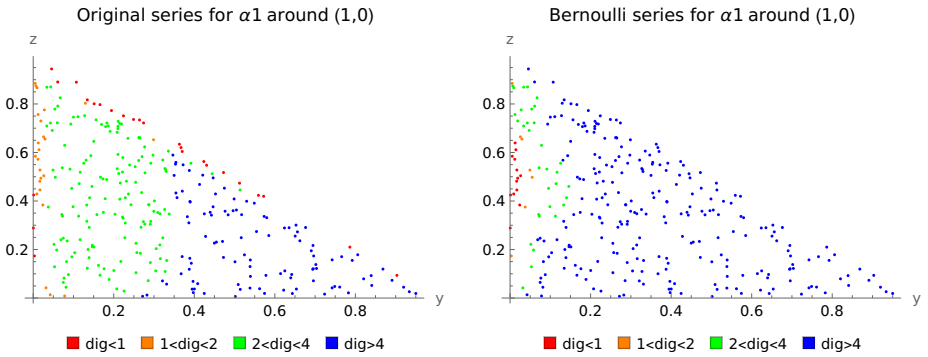

Figure 18: Numerical errors for expansions of α_1 around $(y, z) = (1, 0)$ including 20 orders. On the left there is the expansion in the original variables, on the right the one in Bernoulli variables. Each color corresponds to a certain relative error with respect to the Ginsh evaluation, expressed in terms of digits.

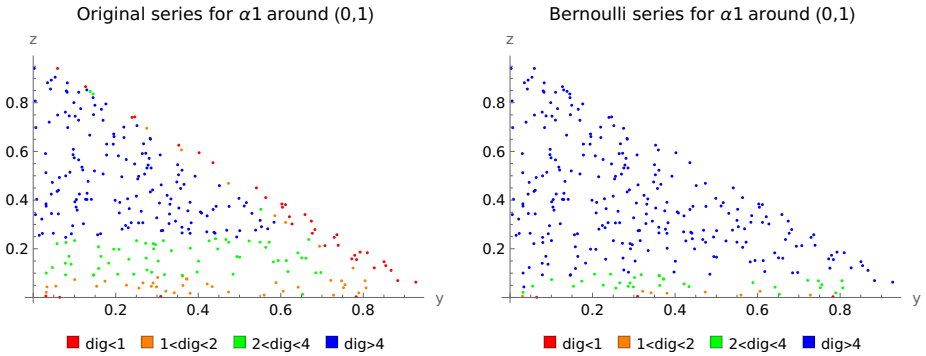

Figure 19: Numerical errors for expansions of α_1 around $(y, z) = (0, 1)$ including 20 orders. On the left there is the expansion in the original variables, on the right the one in Bernoulli variables. Each color corresponds to a certain relative error with respect to the Ginsh evaluation, expressed in terms of digits.

Also in this case, the introduction of two Bernoulli-like variables has extended the region of convergence. We can combine the three accelerated expansions obtaining, with only 9 orders, an accuracy exceeding four digits in the entire kinematic region, as showed in Figure 20. The same also works for the other form factors.

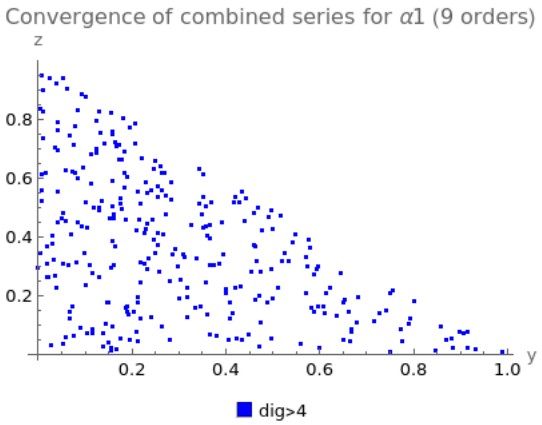

Figure 20: Numerical errors for an optimal combination of the three expansions around the corners of the triangle. Including only 9 orders in both variables, we get an accuracy of more than four digits in the entire physical region.

This shows us that our method for accelerating 2D series expansions also works for an amplitude not expressible in terms of classical polylogarithms. In the next chapter, we will test its applicability to a problem with elliptic geometry.

9 An elliptic 2D case: the two-masses sunrise

In the previous chapter, we started from exact analytic expressions for two-scale amplitudes, expanded them, and applied our acceleration method. In this chapter, by contrast, we directly construct series solutions from differential equations, as we did in simpler one-scale cases.

We focus on the sunrise integral family with two equal masses and a third, distinct mass. The general case with arbitrary masses has been treated analytically in [3]. A series expansion method was proposed in [11], based on expanding the only differential equations in the Mandelstam variable s, treating the problem effectively as one-dimensional. This approach was later extended into a numerical implementation in [10]. In contrast, our goal here is to derive a fully two-dimensional expansion in the relevant scales, capturing the complete structure of the problem.

While our overall strategy parallels that used in *Chapter 7* for the equal-mass case, the presence of two scales introduces additional complications. Although this computation is much less demanding than evaluating a full amplitude, it is conceptually richer than the cases studied in the previous chapter: the underlying geometry is elliptic, rather than polylogarithmic. This makes it a meaningful test case for assessing how well our acceleration method extends beyond MPLs, which is the topic of the final section.

9.1 MIs and differential equations

In this section, we define the integral family, choose a basis of MIs and a set of independent scales and write the DEs for the MIs in those variables.

The topology is the same as for the equal-mass case, but now one of the three internal lines carries a different mass with respect to the other two. Thus, the generic integral of this family is:

$$\begin{aligned} I_{\nu_1,\nu_2,\nu_3,\nu_4,\nu_5} &= \frac{e^{2\gamma_E\epsilon}}{i\pi^D}\int \frac{d^Dk_1 d^Dk_2}{D_1^{\nu_1}D_2^{\nu_2}D_3^{\nu_3}D_4^{\nu_4}D_5^{\nu_5}} \\ \text{with} \qquad & D_1 = k_1^2 - m^2,\ D_2 = k_2^2 - M^2,\ D_3 = (k_1 - k_2 - p)^2 - m^2, \\ & D_4 = (k_1 - p)^2,\ D_5 = (k_2 - p)^2. \end{aligned} \tag{201}$$

As for the equal-mass case, we proceed with the IBP reduction and the derivation of the differential equations. The reduction reveals that there are 5 MIs. In particular,

we choose the following basis of masters:

$$\{I_1 = I_{1,1,0,0,0},\, I_2 = I_{1,0,1,0,0},\, I_3 = I_{1,1,1,0,0},\, I_4 = I_{1,1,2,0,0},\, I_5 = I_{1,1,1,0,-1}\}, \quad (202)$$

of which the first two are two-loops tadpoles, the last three are sunrises.

There are three scales in the problem, of which only two are independent; we can take them to be the symmetric variables: $x = \frac{s}{m^2}$ and $y = \frac{s}{M^2}$. The differential equations for the master integrals in that variables have the form:

$$\partial_x \vec{I}(x,y) = A_x(x,y)\vec{I}(x,y), \qquad \partial_y \vec{I}(x,y) = A_y(x,y)\vec{I}(x,y), \quad (203)$$

where the explicit expressions of matrices A_x and A_y are reported in the *Appendix*.

9.2 Finding a canonical form

Now we aim to write the DEs in canonical form. The procedure is almost identical to the equal-mass case, but there are two main complications: the top sector contains three masters; the presence of two scales leads to two coupled systems of DEs that must be made canonical simultaneously. Consequently, the functions introduced during the rotation must depend on both scales.

We begin by focusing on the matrix A_x of DEs in the variable x, which we aim to make canonical first. We move to a derivative basis, where the second integral in the top sector is taken to be the derivative of the first one (I_3). Looking at the homogeneous part of the differential equations for the three master integrals in the top sector at $\epsilon = 0$, we realize that I_5 decouples from the others, leaving only two coupled masters in the top sector. This implies that the underlying geometry remains elliptic.
For this 2×2 coupled block, we compute the Wronskian matrix and perform a rotation by the inverse of its semi-simple part, just as in the equal-mass case. Next, we rescale the fourth master integral by a factor[49] $1/\epsilon$.

The rotation performed up to now is described by the matrix:

$$R_1 = \begin{pmatrix} \epsilon^2 & 0 & 0 & 0 & 0 \\ 0 & \epsilon^2 & 0 & 0 & 0 \\ 0 & 0 & \epsilon^2 & 0 & 0 \\ 0 & 0 & 0 & \epsilon & 0 \\ 0 & 0 & 0 & 0 & \epsilon^2 \end{pmatrix} \cdot \begin{pmatrix} 1 & 0 & 0 & 0 & 0 \\ 0 & 1 & 0 & 0 & 0 \\ 0 & 0 & \omega_0(x,y) & 0 & 0 \\ 0 & 0 & \partial_x\omega_0(x,y) & \frac{\det W(x,y)}{\omega_0(x,y)} & 0 \\ 0 & 0 & 0 & 0 & 1 \end{pmatrix}^{-1} \cdot \begin{pmatrix} 1 & 0 & 0 & 0 & 0 \\ 0 & 1 & 0 & 0 & 0 \\ 0 & 0 & 1 & 0 & 0 \\ 0 & 0 & 0 & 2 & 0 \\ 0 & 0 & 0 & 0 & 1 \end{pmatrix}, \quad (204)$$

[49] As in the equal-mass case, all three master integrals in the top sector are multiplied by a factor ϵ^2 for conventional normalization.

where the x-dependence of $\omega_0(x,y)$ is fixed by taking the regular solution to the second order partial differential equation(PDE):[50]

$$\partial_x^2\omega(x,y)+\frac{48x^2+(-1+y)^2-16x(1+y)}{x(16x^2+(-1+y)^2-8x(1+y))}\partial_x\omega(x,y)-\frac{2(1-6x+y)}{x(16x^2+(-1+y)^2-8x(1+y))}\omega(x,y)=0. \tag{205}$$

At this stage, we have to remove the remaining non ϵ-factorized terms. However, unlike the equal-mass case, here they are not just total derivatives of rational functions in $x, y, \omega_0(x,y), \partial_x\omega_0(x,y)$. To integrate them out, we need to introduce a new function $G(x,y)$ which is defined by its partial derivatives, constructed to involve ω_0 and its derivatives in such a way that the unwanted terms in A_x exactly cancel.
Specifically, the additional rotation needed to achieve a canonical form for A_x is given by:

$$R_2=\begin{pmatrix}1&0&0&0&0\\0&1&0&0&0\\0&0&1&0&0\\4G(x,y)&-10G(x,y)&6G(x,y)&G(x,y)&6G(x,y)\\0&0&2G(x,y)&0&1\end{pmatrix}\cdot\begin{pmatrix}1&0&0&0&0\\0&1&0&0&0\\0&0&1&0&0\\0&0&f(x,y)\omega_0^2(x,y)&1&0\\0&0&h(x,y)\omega_0(x,y)&0&1\end{pmatrix}, \tag{206}$$

where: $f(x,y)=(80x^2+(-1+y)^2-24x(1+y))/2$, $h(x,y)=2(2x-y-1)$ and $G(x,y)$ must satisfy:

$$\partial_x G(x,y)=-\omega_0(x,y). \tag{207}$$

Up to this point, we have only fixed the x-dependence of ω_0 and G. To make A_y canonical in the same basis, we only need to properly fix the y-dependence of these functions. For $\omega_0(x,y)$, the y-dependence is already fixed by the other partial differential equation[51] for periods:

$$\partial_y\omega(x,y)=\frac{x-y}{(-1+y)y}\omega(x,y)+\frac{x-4x^2+3xy}{2y(1-y)}\partial_x\omega(x,y). \tag{208}$$

Regarding $G(x,y)$, we can require:

$$\partial_y G(x,y)=\frac{-2x(-1+4x-3y)\omega_0(x,y)-x[16x^2+(-1+y)^2-8x(1+y)]\partial_x\omega_0(x,y)}{4y(-1+y)}. \tag{209}$$

This is the only condition that $G(x,y)$ must satisfy for the non ϵ-factorized terms to cancel in A_y. Note that it still remains defined up to a constant, which does not affect the ϵ-factorization of DEs.

[50] This is the homogeneous equation in x at $\epsilon=0$ for the 2x2 coupled subsector.
[51] This is the homogeneous equation in y at $\epsilon=0$ for the 2x2 coupled subsector.

In the final basis, both systems of DEs are in canonical form. However, the canonical matrices $\tilde{A}_x$ and $\tilde{A}_y$ depend explicitly on ω_0 and G; therefore, we need to evaluate these functions. In the next section, we will find series expansions for them by solving the corresponding differential equations.

9.3 Series expansions for $\omega_0(x, y)$ and $G(x, y)$

The goal of this section is to find series expansions for the functions ω_0 and G, which appear in the canonical matrices. Analytical expressions for them are known in terms of elliptic functions [16]; however, since we are interested in numerical evaluations, it is more practical to express them in the form of series expansions.

We know that $\omega_0(x, y)$ is the regular solution to the PDEs (205) and (208). To determine it, we proceed as follows:

- First, we solve the second-order equation (205) via a Frobenius expansion in x. This determines the x-dependence of the solution. The general solution takes the form:
$$\omega(x, y) = c_0(y)\omega_{0,x}(x, y) + c_1(y)\omega_{1,x}(x, y), \tag{210}$$
where $\omega_{0,x}$ and $\omega_{1,x}$ denote respectively partial regular and singular solutions of the system, which differ from the full solutions ω_0 and ω_1 by multiplicative factors depending on y, that for the moment are not fixed.

- The functions $c_0(y)$ and $c_1(y)$ are determined by substituting the ansatz (210) into the second PDE, (208). By requiring the coefficients of x and $x \log x$ to vanish, we obtain ODEs for $c_0(y)$ and $c_1(y)$, which can be solved exactly.

- Finally, we substitute the expressions for $c_0(y)$ and $c_1(y)$ back into (210) and expand in y. The resulting general[52] solution takes the form of a linear combination of two independent solutions: the regular one is ω_0, the one involving logarithms is ω_1.

Here, we just report the first few orders of the series solutions around $(x_0, y_0) = (0, 0)$:

$$\begin{aligned}
\omega_0(x, y) &= 1 + y + y^2 + x(2 + 8y + 18y^2) + x^2(6 + 54y + 216y^2) + ..., \\
\omega_1(x, y) &= 4x + 16x^2 + 2y + 20xy + 144x^2y + 3y^2 + 54xy^2 + 630x^2y^2 + ...+ \\
&\quad + \Big[1 + y + y^2 + x(2 + 8y + 18y^2) + x^2(6 + 54y + 216y^2) + ...\Big] \log x + \\
&\quad + \frac{1}{2}\Big[1 + y + y^2 + x(2 + 8y + 18y^2) + x^2(6 + 54y + 216y^2) + ...\Big] \log y.
\end{aligned} \tag{211}$$

[52] There are two integration constants coming from the solution of the DEs for $c_0(y)$ and $c_1(y)$.

Note that their form is just the two-variable generalization of (166).

The new function $G(x, y)$ is determined by solving the first-order partial differential equations (207) and (209), which respectively determines its dependence on x and y. Since both equations are first order, it is easy to write down the general solution explicitly. We present the strategy in full generality, as it will be useful in later applications.
We are dealing with a coupled system of the form:

$$\begin{cases} \partial_x G(x,y) = f(x,y) \\ \partial_y G(x,y) = h(x,y) \end{cases}, \tag{212}$$

where $f(x, y)$ and $h(x, y)$ are known functions. From the first equation, we obtain a partial solution that captures the x-dependence, up to an integration "constant" that may depend on y:

$$G(x,y) = G_x(x,y) + c(y) = \int f(x,y)dx + c(y). \tag{213}$$

To determine the unknown function $c(y)$, we plug in the second equation, getting:

$$c(y) = \int dy \Big[h(x,y) - \partial_y G_x(x,y) \Big]. \tag{214}$$

Therefore, the full solution of the system (212) can be written as:

$$G(x,y) = \int dx f(x,y) + \int dy \left[h(x,y) - \partial_y \int dx f(x,y) \right]. \tag{215}$$

Note that this is defined up to a constant (indefinite integrals on the rhs) that can be fixed by imposing a boundary condition. In our specific case, $f(x, y)$ and $h(x, y)$ correspond respectively to the right-hand sides of equations (205) and (208), and depend on ω_0 and its derivatives. Therefore, using the series expansion previously obtained for ω_0, we can construct a series representation for G.

For completeness, we now report the first few terms in this expansion:

$$G(x,y) = x(-1-y-y^2-y^3) + x^2(-1-4y-9y^2-16y^3) + x^3(-2-18y-72y^2-200y^3) + ... \tag{216}$$

9.4 Solving the canonical DEs by series

The next step is to find series solutions to the canonical DEs.

We have two coupled systems of first order PDEs:

$$\begin{cases} \partial_x \vec{J}(x,y,\epsilon) = \epsilon \tilde{A}_x(x,y) \vec{J}(x,y,\epsilon) \\ \partial_y \vec{J}(x,y,\epsilon) = \epsilon \tilde{A}_y(x,y) \vec{J}(x,y,\epsilon) \end{cases}, \tag{217}$$

where $\vec{J}$ is the vector of canonical MIs, $\tilde{A}_x$ and $\tilde{A}_y$ are the canonical matrices.

As in the one-variable case, we can look for solutions of the form:

$$\vec{J}(x,y,\epsilon) = \sum_{n=n_0}^{\infty} \epsilon^n \vec{J}^{(n)}(x,y), \tag{218}$$

which leads to the recursive differential equations:

$$\begin{cases} \partial_x \vec{J}^{(n)}(x,y) = \tilde{A}_x(x,y)\vec{J}^{(n-1)}(x,y) \\ \partial_y \vec{J}^{(n)}(x,y) = \tilde{A}_y(x,y)\vec{J}^{(n-1)}(x,y) \end{cases} . \tag{219}$$

As usual, the lowest nontrivial coefficient is a constant: $J^{(n_0)} = c^{(n_0)}$; the generic higher-order coefficient $\vec{J}^{(n)}$ is determined from the previous one by solving (219). This sysyem is a vector-valued generalization of (212), thus its solution will be the following generalization of (215):

$$\begin{aligned} \vec{J}^{(n)}(x,y) = &\int dx \tilde{A}_x(x,y)\vec{J}^{(n-1)}(x,y) + \\ &+ \int dy \left[\tilde{A}_y(x,y)\vec{J}^{(n-1)}(x,y) - \partial_y \int dx \tilde{A}_x(x,y)\vec{J}^{(n-1)}(x,y) \right] + \vec{c}^{(n)}, \end{aligned} \tag{220}$$

where, for each order in ϵ, there is a boundary constant vector to determine.

Series solutions around specific kinematic points can be obtained iteratively, using the same strategy as in the equal-mass case. However, the computation is significantly more involved. In fact, both the canonical matrices and the recursive relation (220) involve more intricate structures, and the series expansions must be performed in both variables, x and y.

In particular, the most computationally expensive part is the expansion of the canonical matrix, due to its complicated form, involving inverse powers of $\omega_0(x,y)$ and high powers of $G(x,y)$. A direct expansion quickly becomes inefficient, especially at high orders. A more efficient approach is to decompose the matrix as:

$$\tilde{A}(x,y) = \sum_{i=0}^{4} \tilde{A}_i(x,y)[G(x,y)]^i, \tag{221}$$

where each coefficient matrix $\tilde{A}_i$ may still involve factors $1/\omega_0$ and $1/\omega_0^2$. We then proceed as follows:

1. Pre-compute the series expansions of $1/\omega_0$ and $1/\omega_0^2$ using the known expansion of ω_0. Since this is the most computationally expensive step, we perform it

only once (for a higher order than the ones we could need) and store the results in a file. For subsequent calculations, we simply truncate these expansions as needed.

2. Substitute them into the matrices $\tilde{A}_i$ and expand.
3. Expand the powers $G^i(x, y)$ using the previously obtained expansion for $G(x, y)$.
4. Multiply each expanded $\tilde{A}_i$ by the corresponding G^i and sum to reconstruct the expansion for the full matrix $\tilde{A}$.

This method significantly improves performance, especially when many orders in the series solutions are required.

For the rest, the procedure follows the same steps as in the equal-mass case. The boundary conditions are also imposed by using the same strategy: we evaluate the MIs numerically near the expansion point, extract the numerical values for the boundary constants, and match them with a proper set of known transcendental constants.

9.5 Study of convergence and Bernoulli-like variables

Our goal is to construct series expansions with good convergence properties using the method proposed in the previous chapter.

The singularities of the DEs in the variables s, m^2, M^2 are located at:

$$\{s = 0,\ s = M^2,\ s = (2m - M)^2,\ s = (2m + M)^2,\ s = \infty\}, \tag{222}$$

where $s = (2m + M)^2$ corresponds to the physical threshold for the production of the three internal particles on-shell.
In the chosen variables (x, y), the singularities of the DEs are:

$$\{x = 0,\ y = 0,\ y = 1,\ (2\sqrt{x} - \sqrt{y})^2 = 1,\ (2\sqrt{x} + \sqrt{y})^2 = 1,\ (x, y) \to \infty\}. \tag{223}$$

Figure 21 shows the x-y plane with these singularities:

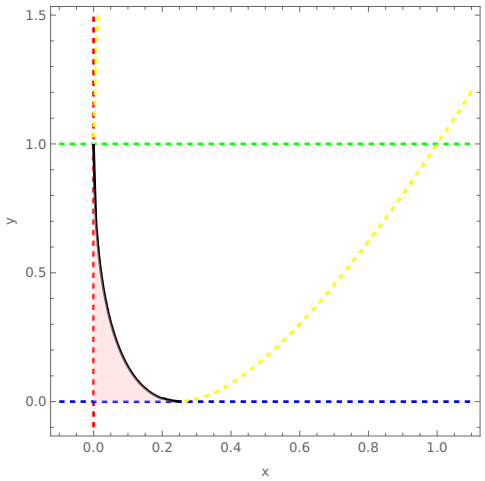

Figure 21: The region of interest(highlighted) in the variables (x,y) and the singularities of the canonical DEs: the solid line corresponds to the physical threshold, the dashed ones are spurious singularities.

We focus on the region beyond the physical threshold, i.e. $s \geq (2m + M)^2$, corresponding to the shaded area in the figure. As expansion point, we choose the origin $(x, y) = (0, 0)$, which corresponds to[53] $s = \infty$. Note that, for this point, the matching of numerical boundary values with known analytic constants is straightforward, since only zeta values are expected to appear.[54]

For this expansion no blow-up is required, as only two singularities intersect at the expansion point. The next step is to decide which singularities to send to infinity via Bernoulli-like changes of variables.

As for the cases previously considered, also here, for similar reasons, it is not convenient to move the true singularity, $(2\sqrt{x} + \sqrt{y})^2 = 1$.
The second closest (spurious) singularity is $(2\sqrt{x} - \sqrt{y})^2 = 1$, corresponding to the yellow curve in Figure 21. One might consider pushing it away via the Bernoulli-like transformation:

$$u = -\log\left[1 - (2\sqrt{x} - \sqrt{y})^2\right] \Longleftrightarrow y = \left(2\sqrt{x} - \sqrt{1 - e^{-u}}\right)^2. \tag{224}$$

However, this choice also turns out to be problematic, as we can see from the following figure:

[53] Or equivalently to: $s = 1$, $m = M = 0$.
[54] This is due to the fact that this is a MUM (maximal unipotent monodromy) point.

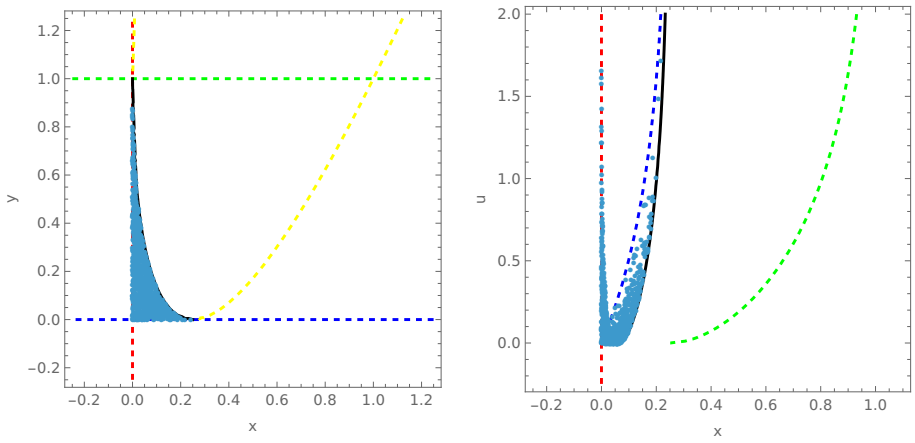

Figure 22: Left: original singularity structure. Right: image of the singular curves under the transformation. Sample points in the region of interest are mapped into an irregular domain that includes the blue singularity.

It is evident that this transformation drastically changes the geometry of our region of interest, mapping it into a domain that contains the blue singularity, corresponding to the original line $y = 0$. Therefore, rather than improving convergence, this change of variables may even make it worse.

The only remaining possibility is to push away just one spurious singularity, namely the line $y = 1$, by introducing the Bernoulli-like variable:

$$v = -\log(1 - y) \Longleftrightarrow y = 1 - e^{-v}. \tag{225}$$

As usual, to test the effectiveness of the new expansion, we generate random points within the region of interest and evaluate both the original and accelerated series at those points, using the same fixed number of terms. The relative precision is estimated by considering as truncation error the relative variation of the partial sums when one more order is added. A comparison of the results for the original and the accelerated expansions of master $I_{1,1,1,0,0}$ is shown in the following figure:

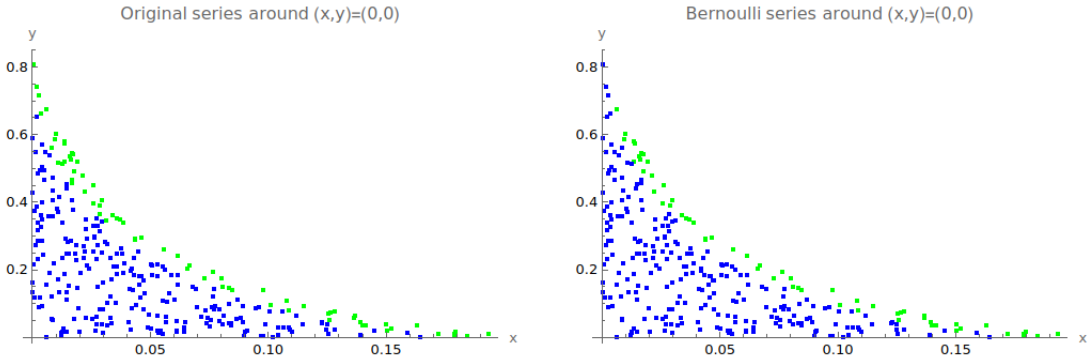

Figure 23: Relative truncation errors for expansions of master I(1,1,1,0,0) including 20 orders. Left: Original series; right: series using one Bernoulli-like variable. As usual, each color corresponds to a different precision; blue: prec.>4 digits, green: 2-4 digits.

The introduction of the Bernoulli-like variable v leads to some improvement in convergence, but the gain is really modest. This is due to the fact that only one singularity can be safely sent to infinity, and it is not the one that most limits convergence. However, two other corners of the region remain available as potential expansion points. In particular, we expect better performance when expanding around $(x, y) = (1/4, 0)$, since in that case two singular lines ($x = 0$ and $y = 1$) can be safely pushed to infinity. We leave the study of this expansion to future work.

This case study already shows that the acceleration method remains effective for two-dimensional problems beyond the polylogarithmic case, as expected.[55] However, it also reveals a fundamental limitation: the method's effectiveness strongly depends on the geometrical shape of the singular curves being pushed away. Bernoulli-like variable changes work particularly well for straight-line singularities, though not exclusively, as shown in the previous chapter, when dealing with the transformed singular lines after the blow-up. However, they fail when applied to more complicated curves, such as those encountered in this example. Attempting to move such curves typically distorts the geometry of the region of interest and may cause external singularities to enter it, ultimately undermining the convergence of the expansion.

[55] We already applied a Bernoulli-like change of variable to the equal-mass sunrise, which is a 1D problem, but already involves an elliptic geometry.

10 Conclusions

Loop Feynman diagrams are a fundamental ingredient for high-precision predictions in quantum field theory. However, computing the associated Feynman integrals remains a challenging task. The state-of-the-art approach involves reducing integrals to a set of master integrals (MIs) via integration-by-parts (IBP) identities, followed by solving the corresponding differential equations in the relevant kinematic variables.

In this work, we focused mainly on the second step, using in particular series expansion techniques. For each integral family under study, we first cast the differential equations in canonical form. In this form, we solved the system using an iterative approach in ϵ, combined with a series expansion in the relevant kinematic scales. The key advantage of this method is that, once a canonical basis is found — a step whose complexity depends on the geometry of the problem — the remaining procedure becomes fully algorithmic and general. In fact, unlike analytic methods, whose complexity rapidly increases with the number of loops and external legs, this method handles only power series and logarithms at each step, making it broadly applicable regardless of the underlying mathematical structure.

A central challenge in this approach is the restricted region where the series solution converges, and the progressively slower convergence near its boundary. To address it, we investigated a class of variable transformations, called Bernoulli-like variables, that can push nearby singularities to infinity, thereby extending the domain of validity of the series and accelerating its convergence. Although these techniques had been previously applied empirically to one-scale problems, no systematic study of their properties had been performed.

In the first part of this work, starting from the study of simple one-scale problems and some general considerations, we carried out a detailed analysis and identified several key features of Bernoulli-like variables:

- The improvement in convergence is not solely due to mapping singularities to infinity, but is also linked to the structure of the series coefficients in the new variable.
- The gain in precision with the number of orders is most significant at low orders; at higher orders, the relative improvement tends to saturate.
- Even spurious singularities can affect convergence and must be considered when choosing the right transformation.
- In the presence of multiple singularities, the next-limiting singularity after the first is not necessarily the second closest in the original variable, but the one

that appears nearest in the new coordinate. However, pushing it further away with the same approach does not always help and can worsen convergence due to multivaluedness and branch cut effects. We leave to future work a deeper investigation of generalized Bernoulli-like variables capable of handling multiple singularities effectively.

Then, we moved to multi-scale problems and proposed a procedure to improve convergence based on the introduction of several Bernoulli-like variables, eventually after performing blow-ups. In particular, each original variable is replaced by a Bernoulli-like variable designed to push away the singularity that most limits convergence. Unlike the one-dimensional case, identifying which singularities to remove is less straightforward. The optimal choice depends on how the transformation affects the geometry of the singularities and the physical region of interest. We also found that this method is more effective when the singularities are straight lines or simple curves, as more involved shapes tend to distort the geometry of the physical region, causing eventually external singularities to enter in.

We tested this method on two physically relevant two-loop amplitudes: the decays respectively of a Higgs and a Z boson into three gluons, both expressed in terms of MPLs. Using three expansion points and Bernoulli-like transformations, we covered the full physical region with relative precision better than four digits, requiring only 9–10 orders in each expansion. In contrast, expansions in the original variables needed over 20 orders per variable to reach comparable precision.

We also explored an elliptic two-scale example: the sunrise integral with two equal masses and one different mass. In this case, due to the complicated geometry of the singularities, only the (spurious) singular line $y = 1$ could be safely pushed away. Although this produced only modest improvements, it suggests that the our acceleration method remains valid even beyond the polylogarithmic case. Notably, the difficulty was not tied to the elliptic nature of the problem, but to the complicated shape of some of the singular curves.

A possible refinement of the method could involve first performing a suitable change of variables to simplify the geometry of some singular curves and then applying Bernoulli-like transformations to push them away. We leave this to future work.
Another promising direction is the application to integrals with more than two scales, where identifying and controlling the dominant singularities becomes increasingly challenging. Finally, this method could be particularly valuable for high-loop amplitudes, where the extremely large size and the involved mathematical structure of the expressions often make direct expansions impractical, as too many terms would be required to get accurate results. In such cases, accelerated expansions may offer a viable and efficient alternative.

Appendix

In the following, we report the matrices A_x and A_y of the differential equations for the sunrise integral family with two equal masses m and a different mass M:

$$A_x = \begin{pmatrix} -\frac{\epsilon}{x} & 0 & 0 & 0 & 0 \\ 0 & -\frac{2\epsilon}{x} & 0 & 0 & 0 \\ 0 & 0 & 0 & 2 & 0 \\ a & b & c & d & e \\ \frac{2\epsilon}{x} & -\frac{4\epsilon}{x} & -2(2\epsilon+1) & -4(2x-y-1) & 0 \end{pmatrix}, \tag{226}$$

with:

$$\begin{aligned} a &= \frac{2\epsilon(1+6\epsilon)}{x(1-8x+16x^2-2y-8xy+y^2)}, \\ b &= -\frac{\epsilon(5x-\epsilon+14x\epsilon+y\epsilon)}{x^2(1-8x+16x^2-2y-8xy+y^2)}, \\ c &= -\frac{(1+2\epsilon)(-1+6x-y+2\epsilon+16x\epsilon+2y\epsilon)}{x(1-8x+16x^2-2y-8xy+y^2)}, \\ d &= -\frac{1-16x+48x^2-2y-16xy+y^2+\epsilon-24x\epsilon+80x^2\epsilon-2y\epsilon-24xy\epsilon+y^2\epsilon}{x(1-8x+16x^2-2y-8xy+y^2)}, \\ e &= \frac{3\epsilon(1+2\epsilon)}{x(1-8x+16x^2-2y-8xy+y^2)}. \end{aligned} \tag{227}$$

$$A_y = \begin{pmatrix} -\frac{\epsilon}{y} & 0 & 0 & 0 & 0 \\ 0 & 0 & 0 & 0 & 0 \\ -\frac{\epsilon}{(y-1)y} & \frac{5\epsilon}{2(y-1)y} & -\frac{-4x\epsilon-2x+y\epsilon+2y-5\epsilon}{2(y-1)y} & \frac{x(4x-3y-1)}{(y-1)y} & -\frac{3\epsilon}{2(y-1)y} \\ f & g & h & i & l \\ -\frac{(3y+1)\epsilon}{(y-1)y} & \frac{5(3y+1)\epsilon}{2(y-1)y} & m & \frac{x\left(12xy+4x-5y^2-10y-1\right)}{(y-1)y} & -\frac{3(3y+1)\epsilon}{2(y-1)y} \end{pmatrix}, \tag{228}$$

with:

$$
\begin{aligned}
f &= \frac{\epsilon\left(8x^2\epsilon + 4x^2 - 10xy\epsilon - 3xy + 2x\epsilon - x - y^2\epsilon + 2y\epsilon - \epsilon\right)}{x(y-1)y\left(16x^2 - 8xy - 8x + y^2 - 2y + 1\right)},\\
g &= -\frac{\epsilon\left(40x^2\epsilon + 20x^2 - 30xy\epsilon - 15xy - 10x\epsilon - 5x - 4y^2\epsilon + 4y\epsilon\right)}{2x(y-1)y\left(16x^2 - 8xy - 8x + y^2 - 2y + 1\right)},\\
h &= \frac{(2\epsilon+1)\left(-16x^2\epsilon - 8x^2 + 16xy\epsilon + 14xy - 16x\epsilon + 2x + 9y^2\epsilon - 2y^2 + 2y\epsilon - 6y + 5\epsilon\right)}{2(y-1)y\left(16x^2 - 8xy - 8x + y^2 - 2y + 1\right)},\\
i &= -\frac{(2\epsilon+1)\left(16x^3 - 24x^2y - 8x^2 + xy^2 + 14xy + x + y^3 - 2y^2 + y\right)}{(y-1)y\left(16x^2 - 8xy - 8x + y^2 - 2y + 1\right)},\\
l &= -\frac{3\epsilon(2\epsilon+1)(-4x + 3y + 1)}{2(y-1)y\left(16x^2 - 8xy - 8x + y^2 - 2y + 1\right)},\\
m &= \frac{12xy\epsilon + 6xy + 4x\epsilon + 2x + 5y^2\epsilon + 6y\epsilon - 8y + 5\epsilon}{2(y-1)y}.
\end{aligned}
\tag{229}
$$

References

[1] Gerard 't Hooft and M. J. G. Veltman. "Scalar One Loop Integrals". In: *Nucl. Phys. B* 153 (1979), pp. 365–401. DOI: 10.1016/0550-3213(79)90605-9.

[2] Samuel Abreu, Ruth Britto, and Claude Duhr. "The SAGEX review on scattering amplitudes Chapter 3: Mathematical structures in Feynman integrals". In: *J. Phys. A* 55.44 (2022), p. 443004. DOI: 10.1088/1751-8121/ac87de. arXiv: 2203.13014 [hep-th].

[3] Luise Adams, Christian Bogner, and Stefan Weinzierl. "The two-loop sunrise graph with arbitrary masses". In: *J. Math. Phys.* 54.5 (2013), p. 052303. DOI: 10.1063/1.4804996. arXiv: 1302.7004 [hep-ph].

[4] Simon Badger et al. *Scattering Amplitudes in Quantum Field Theory*. Vol. 1021. Lecture Notes in Physics. Springer, 2024. DOI: 10.1007/978-3-031-46987-9.

[5] Christian Bogner and Stefan Weinzierl. "Periods and Feynman integrals". In: *Journal of Mathematical Physics* 50.4 (2009), p. 042302. DOI: 10.1063/1.3106041. arXiv: 0711.4863 [hep-ph].

[6] C. G. Bollini and J. J. Giambiagi. "Dimensional renormalization: The number of dimensions as a regularizing parameter". In: *Il Nuovo Cimento B* 12.1 (1972), pp. 20–26. DOI: 10.1007/BF02895558.

[7] William E. Boyce and Richard C. DiPrima. *Elementary Differential Equations and Boundary Value Problems*. 10th ed. Hoboken, NJ, USA: Wiley, 2012. ISBN: 9780470458310.

[8] Johannes Broedel et al. "Elliptic polylogarithms and Feynman parameter integrals". In: *Journal of High Energy Physics* 5 (2019), p. 120. DOI: 10.1007/JHEP05(2019)120. arXiv: 1902.09971 [hep-ph].

[9] Johannes Broedel et al. "Elliptic polylogarithms and iterated integrals on elliptic curves. II. An application to the sunrise integral". In: *Phys. Rev. D* 97.11 (2018), p. 116009. DOI: 10.1103/PhysRevD.97.116009. arXiv: 1712.07095 [hep-ph].

[10] Michele Caffo et al. "BOKASUN: A fast and precise numerical program to calculate the Master Integrals of the two-loop sunrise diagrams". In: *Comput. Phys. Commun.* 180 (2009), pp. 427–438. DOI: 10.1016/j.cpc.2008.10.011. arXiv: 0807.1959 [hep-ph].

[11] Michele Caffo et al. "The master differential equations for the 2-loop sunrise self-mass amplitudes". In: *Nuovo Cim. A* 111.4 (1998), pp. 365–389. arXiv: hep-th/9805118 [hep-th].

[12] K. G. Chetyrkin and F. V. Tkachov. "Integration by Parts: The Algorithm to Calculate beta Functions in 4 Loops". In: *Nucl. Phys. B* 192 (1981), pp. 159–204. DOI: 10.1016/0550-3213(81)90199-1.

[13] Claude Duhr. "Hopf algebras, coproducts and symbols: An application to Higgs boson amplitudes". In: *Journal of High Energy Physics* 2012.8 (2012), p. 43. DOI: 10.1007/JHEP08(2012)043. arXiv: 1203.0454 [hep-ph].

[14] Claude Duhr. "Mathematical aspects of scattering amplitudes". In: *Theoretical Advanced Study Institute in Elementary Particle Physics: Journeys Through the Precision Frontier: Amplitudes for Colliders*. 2015, pp. 419–476. DOI: 10.1142/9789814678766_0010. arXiv: 1411.7538 [hep-ph].

[15] Claude Duhr and Falko Dulat. "PolyLogTools – polylogs for the masses". In: *J. High Energy Phys.* 2019.08 (2019). Package URL: https://gitlab.com/pltteam/plt, p. 135. DOI: 10.1007/JHEP08(2019)135. arXiv: 1904.07279.

[16] Claude Duhr et al. "Aspects of canonical differential equations for Calabi-Yau geometries and beyond". In: *JHEP* 06 (2025), p. 128. DOI: 10.1007/JHEP06(2025)128. arXiv: 2503.20655 [hep-th].

[17] Claude Duhr et al. "Elliptic polylogarithms and two-loop Feynman integrals". In: *13th International Symposium on Radiative Corrections (LL2018)*. 2018, p. 005. DOI: 10.22323/1.303.0005. arXiv: 1807.06238 [hep-ph].

[18] Thomas Gehrmann and Ettore Remiddi. "Numerical Evaluation of Harmonic Polylogarithms". In: *Comput. Phys. Commun.* 141 (2001), pp. 296–312. DOI: 10.1016/S0010-4655(01)00411-8. arXiv: hep-ph/0107173 [hep-ph].

[19] Thomas Gehrmann and Ettore Remiddi. "Numerical Evaluation of Two-Dimensional Harmonic Polylogarithms". In: *Comput. Phys. Commun.* 144 (2002), pp. 200–223. DOI: 10.1016/S0010-4655(02)00139-X. arXiv: hep-ph/0111255 [hep-ph].

[20] Thomas Gehrmann et al. "Two-loop helicity amplitudes for $H+$jet production to higher orders in the dimensional regulator". In: *J. High Energy Phys.* 2023.4 (2023), p. 016. DOI: 10.1007/JHEP04(2023)016. arXiv: 2301.10849 [hep-ph].

[21] Thomas Gehrmann et al. "Two-loop helicity amplitudes for $V+$jet production including axial vector couplings to higher orders in ϵ". In: *J. High Energy Phys.* 09 (2023), p. 192. DOI: 10.1007/JHEP09(2023)192. arXiv: 2306.10170 [hep-ph].

[22] Lennard Görges et al. "On a procedure to derive ϵ-factorised differential equations beyond polylogarithms". In: *JHEP* 2023.7 (2023), p. 206. DOI: 10.1007/JHEP07(2023)206. arXiv: 2305.14090 [hep-th].

[23] Johannes M. Henn. "Multiloop integrals in dimensional regularization made simple". In: *Phys. Lett. B* 766 (2017), pp. 193–197. DOI: 10.1016/j.physletb.2016.12.039. URL: https://doi.org/10.1016/j.physletb.2016.12.039.

[24] G. 't Hooft and M. J. G. Veltman. "Regularization and renormalization of gauge fields". In: *Nuclear Physics B* 44.1 (1972), pp. 189–213. DOI: 10.1016/0550-3213(72)90279-9.

[25] A. V. Kotikov. “Differential equations method: New technique for massive Feynman diagrams calculation”. In: *Phys. Lett. B* 254.1-2 (1991), pp. 158–164. DOI: 10.1016/0370-2693(91)90413-K.

[26] S. Laporta and E. Remiddi. “The structure of the differential equations for the master integrals of the two-loop on-shell electroweak form factor”. In: *Acta Physica Polonica B* 28.3 (1997), pp. 959–968.

[27] Sergio Laporta. “High-precision calculation of multi-loop Feynman integrals by difference equations”. In: *International Journal of Modern Physics A* 15.28 (2000), pp. 5087–5159. arXiv: hepâĂŘph/0102033 [hep-ph].

[28] Stefano Laporta and Ettore Remiddi. “Analytic treatment of the two-loop equal mass sunrise graph”. In: *Nuclear Physics B* 704.1-2 (2005), pp. 349–386. DOI: 10.1016/j.nuclphysb.2004.10.044. arXiv: hep-ph/0406160 [hep-ph].

[29] Nathaniel Larson. *The Bernoulli Numbers: A Brief Primer*. Whitman College Technical/Expository Paper. May. 2019. URL: https://www.whitman.edu/Documents/Academics/Mathematics/2019/Larson-Balof.pdf.

[30] R.N. Lee. “Dimension-shift relations for Feynman integrals”. In: *J. High Energy Phys.* 2009.10 (2009), p. 074. DOI: 10.1088/1126-6708/2009/10/074.

[31] Xiao Liu and Yan-Qing Ma. “AMFlow: a Mathematica package for Feynman integrals computation via Auxiliary Mass Flow”. In: *Computer Physics Communications* 283 (2023), p. 108565. DOI: 10.1016/j.cpc.2022.108565. arXiv: 2201.11669 [hep-ph].

[32] Andreas von Manteuffel and Cedric Studerus. “Reduze 2 - Distributed Feynman Integral Reduction”. In: *arXiv e-prints* (2012). DOI: 10.48550/arXiv.1201.4330. eprint: 1201.4330.

[33] Stefan Müller-Stach, Stefan Weinzierl, and Raphael Zayadeh. “Picard–Fuchs equations for Feynman integrals”. In: *Communications in Mathematical Physics* 326.1 (2014), pp. 237–249. DOI: 10.1007/s00220-013-1838-4. arXiv: 1212.4389 [hep-ph].

[34] Christoph Nega et al. *Calabi-Yau Geometries and Feynman Integrals – Bananas & Ice Cones*. Talk presented at the workshop "Elliptic Integrals in Fundamental Physics". Sept. 2022. URL: https://indico.mitp.uni-mainz.de/event/212/contributions/4066/.

[35] Tiziano Peraro. “FiniteFlow: Multivariate Functional Reconstruction Using Finite Fields and Dataflow Graphs”. In: *J. High Energy Phys.* 2019.07 (2019), p. 031. DOI: 10.1007/JHEP07(2019)031. arXiv: 1905.08019 [hep-th].

[36] Michael E. Peskin and Daniel V. Schroeder. *An Introduction to Quantum Field Theory*. Boulder, Colorado: Westview Press, 1995. ISBN: 978-0201503975.

[37] S. Pozzorini and E. Remiddi. “Precise numerical evaluation of the two loop sunrise graph Master Integrals in the equal mass case”. In: *Comput. Phys. Commun.* 175 (2006), pp. 381–387. DOI: 10.1016/j.cpc.2006.05.005. arXiv: hep-ph/0505041 [hep-ph].

[38] Amedeo Primo and Lorenzo Tancredi. “On the maximal cut of Feynman integrals and the solution of their differential equations”. In: *Nucl. Phys. B* 916 (2017), pp. 94–116. DOI: 10.1016/j.nuclphysb.2016.12.021. arXiv: 1610.08397 [hep-ph].

[39] E. Remiddi. “Differential equations for Feynman graph amplitudes”. In: *Il Nuovo Cimento A* 110 (1997), pp. 1435–1452. DOI: 10.1007/BF03185566.

[40] Ettore Remiddi and Lorenzo Tancredi. “An Elliptic Generalization of Multiple Polylogarithms”. In: *Nucl. Phys. B* 925 (2017), pp. 212–251. DOI: 10.1016/j.nuclphysb.2017.10.007. arXiv: 1709.03622 [hep-ph]. URL: https://doi.org/10.1016/j.nuclphysb.2017.10.007.

[41] Cesare Rossetti. *Metodi matematici della fisica*. 2nd ed. Seconda edizione, completamente riveduta. Torino, Italia: Levrotto & Bella, 2000, p. 596. ISBN: 978-8882180607.

[42] Matthew D. Schwartz. *Quantum Field Theory and the Standard Model*. Cambridge, UK: Cambridge University Press, 2014. ISBN: 978-1107034730. DOI: 10.1017/CBO9780511813900. URL: https://doi.org/10.1017/CBO9780511813900.

[43] Joseph H. Silverman. *The Arithmetic of Elliptic Curves*. 2nd ed. Vol. 106. Graduate Texts in Mathematics. Springer, 2009. DOI: 10.1007/978-0-387-09494-6.

[44] Alexander V. Smirnov and Alexey V. Petukhov. “The number of master integrals is finite”. In: *Lett. Math. Phys.* 97 (2011), pp. 37–44. DOI: 10.1007/s11005-010-0450-0. arXiv: 1004.4199 [hep-th]. URL: https://doi.org/10.1007/s11005-010-0450-0.

[45] O.V. Tarasov. “Connection between Feynman integrals having different values of the space-time dimension”. In: *Phys. Rev. D* 54.11 (1996), pp. 6479–6487. DOI: 10.1103/PhysRevD.54.6479.

[46] F. V. Tkachov. “A Theorem on Analytical Calculability of Four Loop Renormalization Group Functions”. In: *Phys. Lett. B* 100 (1981), pp. 65–68. DOI: 10.1016/0370-2693(81)90288-4.

[47] Steven Weinberg. *The Quantum Theory of Fields, Volume I: Foundations*. Cambridge, UK: Cambridge University Press, 1995. ISBN: 978-0521550017.

[48] Stefan Weinzierl. *Feynman Integrals: A Comprehensive Treatment for Students and Researchers*. Cham, Switzerland: Springer, 2022. DOI: 10.1007/978-3-030-99558-4. URL: https://doi.org/10.1007/978-3-030-99558-4.

[49] E. T. Whittaker and G. N. Watson. *A Course of Modern Analysis*. 4th ed. Cambridge, UK: Cambridge University Press, 1927. ISBN: 9780521588072.

[50] Simone Zoia. *Modern Analytic Methods for Computing Scattering Amplitudes: With Application to Two-Loop Five-Particle Processes*. Springer Theses. Springer, 2022. DOI: 10.1007/978-3-031-01945-6.